Faculty of Science & Engineering
Cyfadran Gwyddoniaeth a Pheirianneg

Swansea University
Prifysgol Abertawe

Modelling of High Temperature Hot-Rolled Steel

Project Dissertation submitted to Swansea University in Partial Fulfilment for the Degree of Master of Science

Material Science MSc

Dissertation Author: Ahmad Sajjad

Submission: September 2023

Supervisor: Prof. Nicholas Lavery

2nd Supervisor: Prof Steve Brown

Abstract

The coilbox is a non-compulsory process used in hot strip milling to produce diverse alloys of hot-rolled steel products. Unlike other hot strip processes, the Coilbox is a passive process usually placed between the roughing and finishing mills which does not introduce any extra heat or mechanical stress into the steel strip. The coilbox wraps the steel strip around itself, forming a tight coil and shortening the overall length of the steel strip, and in turn, reduces the overall size of the hot strip mill. The coilbox also reduces heat loss from the steel strip by reducing the total surface area exposed to the environment. Lastly, the coilbox allows the strip to be stored temporarily on the mill while still hot in case of a fault or congestion ahead.

Temperature control throughout the hot strip milling process is essential to ensure the end steel product has the correct and expected mechanical properties. Temperatures too high or low can introduce unexpected stresses and damage mill equipment. Due to the importance of temperature control, many mills have thermal models or simulation software that predict the temperature of the steel strip throughout every stage of the milling process.

Thermal models of the hot strip are often implemented in-house and specific to manufacturers' requirements and setups. TATA Steel is no different, having developed a strip mill simulation software called TiTAN. This study looks at modifying and implementing a thermal model into TiTAN using the finite element method to allow the user to test and understand the thermal losses of a steel strip as it passes through the coilbox.

TiTAN is a quick and efficient modelling software for hot and cold strip mills, although currently, it cannot model temperature changes that may occur during the coilbox process. TATA Steel would like to implement a new module into TiTAN that would allow this functionality. The new model must integrate seamlessly with TiTAN whilst also accurately modelling the steel strip temperature up to 80% of the actual temperature of the steel strip as measured from on-site data.

Temperature data from TATA Steels Port Talbot site were analysed to understand the thermal properties of the strip as it passes through the coilbox. Furthermore, how the strip moves through the coilbox was studied to determine if the physical properties of the strip, such as position and speed, would impact the temperature. After building up a good understanding of the properties of the strip as it passes through the coilbox, a model of the coilbox process was developed in TiTAN.
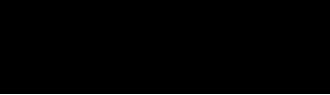
Declaration

This work has not previously been accepted in substance for any degree and is not being concurrently submitted in candidature for any degree.

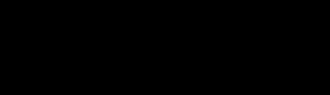Signed: ███████████   Date: 05/09/2023

Statement 1

This dissertation is the result of my own independent work/investigation, except where otherwise stated. Other sources are acknowledged by giving explicit references. A bibliography is appended.

Signed: ███████████   Date: 05/09/2023

Statement 2

I hereby give consent for my dissertation, if accepted, to be available for photocopying and for interlibrary loan and for the title and summary to be made available to outside organizations.

Signed: ███████████   Date: 05/09/2023

Acknowledgements

Contents

1 Introduction

Tata Steel is one of the most geographically diverse steel producers, conducting operations in many countries and continents. In Europe, Tata Steel is one of the largest steel producers with major plants at Ijmuiden in the Netherlands, which produces more than 7 million tonnes of coated steel in the form of rolls annually [1] and Port Talbot in South Wales. Tata Steel has operations in many locations throughout the United Kingdom. This paper will focus on the Tata Steel plant in Port Talbot, Wales.

Port Talbot's integrated steelworks is responsible for producing high-quality steel alloys. The site can process raw iron ore and coal into 'Slabs' and then to finished steel products. Steel slabs are semi-finished steel products. The slabs are flat and have rectangular cross-sections, typically having a thickness of 160mm or more [2].

At Port Talbot, the hot strip mill performs a series of operations by reheating thick steel slabs and rolling this material to produce steel strip products mainly in the form of hot rolled coils. The hot strip process causes the steel slab to experience many physical alterations and heat cycles. Although traditional strip mills had limited features, hot strip mills have developed significantly from the original tinplate and sheet rolling mills [3]. Modernisation has bought many changes to meet current customer demands allowing the production of large-diameter low, medium, and high-carbon steel coils used in sectors such as automotive, construction, and packaging [4]. During the hot milling process, after the initial casting of the slab, the steel slabs are first reheated in a reheating furnace to the required temperature. Once the desired temperature is attained the slabs pass through the roughing mill, generally consisting of one or two roughing stands [5]. The slab is rolled reversibly and usually passes through the roughing mill multiple times until the desired thickness of the slab is reached, typically around 30-50mm [6].

Figure 1.1 - Tata Steel, Netherlands roughing mill [7]

After the roughing process, the head and tail of the strip are cropped in the crop shear. Thereby ensuring the strip is fed correctly into the finishing mill without causing complications. The strip is then passed through the finishing mill, which usually has five to seven finishing roller stands [5-6]. The finishing mill reduces the thickness of the strip to the gauge required by the customer. The finishing speed must be adjusted to allow the final stand in the assembly to perform the thickness reduction at the correct temperature, as this will determine the mechanical properties of the hot rolled strip [8]. The finishing rolls must be monitored very closely. To avoid stretching or tearing the strip.

Figure 1.2 - Tata Steel, Port Talbot finishing mill [7]

After exiting the finishing mill the strip is now at the desired thickness and is carried down through a cooling table with water being sprayed onto the strip to cool it down from an initial temperature of around 1000°C to around 400°C at the end of the finishing mill, allowing the finished product to be coiled and then transported to the customer or another manufacturing process [9].

Figure 1.3 - Tata Steel, Netherlands cooling stands [7]

With the demand for high-quality yet affordable steel ever present it is important to tightly control the manufacturing process, ensuring that the mechanical properties of the steel are as the customer expects while reducing the defects and failures in the hot strip milling process in turn reducing the costs and lead time.

The mechanical properties of strip steel rely heavily on the temperature of the strip as it moves throughout the various process of hot strip milling, especially towards the finishing mill. As the steel must be malleable enough to pass through the rollers, reducing the thickness to final dimensions, however, excess heat may induce stresses as the steel cools changing the characteristics of the finished steel.

To achieve a higher level of control and predictability throughout the hot strip milling process many mathematical models have been previously developed using various techniques such as finite element modelling and computational fluid dynamics, by various mills. Simulations can predict rolling forces, such as roll speed, reduction ratio, and temperature as well as being able to describe metallurgical phenomena such as recrystallization, and grain growth [10]. Many models have been designed and implemented in steel plants across the world to help control the hot strip mill process [10-11].

Tata Steel has also developed its simulation software, coded using Delphi [13], called TiTAN to simulate a strip of steel as it goes through a hot or cold mill. The simulation software is quite complete allowing the user to input material composition and calculate material properties such as temperature, scaling, and oxide formation.

Whilst the software is quite competent it is missing a 'coilbox module', which is not a necessary process during the hot strip process and the Netherlands division of Tata Steel does not have a coilbox in their plant. However, the Port Talbot site does. As Tata Steel Europe was split into two companies, Tata Steel UK, and Tata Steel Dutch, there is now an opportunity to develop TiTAN for the UK division of Tata Steel by implementing a new coilbox component. This report describes the attempt to enhance the TiTAN software package to be able to accurately simulate strip behaviour as it moves through the coilbox.

1.1   Literature Review

The finite element method has been used several times to model the hot strip milling process although usually without the coilbox module. However, from these studies, the methods and modelling used can be extrapolated which can then be applied to the coilbox module in the future.

Previous works have considered several heat transfer mechanics. The phenomena which are considered are the following (i) Heat losses due to radiation and convection to the atmosphere. (ii) Heat conduction to the work roll. (iii) Heat losses due to boiling and forced convection of water employed in descaling the surface of the strip. (iv) Adiabatic heating produced by deformation. (v) Heat conduction within the stock [14]. Further studies focus on dynamic modelling, accounting for speed, heat flux, and deformation, the model below shows an example from this model showing all the modules that the program frequently calls on for multiple processes, like TiTAN [11],[12].
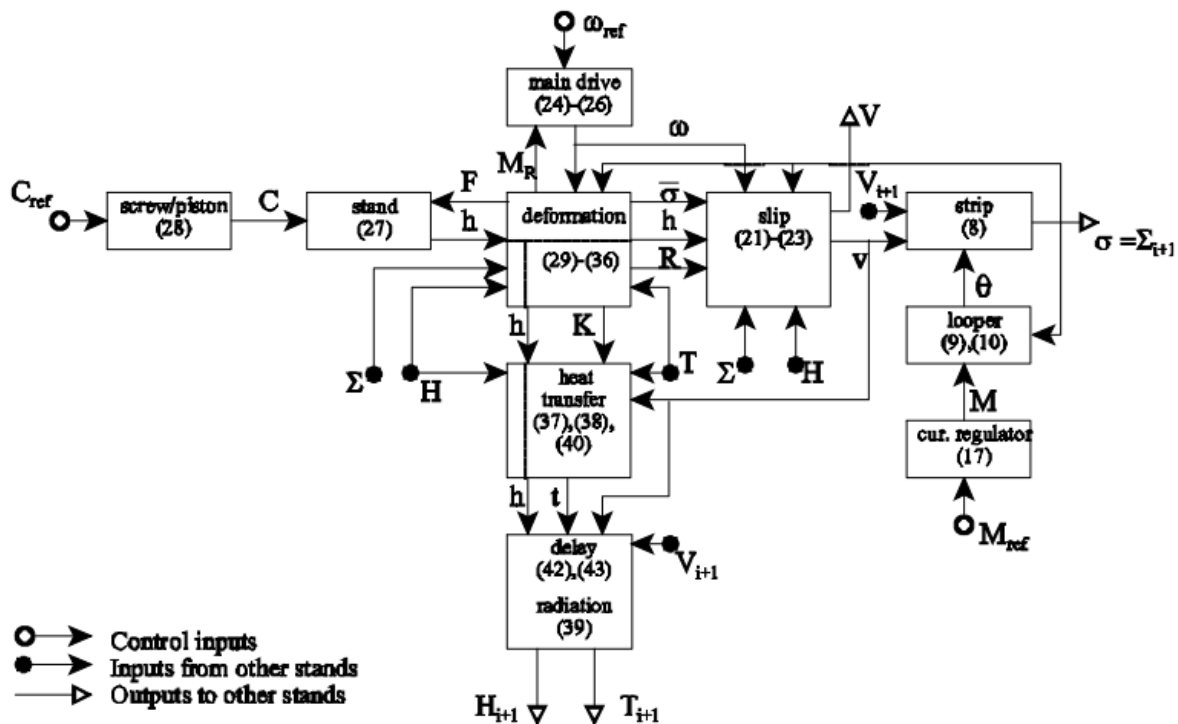
Figure 1.4 - Block diagram representation of the basic mill unit simulation [12]

Inspiration can be drawn from previous studies about how to discretize and model heat transfer in the coil by looking at heat transfer models made to simulate the cooling of hot-rolled coils. FEM has again been used in this context to model temperature as well as stress inside a cooling coil which is like the coils produced in the coilbox process, furthermore, these studies also help with the discretization of the model [15],[16].
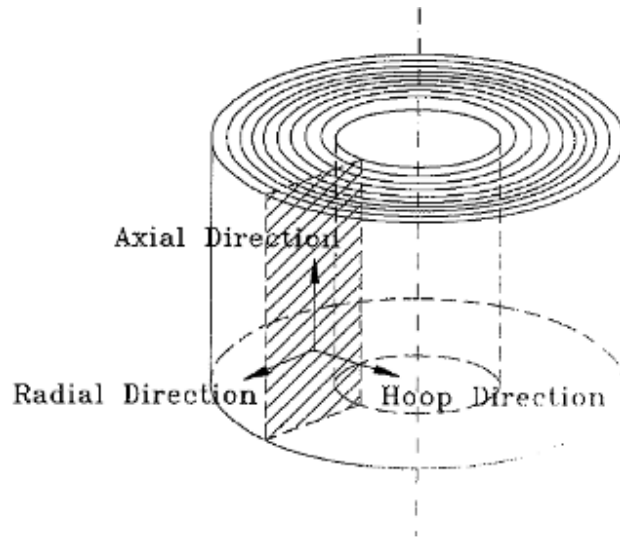
Figure 1.5 - Spatial discretization of the FEM Model in coil cooling [17]

The finite element method has been used in previous works to model coiling conditions, although not much research is available, such as bending angle and contact angle for coiling and uncoiling the material, [18] as well as temperature losses [19]. Although these papers focus solely on the coilbox and can go into much greater depth in much more resolution than possible for TiTAN.

1.2   The Coilbox

During the hot rolling process the steel strip must travel through the roughing mill, which significantly reduces the thickness of the steel plate, before entering the finishing mill, where the strip is adjusted to its final thickness [20].

However, when the mill is busy due to the manufacturing of multiple strips simultaneously. The hot strip process can become unsynchronized. This means that if there is a strip currently in the finishing mill, the strip in the roughing mill would need to wait until the finishing mill is free. If a coilbox is not incorporated in the mill layout, the strip would wait on roller tables between the roughing and finishing mills exposing the entire strip surface to the environment which would cause uneven temperature losses across the length of the strip. Uneven temperature loss in the strip can lead to an increase in the flow stresses present in turn making it more difficult to roll and reducing the uniformity of the mechanical properties of the finished product.

Figure 1.6 - TATA Steel Port Talbot hot mill coilbox [7]

One solution to this problem is installing a coilbox between the roughing and finishing mill. A coilbox is designed to wrap the steel strip around itself forming a coil of steel. In this configuration the strip takes up less space overall in the mill, reducing the length of the mill, although a much bigger benefit to this process is that it greatly reduces the surfaces of the coil exposed to the environment thus reducing temperature losses.
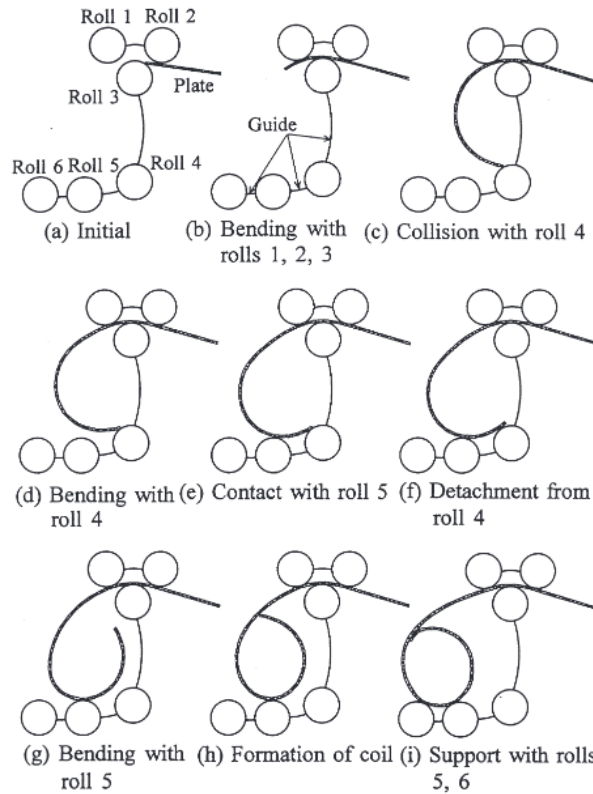
Figure 1.7 - Schematic showing how the coiling process is performed [18]

During the coiling process, no heat is added, and the thickness of the strip remains unchanged. The coil is wrapped around itself using six rollers seen in Figure 1.7. The inner diameter is previously determined by the contact angle of roller 4 [18]. The characteristics of the coil, such as the number of revolutions and the outer diameter, are functions of the length of the strip which can vary depending on the length of the strip being rolled.

Another benefit of the coilbox is that the strip is wrapped around itself. Meaning, that through heat diffusion, the temperatures in the steel strip are allowed to even out throughout the coil reducing hot and cold spots and allowing a more uniform temperature in the strip overall. The steel coil can also be held in the coilbox until the finishing mill is free. However, if held for too long the temperature will fall below the minimum temperature required for the strip to pass through the finishing mill, in this case, the steel strip is lost and scrapped, and this is the main motivation for Tata Steel to develop a coilbox module for their hot mill simulation software.

Another consequence of the coilbox is that the top and bottom surfaces of the steel strip are flipped as well as the head and tail switch positions due to the coiling and uncoiling processes. Figures 1.8 and 1.9 show an annotated example of the properties of the steel strip changing as it enters and exits the coilbox.
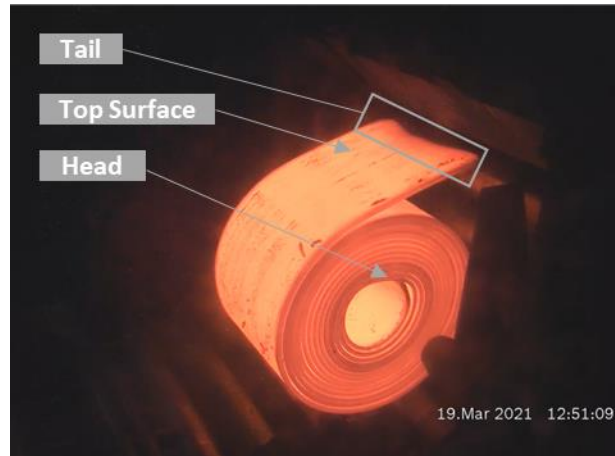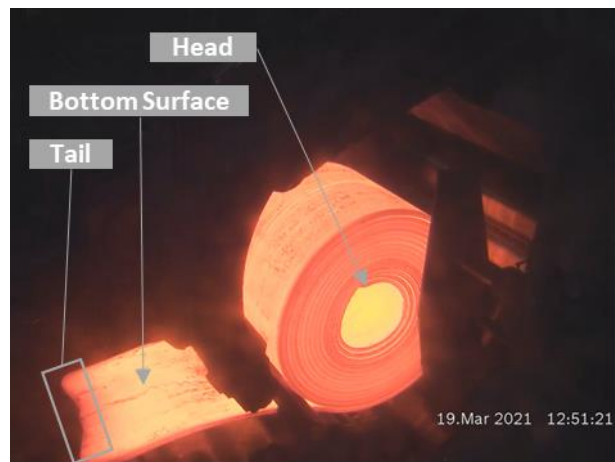
Figure 1.8 - Strip entering the coilbox.

Figure 1.9 - Strip leaving the coilbox.

1.2.1 Cradle Position

The coilbox is 8 metres in length. As the strip enters the coilbox, the coiling process begins immediately. Once the strip has been coiled, it can travel through the coilbox whilst remaining coiled. In this state, the coil may travel to three distinct positions within the coilbox depending on the set-up and conditions of strips ahead in the hot rolling process.

Figure 1.10 - Strip in cradle one

The first cradle position, cradle roll 1, is where the strip is coiled and where uncoiling begins. During the coiling process, the internal diameter of the coil is predetermined and achieved through the roller setup shown previously in Figure 1.7. Once the strip has been coiled, it may rest in cradle 1 for a specified time depending on any obstructions ahead of the hot mill. However, if there are no obstructions, or the coil has been held for the allotted time, uncoiling can begin. The outermost layers of the coil are uncoiled in this step, meaning they are coiled for the shortest duration.

Figure 1.11 - Strip in cradle two

Once the outer layers are uncoiled, the strip can move to cradle roll 2. Moving to the second cradle position allows the coiling arm and centring rolls to reset and prepare for another strip to enter the coilbox. Once in the second cradle more layers of the coil are uncoiled, in this instance, as cradle roll 2 is further into the coilbox and the layers have been coiled for longer, this section of the strip should see temperatures higher than those removed in the previous cradle. This position can be skipped in the setup of the coilbox, allowing the coil to move from cradle 1 directly to cradle 3 which is usually the case if the coil is not being held.

Figure 1.12 - Strip in cradle three

Cradle roll three is the last position of the coil within the coilbox. The coil is unable to move past this point due to the crop shear blocks. Layers uncoiled from this point will have little to no exposure to the environment as they leave the coilbox.
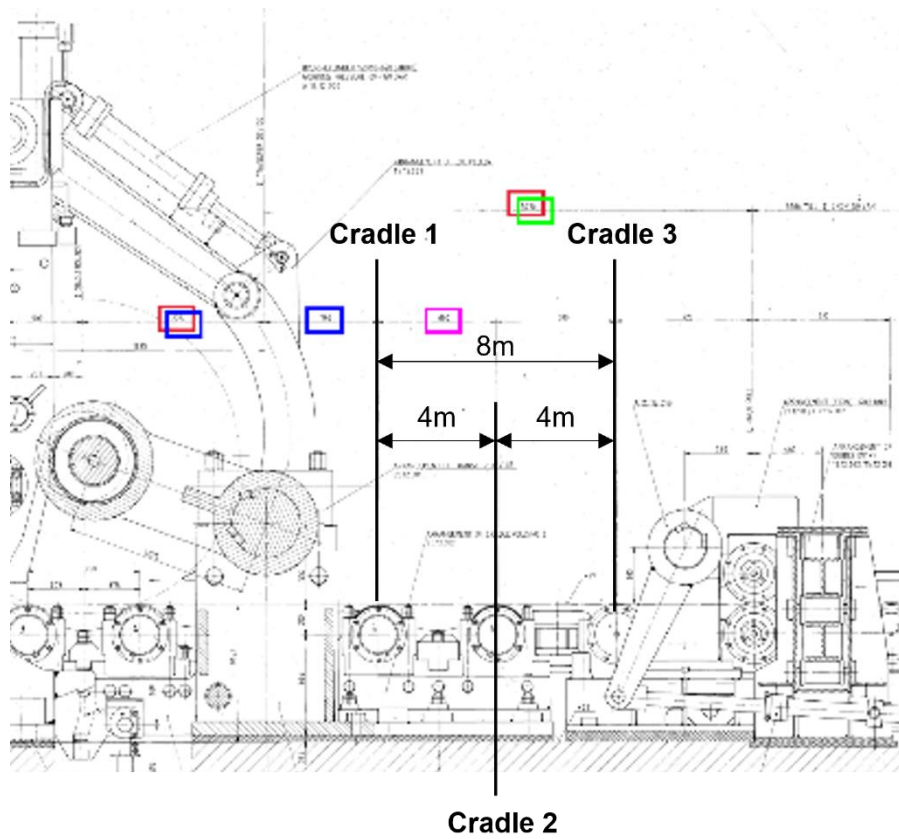

Figure 1.13 - Diagram of cradle positions along the coilbox

Figure 1.13 shows the cradle positions as well as the overall length the coil can traverse in the coilbox. The movement of the strip through the coilbox determines how long each layer of the strip is in contact with each other, therefore determining how much heat transfer occurs within the coil itself.

1.3 TiTAN Overview

TiTAN is Tata Steels' in-house developed software that is used mainly to model how steel strips will behave in the hot or cold mill. TiTAN was designed to allow for quick but accurate simulations of many strip properties at any stage of the hot or cold milling process. TiTAN can simulate many aspects of the strip such as oxidation, scale, deformation, and softening however the new coilbox module will focus mainly on temperature, radiation, position, and acceleration of the strip.
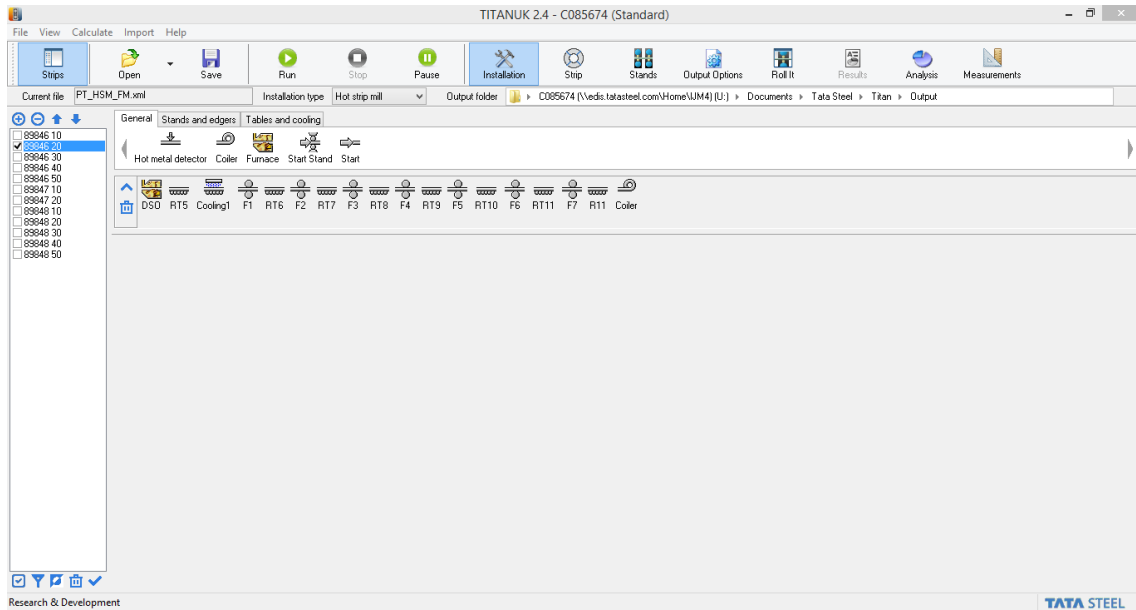
Figure 1.14 - TiTAN installation page

Figure 1.14 shows the main installation page of TiTAN. TiTAN is designed with many modules that represent different mill components. The components are free to be placed and have their characteristics modified by the user allowing any mill process to be simulated.
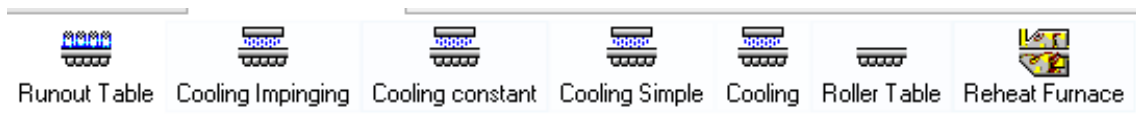
Figure 1.15 - TiTAN tables and cooling modules

Figure 1.15 shows some examples of the modules present in TiTAN. The coilbox module will need to be consistent with all the other modules present and must be compatible with other mill processes even if the mill setup may be unrealistic.

| General Properties | MetalMatrix | Scale | Transformation | Deformation | Softening | Thermal properties | Precipitation | MechProperties |

General strip properties

| Strip length [m]	10.0 m
Strip thickness [mm]	40.000 mm
Strip width [mm]	1267.0 mm
Position on strip [m]	1.00 m
Initial speed [m/s]	0.48 m/s
Initial temperature (average) [°C]	1145.0 °C
Estimated end temperature [°C]	900.0 °C
Initial surface top temperature [°C]¹	0.0 °C
Initial surface bottom temperature [°C]¹	0.0 °C

¹ = 0 means same as average temperature.

Metal properties

Top side emission coefficient [-]	0.83
Bottom side emission coefficient [-]	0.83
Initial Deformation Strain [-]	0.00

Options:

Cell distribution	Parabolic
Adaptive cell distribution	☑
Use minimum cell size	☐
Minimum cell size [mm]	0.025 mm
Number of cells [-]	55
Maximum number of cells [-]	21
Thermal calculation	☑
Convection	top & bottom
Radiation	top & bottom
Material model calculations per cell	☐
Solve transformation temperature	☐
Roll-it calculation type	None

MetalMatrix output options

Lattice	☑
Texture	☐
Metal Properties	☐
Composition	☐
Steel Phase	☐
Steel Precipitate	☐
Steel Phase Details	☐
Steel Precipitate Details	☐
Aluminium Phase	☐
Aluminium Precipitate	☐
Aluminium Phase Details	☐
Aluminium Precipitate Details	☐

Figure 1.16 - TiTAN strip properties

Another way TiTAN is flexible is through strip setups. TiTAN allows multiple configurations of strips to be simulated one after the other. Each strip has many properties that can be adjusted such as

length, speed, and initial temperature. TiTAN also allows the user to modify how it calculates the properties of the strip.
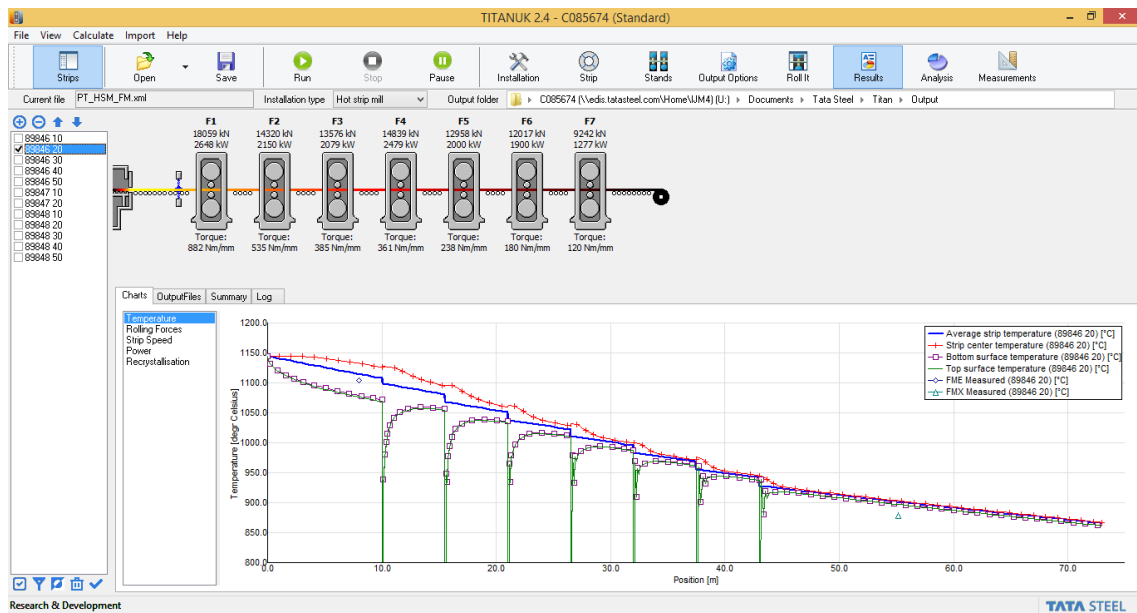
Figure 1.17 - TiTAN temperature results from the simulation

Figure 1.17 shows a typical graphical output from TiTAN. In this case, a finishing mill process was simulated with seven finishing stands. The figure shows the temperature of the strip varying as it travels through each stand and the temperature of the strip as it exits the finishing mill. This gives the mill operator an idea as to how the strip will react in the finishing process and whether the final product will emerge at the desired temperature.

1.4 TiTAN Calculation Method

TiTANs use within TATA Steel is as a quick and efficient tool to provide accurate data about the behaviour of the steel strip as it moves throughout the hot strip mill. As such, TiTAN is optimised to reduce both computational time and power required to run the simulations. TiTAN offers incredible flexibility within its simulations, allowing the user to run individual or processes in series, thereby simulating the entire hot strip process. The new coilbox module must integrate seamlessly with TiTAN by running quick and accurate simulations whilst remaining compatible with existing modules and differing strip layouts.

To do so, an understanding of how TiTAN works must be achieved. TiTAN uses the finite element method (FEM) to calculate heat transfer through conduction and radiation. As well as the deformation of the steel strip as it passes through the mill. To reduce the complexity and, in turn, computational time to run these simulations TiTAN views the strip in 1 dimension bringing down the runtime of the simulation dramatically.

TiTAN cannot simulate the entire strip and instead views the steel strip at a single point along the strip called the calculation position. At this point, TiTAN produces a 1-dimensional mesh through the thickness of the strip, this position is called the calculation position and can be placed anywhere along the length of the steel strip with the user able to adjust parameters such as the number and positioning of the nodes.
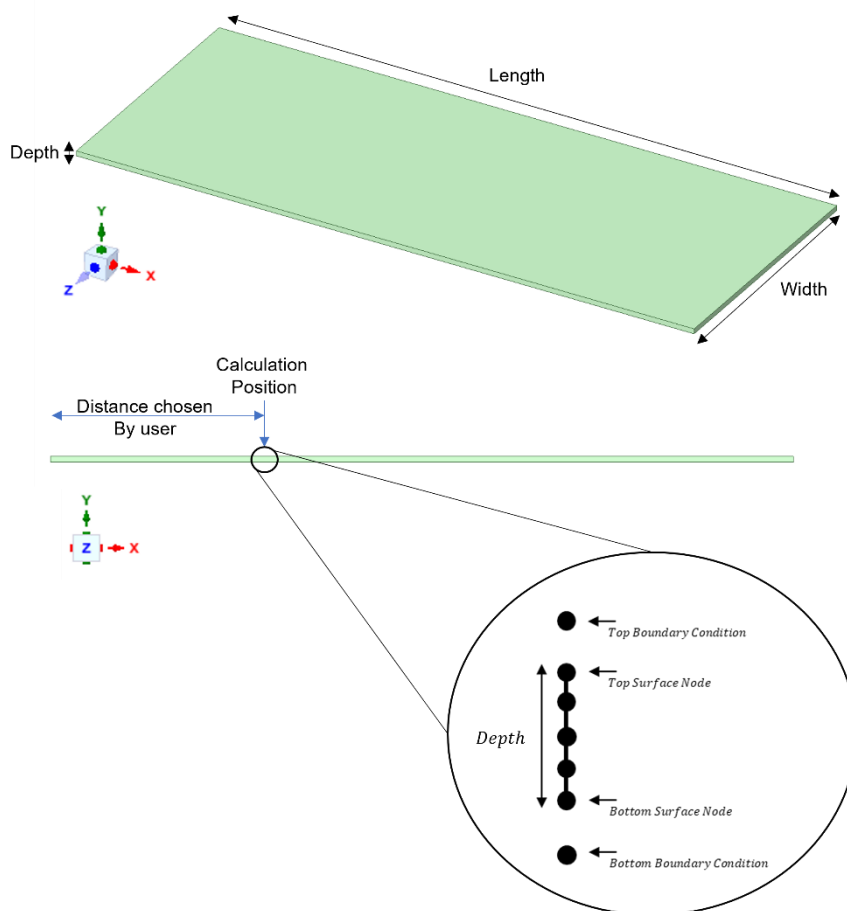

Figure 1.18 – TiTAN 1-Dimensional mesh diagram

21

Due to how TiTAN simulates the steel strip, environmental losses can only occur on two nodes, the top and bottom surface nodes. As such these nodes have special characteristics that allow them to experience radiation and convection. Although convective losses are small and can often be ignored TiTAN can account for them. The main source of environmental losses at high temperatures is through radiation and as such the most important boundary condition for coilbox level temperatures, which are around 1200°C, is through thermal radiation.

$$T^2_{Rad} = \sqrt{\frac{kA(T_2 - T_1)t}{d} + T^4_S}$$ Eq. 1. Titan Radiation Equation

Where k is the thermal conductivity (Wm^{-1}K^{-1}) of the strip, A is the cross-sectional area (m^2), T_1 is the strip temperature (°C), T_2 is the environmental (°C), Ts is the average strip temperature, t is the timestep (seconds), and d is the thickness of the strip (m).

TiTANs' simulation model assumes the steel strip is uniform through its length, meaning the properties of the steel strip at a single point may be expanded to the entire strip. However, in reality, this is not true, and as will be seen in Chapter 2, temperature can vary along the length of the steel strip.

Although this is a limitation of TiTAN, for its use, assuming uniformity makes sense as relatively small temperature differences, of around 30°C, can be disregarded. This is because, in terms of the average temperature of the strip, it is not too significant and still shows reliable and accurate data on how the strip would react in the hot mill.

TiTAN also tracks the displacement of the strip, as it moves through the hot mill. These calculations are separate from the finite element calculations used to calculate the properties of the coil. Instead, the position of the strip is calculated using its velocity and the length of the various process. Three different points are tracked along the length of the steel strip throughout its journey. The head position, tail position, and calculation position.

Most hot mills without a coilbox only move in 1 dimension, forwards, or reverse, and as such TiTAN stores its coils displacement in only 1 axis which is along the length of the mill. However, in the coilbox, the coil also moves in the vertical axis, up and down as it is coiled.

1.5   Titan Discussion

The main challenge of implementing a coilbox module into TiTAN is the lack of temperature information along the length of the steel strip. When the steel strip is coiled it is important to know the surrounding temperature of the layers above and below the calculation position. However, as the temperature of the strip is calculated at a single point, this is not something that can readily be accessed by TiTAN. Furthermore, being restricted to 1 dimension for both the thermal and positional calculations make it difficult to accurately understand all the mechanics of the process, so a 2-dimensional implementation may be investigated.

The model produced also must be able to integrate and feel like a part of TiTAN. This limits the model to use the same thermal model that TiTAN is currently using to calculate temperature losses namely the finite element method. The model must also produce outputs in the same style as TiTAN to allow for clarity within the program and ease of understanding the outputs.

In conclusion, to implement the coilbox module it is important to understand the mechanics of the coiling process, and what amount and method of heat transfer occurs to the strip when it is coiled. As well as whether representing the data in 1 dimension would be suitable for both the user to understand as well as for the accuracy of the data.

2 Plant Data Analysis

Before a model in TiTAN can be developed it is important to understand how the coiling processes affect the steel strip. Understanding how heat transfer occurs within the system and what factors affect the temperature of the coil the most allows the model to focus on the most important aspects of the coiling process concerning heat transfer.

The hot strip mill has cameras and pyrometers placed throughout each of the hot strip processes mentioned in Chapter One. This data is stored in Tata Steels data logger software and all data is made available for users to look over. However, Tata Steel produces various alloys and special steels for customers. The data logger software does not keep track of the specific alloy of steel or whether a special alloy was being milled on a particular day. Therefore, it is important to spread out the data used for the analysis. If all the data is collected on the same day, it is possible that the data would not be reflective of a general steel alloy and may be from a specific customer order.

Another attempt at gaining a representative view of the heat transfer mechanisms during the coilbox process is by choosing coils with consistent sizes. This can be done by using the coiling speed and time it takes for the strip to pass over the pyrometer to determine the length in meters. Furthermore, by using the camera to monitor the strips, only coils that formed 14 layers were chosen, meaning that each layer is in the same position for each data point allowing for direct comparisons between all data points. Figure 2.1 shows the program used with the relevant signals displayed.
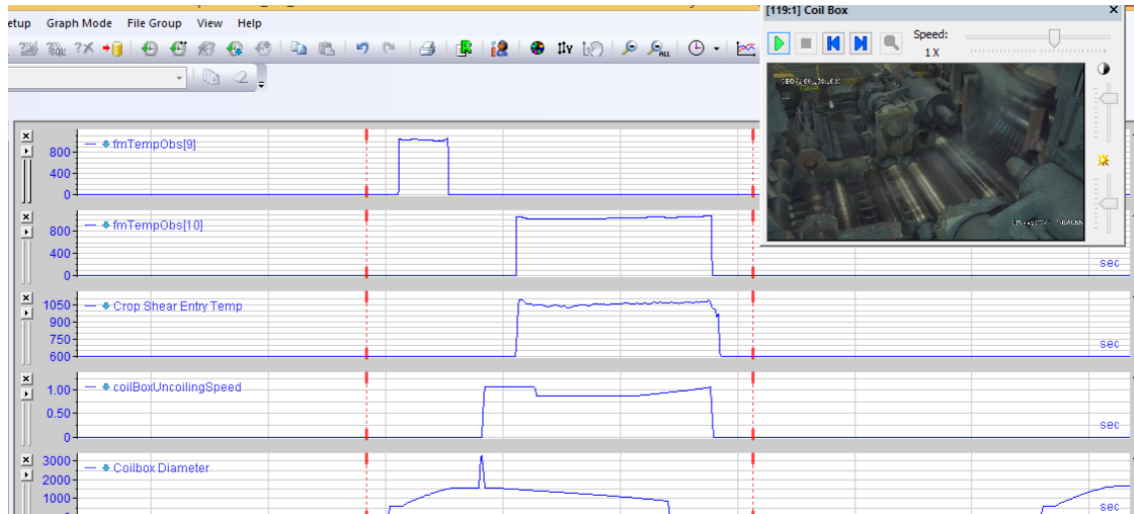

Figure 2.1 - Signal data from IBAnalyzer

2.1 Data Collection

Using the data logger software 10 datasets were gathered throughout a month from Tata Steels hot strip mill in port talbot. For each dataset, three sets of temperature data were gathered. The first temperature data point came from a pyrometer placed at the entry of the coilbox, providing an initial temperature. The second data point came from a pyrometer placed at the end of the coilbox and the entry to the crop shear, which is the next process after the coilbox, providing a final or exit temperature.
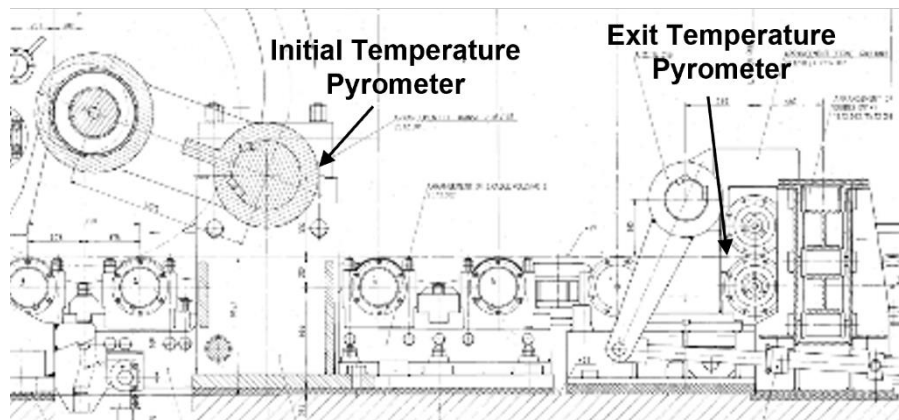

Figure 2.2- Locations of pyrometers on the coilbox

Recording initial and final temperature data allows for the delta temperatures of each section of the coil to be calculated. This would show how much heat transfer occurs between the layers of the coil, and whether the layers closer to the exposed surface of the coil would experience greater heat transfer.

To keep datasets consistent and allow for comparison the criteria for a dataset to be chosen was based on the following.

- The strip produces a coil with 14 layers.
- The internal diameter of the coils produced is approximately 0.5m.
- The thickness of the steel strips is approximately 40mm.

Following the criteria set out above allows the datasets to be consistent, allowing for comparisons and averages to be calculated from all the data gathered.

As well as the two pyrometers recording real-time data another data point was also collected. This data point also represents the exit/final temperature of the steel strip as it leaves the coilbox, however, this data point is simulated, and the temperature values are computed by an external simulation. The simulation data itself is computed by a program made by another company that works with Tata Steel and therefore this study does not have any information about how the calculations are produced. It is assumed the simulation also uses the initial temperature data from the initial temperature pyrometer as there is no other method of acquiring this data. Although the mechanics of the simulation are unknown this does provide an interesting opportunity to compare data produced by TiTAN when the coilbox module is developed and with the already present simulation of the coilbox exit temperatures.

2.2   Plant Data Preprocessing

Once the strips with comparable properties mentioned at the start of this chapter were selected the relevant temperature data was exported into Excel so they could be collated and presented in such a way that would help identify trends in heat transfer.

The raw pyrometer data, however, includes a lot of artefacts which need to be removed, to only include relevant data and increase the clarity of the data collected.
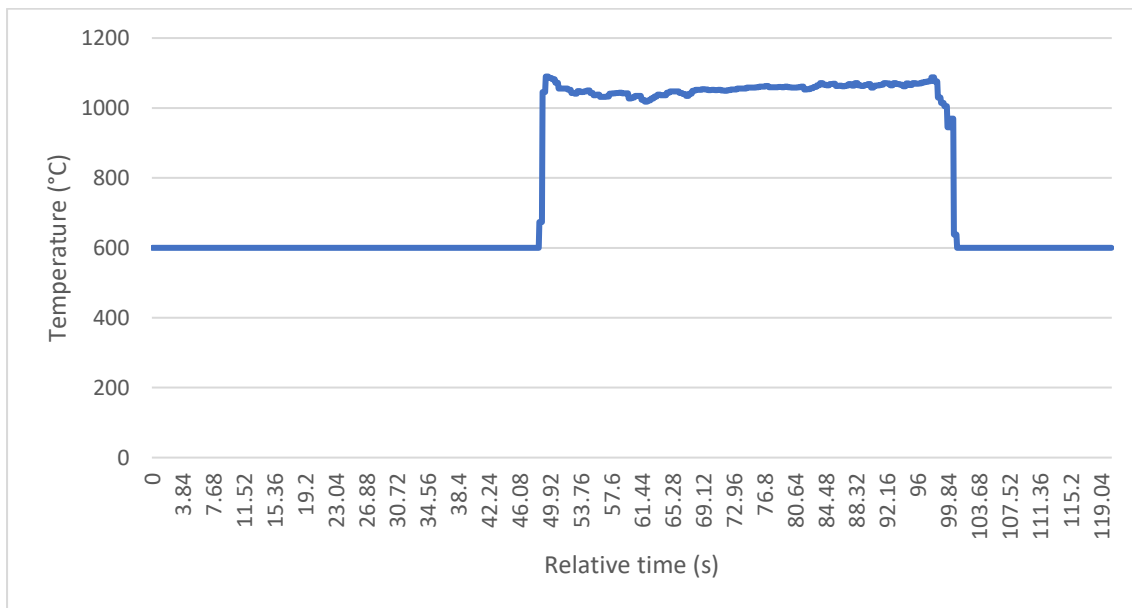

Figure 2.3 - Graph showing pyrometer exit temperature over time.

Figure 2.3 shows the raw pyrometer data from the real exit temperature of the coilbox. The pyrometer itself is calibrated at a minimum temperature of 600°C, populating fields that otherwise would be empty. The first step to refining the data is to remove all data points that are equal to 600°C.

A further issue from collecting the plant data is that as the steel strip comes into and out of contact with the pyrometer the temperature climbs and drops respectively, this can be seen in Figure 2.4 below at the beginning and end of the graph, these features make it difficult to determine the actual temperature at the start and end of the strip. This means that although the plant data is a good reference it cannot be represented as perfect data.
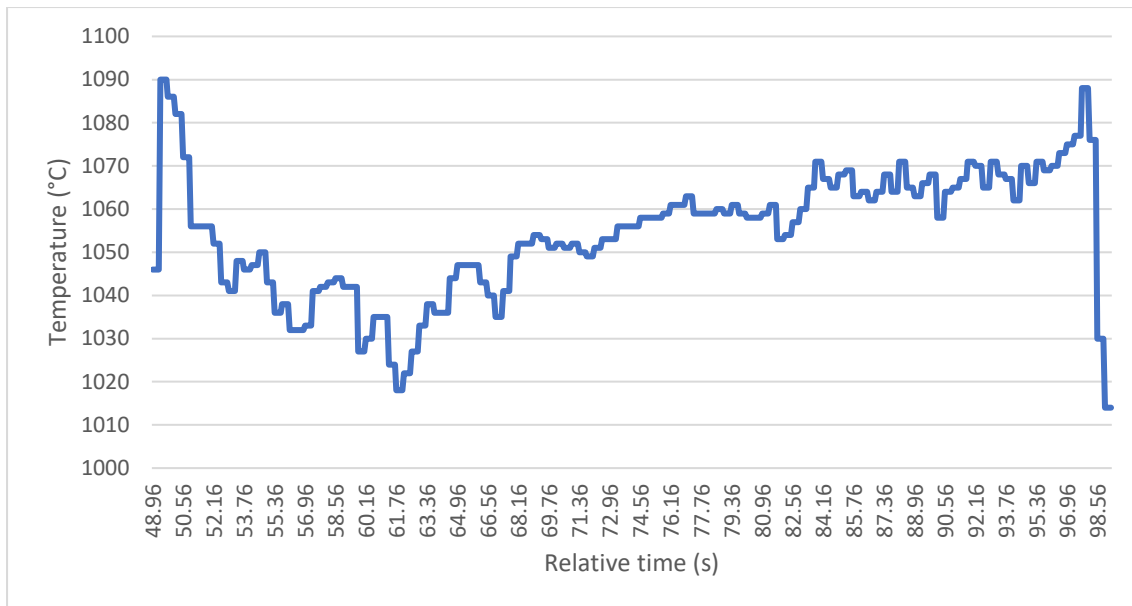
Figure 2.4 - Exit pyrometer data over time after data refinement

To minimize this impact an algorithm was written in MATLAB to identify the minimum temperature in between the two spikes caused by the strip coming into and out of contact with the pyrometer. In figure 2.4 this temperature was taken in between relative time 60.76 and 63.36. All other temperature values below this point are discarded.

Using the overall length of the strip and number of layers, it is possible to determine the length of each layer. By combining the temperature data, with its relative position on the strip, the temperature at every point along its length can be determined. These can then be averaged based on where in the coil the position lies. In this case, all points in the same layer in the coil are averaged together.

This is done to show how different layers of the coil interact with each other due to their position in the coil. The specific temperature of a point within the coil is not as important as the overall activity of the layer interacting with the others.

Table 1 - Dataset 1 average layer temps for each signal

Layer	Initial Temperature (°C)	Exit Temperature (°C)	Simulated Exit Temperature (°C)
1	1057.68	1070.26	1057.69
2	1039.36	1056.20	1070.50
3	1032.51	1048.46	1067.34
4	1033.64	1048.33	1065.80
5	1038.54	1045.67	1065.29
6	1049.55	1052.62	1066.24
7	1049.45	1043.93	1057.56
8	1040.63	1040.29	1060.17
9	1040.58	1035.42	1055.53
10	1030.61	1026.08	1051.50
11	1026.60	1020.11	1041.74
12	1021.97	1018.76	1030.84
13	1021.67	1022.19	1040.08
14	1042.10	1034.54	1059.97

It is important to note that due to how the coiling occurs when the steel strip enters the coilbox, layer 1 is the first to be coiled (innermost layer) with layer 14 being last (outermost layer). When uncoiled the layers are removed from 14 down to 1.

10 datasets in total were analysed, from different days to mitigate days when special alloys were manufactured. All the datasets chosen have coils with 14 layers, to keep strip length and thickness consistent and allow comparisons to be made between the datasets. Lastly, all the coils skipped cradle 2 moving from cradle 1 directly to cradle 3. This was done as it seemed to be the norm, and coils would often only wait in cradle 2 if there was an issue ahead on the hot strip mill.

2.3 Trends in Data

The data collected from all datasets showed consistent results, with the same trends occurring in all datasets analysed. Therefore, in this section, dataset 6 will be shown as this dataset shows the trends the clearest. All other datasets are included in the appendix.
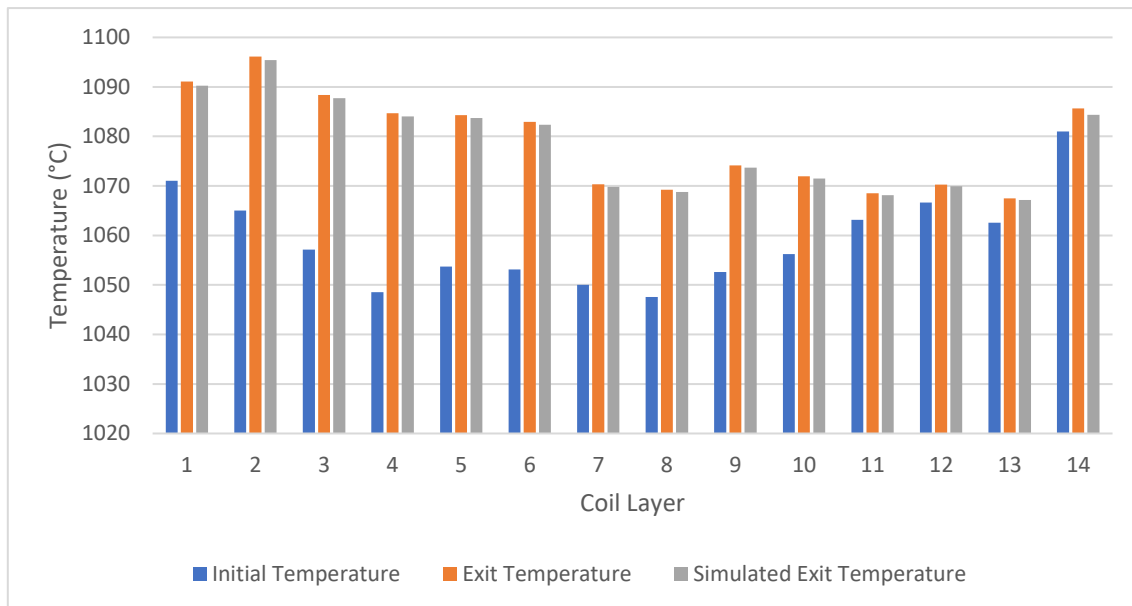

Figure 2.5 - Average temperature data per layer in data set 6

Figure 2.5 shows the average layer temperatures for dataset 6. The first and last layers show the highest initial temperatures. However, as discussed in Chapter 2.2 this could be due to the temperature spikes caused by the plates meeting the pyrometers.

Furthermore, both the real and simulated exit temperature show trends in declining temperature as coil layers increase, suggesting that the outer layers of the coil experience more temperature loss. However, the final layer again shows a temperature jump in both real and simulated which does not follow the trend of decreasing final temperature. All data sets show a rise in the final layer across all collected data points. This can be due to the pyrometer spikes as discussed in the plant data preprocessing section. To mitigate some of the uncertainties caused by this process a different method of visualizing the data was tested.
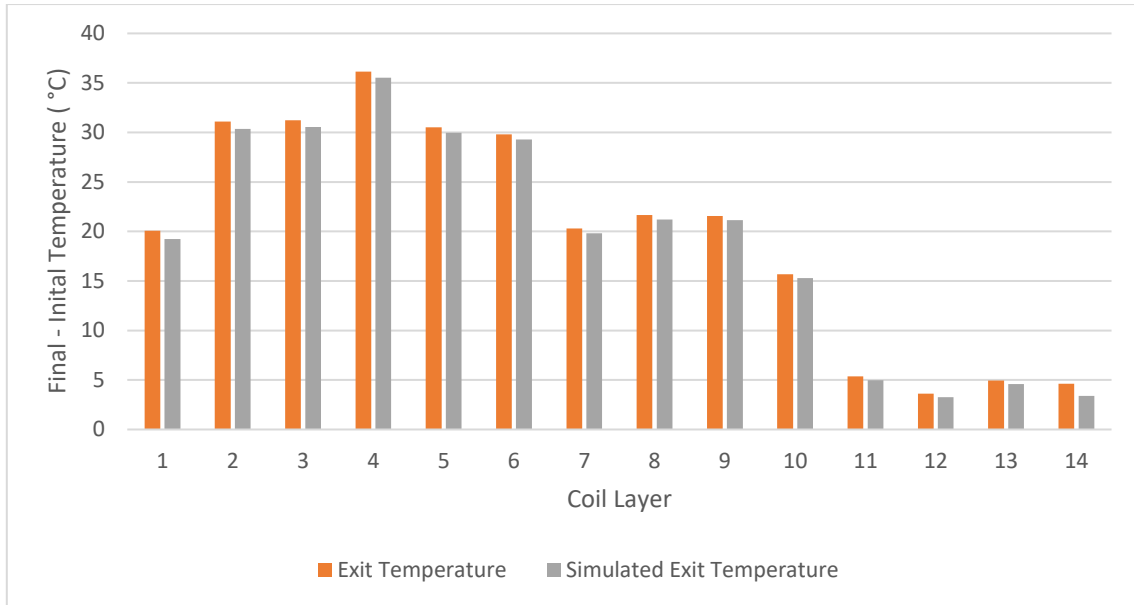
Figure 2.6 - Delta temperature per layer (final - initial) for data set 6

Figure 2.6 shows the delta temperature per layer from the coilbox process. This is calculated from the final/exit temperature subtracted from the initial temperature. This method of showing the temperature allows trends to be seen by how much each layer differs from entry to exit temperatures. This means that the spikes caused by the steel strip coming into contact with the pyrometers are taken into account and the data is independent of the overall temperature values, allowing more focus on temperature change per layer.

From Figure 2.6 the temperature trends downwards from layer 4 to layer 14, indicating that the centre of the coil is the hottest part and heat lost through radiation in this region is often reabsorbed by the coil. Another trend in the data is a temperature rise from layer 6 backwards, this can be seen clearly in Figure 2.6. This shows that the movement of the coil is especially important to the heat transfer, as the temperature rise is caused by the coil moving from cradle 1 to cradle 3 as the layers uncoiled in the third cradle were exposed to the environment for much less time, as explained previously in Chapter 1.2.1.

However, again from Figure 2.6, all the delta temperatures are positive meaning that the exit temperatures for all layers are higher than the initial temperatures. As the coilbox adds no heat to the steel strip it is difficult to explain this heat gain.
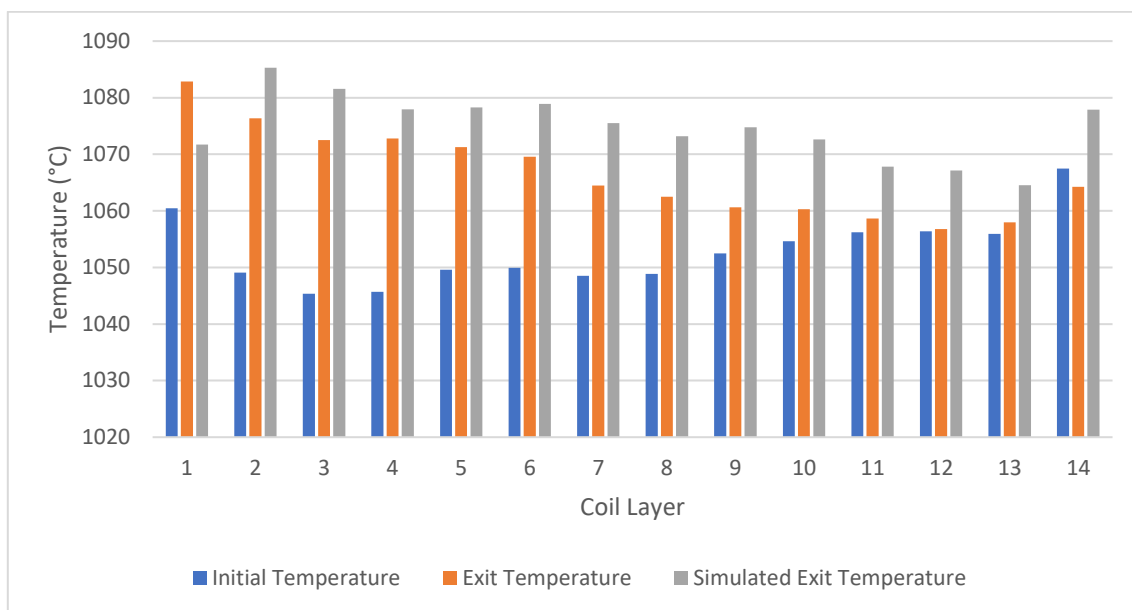
2.4   Discussion of Plant Data

Figure 2.7 - Average temperature values per layer of all data sets
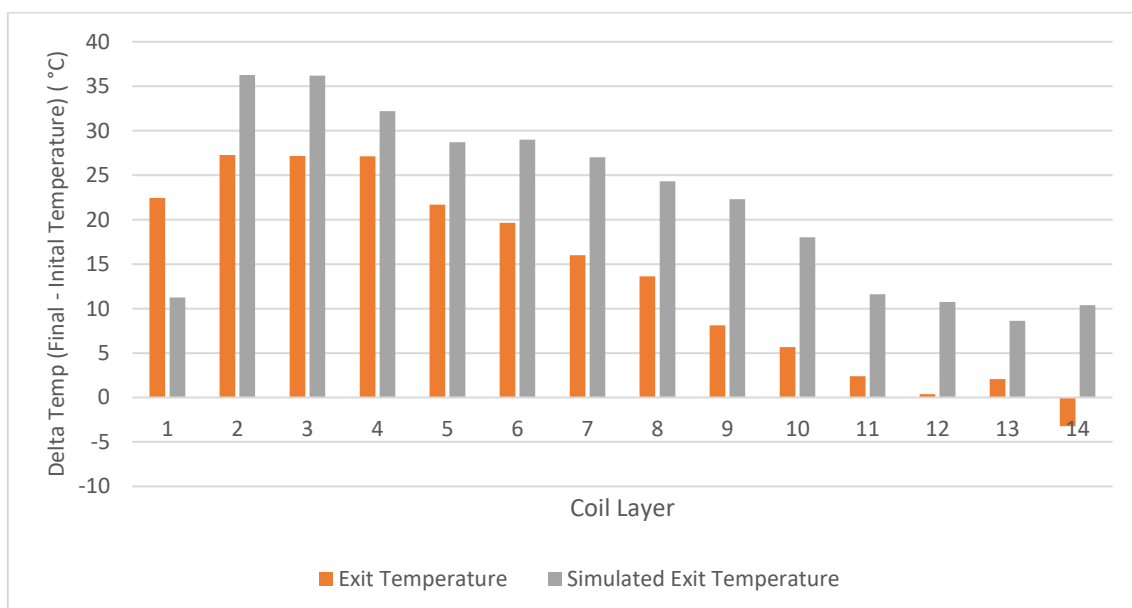

Figure 2.8 - Average delta temperature per layer of all data sets

Figure 2.7 shows the average temperatures from all 10 datasets combined and Figure 2.8 shows the delta temperatures just as Figure 2.6. Both graphs show the strip gaining heat from the coilbox process. Every dataset showed the same trend in the strip gaining heat from the coiling process. This is an issue as this is not expected to happen as there is no heat added to the coiling process.

A plausible reason for the data showing this disparity could be that the initial temperature reading is from the top surface of the strip, however as the strip exits the coilbox the top and bottom faces are

flipping, meaning that the exit temperature is taken from the bottom surface. This can cause disparities in the temperature readings but the temperature gradient of the strip through its thickness of approximately 40mm is not likely to be this great.

Furthermore, some sources of heat gain could come from the friction and work done by the metal rollers on the steel strip as it is coiled. However, although some heat and work may be generated it should not be enough to increase the temperature of the strip by up to 35°C in some cases.

Another plausible reason for the data being inaccurate can be that the pyrometers are inaccurately calibrated. A temperature gain of 35°C may not be that important in the overall hot mill process and as such it is not curial that the pyrometers be calibrated to a high level of accuracy.

2.5   Plant Data Conclusions

By allowing access to the pyrometers and internal simulation data, temperature data of the steel strip before and after the coiling process was analysed to better understand the heat transfer that occurs in the steel strip during the coiling process. Data was collected from 10 steel strips over different days with the same amount of coil layers, similar thicknesses, and similar lengths to allow temperature data to be split by layer. This gave an overview as to how each layer interacted with each other.

The data showed rises in temperature at points where the coiled steel strip moved from cradle 1 to cradle 2. The temperature rise is due to the decreased length the strip now must travel from cradle 2 to the exit of the coilbox. A reduction in uncoiled distance travelled reduces the amount of time the surface is exposed to the environment resulting in higher temperatures. This shows why it is necessary to be able to capture this movement in TiTAN, this will be looked at in more detail in Chapter 4.

Although the plant data helped uncover how the movement of the coil through the coilbox affects the steel strip temperature, the overall accuracy of the data received from the pyrometers is questionable. For each data set when plotting delta temperatures (exit temperature – initial temperature), each layer showed an increase in temperature. This is not what was expected to be seen and may be due to factors outside the control of this study, discussed in previous chapter 2.4.

The problems faced with the plant data mean that they cannot be viewed as perfect and therefore it will be difficult to prove the accuracy of the TiTAN coilbox model as the accuracy of the plant data model cannot be verified. However, there are still interesting trends and takeaways learned from the plant data that can be implemented into TiTAN. The biggest trend that can be seen is a temperature decrease as the coil layers increase, indicating that the innermost layers of the coil retain the most heat. Furthermore, the rise in temperature of layers that are uncoiled in cradle 3 as compared to cradle one is an interesting phenomenon and must be included in the TiTAN model to accurately portray the effect of the coilbox on the steel strip.

3   Modelling TiTAN in MATLAB

As Titan is a propriety software developed by TATA Steel an NDA (non-disclosure agreement) was signed before access to their software was granted. Unfortunately, there were some delays as Tata Steel Europe had been split into two different entities, Tata Steel UK, and Tata Steel Netherlands, causing delays within their legal teams.

While access to TiTAN was unavailable the project focused on developing a 1-dimensional heat transfer model using FEM developed in MATLAB. The MATLAB model would allow for a deeper understanding of how heat transfer is calculated within TiTAN, and the idea of expanding the 1-dimensional model to allow for 2-dimensional heat transfer could be evaluated in MATLAB first to decide if a similar model could integrate well with TiTAN.

The finite element method (FEM) is a commonly used method for numerical analysis [22]. Originally used for solving solid-state mechanical problems such as plate bending but has since been used in a wide variety of applications of physics and engineering, such as topological optimisation, CFD and even Biomedical research in solid-state and transient models [23]. For use in understanding TiTAN in 1 dimension, the FEM model will focus on heat transfer through conduction.

The basic concept of FEM is to split, or discretise, the problem domain into smaller parts, often called elements, thereby creating a mesh allowing the method to be applied in as many dimensions as needed. Elements are usually linear for 1-dimensional domains, triangles, or squares for 2-dimensional domains, and tetrahedra or cuboids for 3-dimensional domains. The points of contact between the elements are known as nodes. Each node forms part of a mass and stiffness matrix which are calculated using material properties from the domain, the sizes of the matrices depend on the number of elements and nodes in the domain. Boundary and initial conditions, as well as external forces, are also included as vectors. They include initial temperature of the nodes and radiation and convection conditions on certain nodes. Local solutions are found at each node and by combining the local solutions of each element and node the global solution to the domain can be calculated [24].
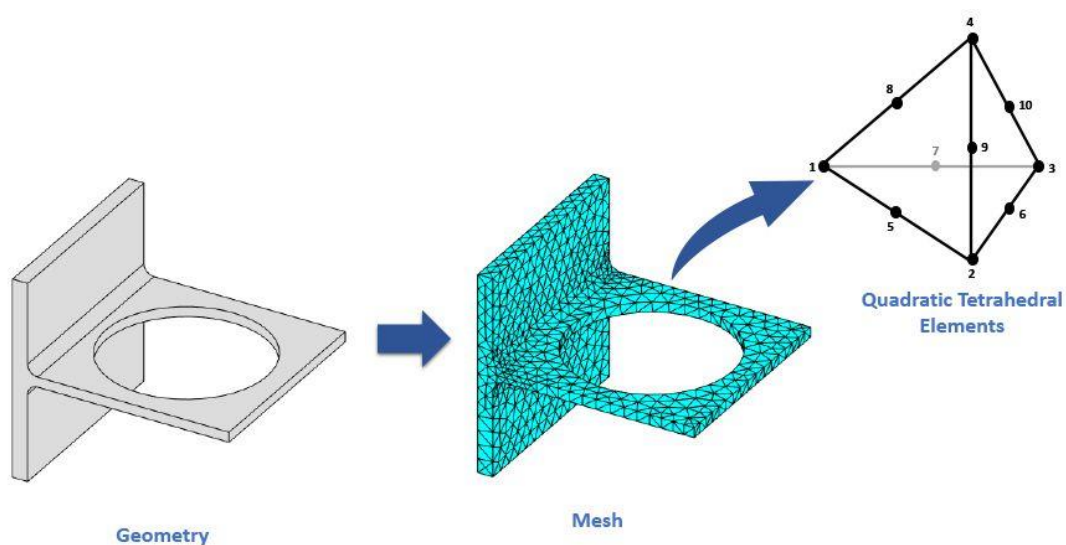

Figure 2.1 - Demonstration of FEM meshing on a geometry

3.1 1-Dimensional Conductive Heat Transfer Model

As previously mentioned in Chapter 1.4, TiTAN uses 1-dimensional FEM to model a single point along the length of the steel strip thus the heat transfer is happening vertically relative to the position and direction of the steel strip. The internal heat transfer of the strip uses a conduction model and any losses to the environment are handled by radiations models that only affect the surface nodes. In TiTANs case that means that radiative heat transfer losses only occur on the top and bottom surface nodes.

The 1-dimensional model developed in MATLAB is intended to be a representation of TiTAN, with conduction only occurring through one axis. However, the 1-dimensional MATLAB model does not look at radiative heat losses through the outermost nodes, as this section focuses on expanding TiTANs 1-dimensional model into 2 dimensions.
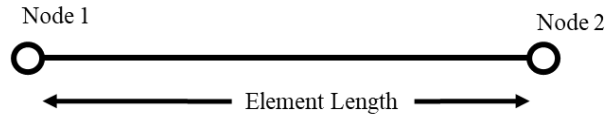

Figure 3.2 - 1 dimensional FEM element

Figure 3.2 shows a linear 1-dimensional element with two nodes labelled 1 and 2, and an element length h_e defined over the range $-1 \leq \xi \leq 1$.

The finite element approximation can be determined from the equation expressed in matrix from equation 2 shown below.

$$\mathbf{K}_e \mathbf{T}_e = \mathbf{M}_e \mathbf{Q}_e - \mathbf{q}_e \quad \text{Eq.2 [25]}$$

$\mathbf{K}_e$ and $\mathbf{M}_e$ represent the one-dimensional stiffness and mass matrices respectively.

$$[\mathbf{K}_e]_{ij} = \frac{2}{h_e} \int_{-1}^{1} k \frac{dN_j}{d\xi} \frac{dN_i}{d\xi} d\xi \quad and \quad [\mathbf{M}_e]_{ij} = \frac{h_e}{2} \int_{-1}^{1} N_j N_i d\xi$$

$$\mathbf{K}_e = \frac{k_e}{h_e} \begin{bmatrix} 1 & -1 \\ -1 & 1 \end{bmatrix} \quad and \quad \mathbf{M}_e = \frac{h_e}{6} \begin{bmatrix} 2 & 1 \\ 1 & 2 \end{bmatrix} \quad \text{Eq.3\&4 [25]}$$

As in this example there is no radiation or convection boundary conditions, and the strip is insulated only diffusion across the length of the steel strip is being modelled and therefore $\mathbf{Q}_e$ and $\mathbf{q}_e$ are equal to zero. The element vector $\mathbf{T}_e$ is given by.

$$\mathbf{T}_e = \begin{bmatrix} T_1 \\ T_2 \end{bmatrix} \quad \text{Eq.5 [25]}$$

As the temperatures vary with time during an arbitrary time interval, the problem is transient and requires time-dependent equations which can calculate the temperature at any given time interval.

Using the finite difference equation, the forward, backward, and central differences can be used as time-stepping schemes giving the θ -method (where $0 < \theta < 1$). θ allows the time stepping scheme to vary between the two extremes, if $\theta = 0$, it produces the explicit forwards difference scheme whereas if $\theta = 1$, the implicit backwards difference [7]. For Crank Nicolson $\theta = 0.5$ was used as this is proven to be unconditionally stable [17].

$$(\boldsymbol{M} + \theta \Delta t \boldsymbol{K})\boldsymbol{T}^{n+1} = (\boldsymbol{M} - (1 - \theta)\Delta t \boldsymbol{K})\boldsymbol{T}^n + \Delta t \boldsymbol{f}^n \qquad \text{Eq.6 [25]}$$

Programming the system in MATLAB gives the code.

```
K = ((A*HC)/h) *[1 -1; -1 1].
M = ((HCap*A*h)/6) *[2 1;1 2].

TempNew = M+0.5*dt*K\((M-0.5*dt*K) *TempInitial)
```

Where h is the length of an element in metres, HC is the heat conductivity of the material in W/(mK), HCap is the heat capacity in J/(kg-K), and A is the cross-sectional area in m². For all MATLAB simulations in this section, the material was assumed to be steel and as such the heat conductivity of the material was set at 45W/(mK), heat capacity of 460J/(kg-K), and cross-sectional area set to 1m².

To test how well the code works three simulations were performed in MATLAB. Each simulation has 45 nodes. The temperatures of each node are randomly generated values between 1000°C and 1200°C, the table is shown in the appendix, this was chosen as the temperature of the strip as it enters the coilbox is around 1100°C and so the simulation will deal with the temperature that is expected to be present. The simulations were run for 1, 10, and 100 seconds respectively with a timestep of 0.1 seconds.
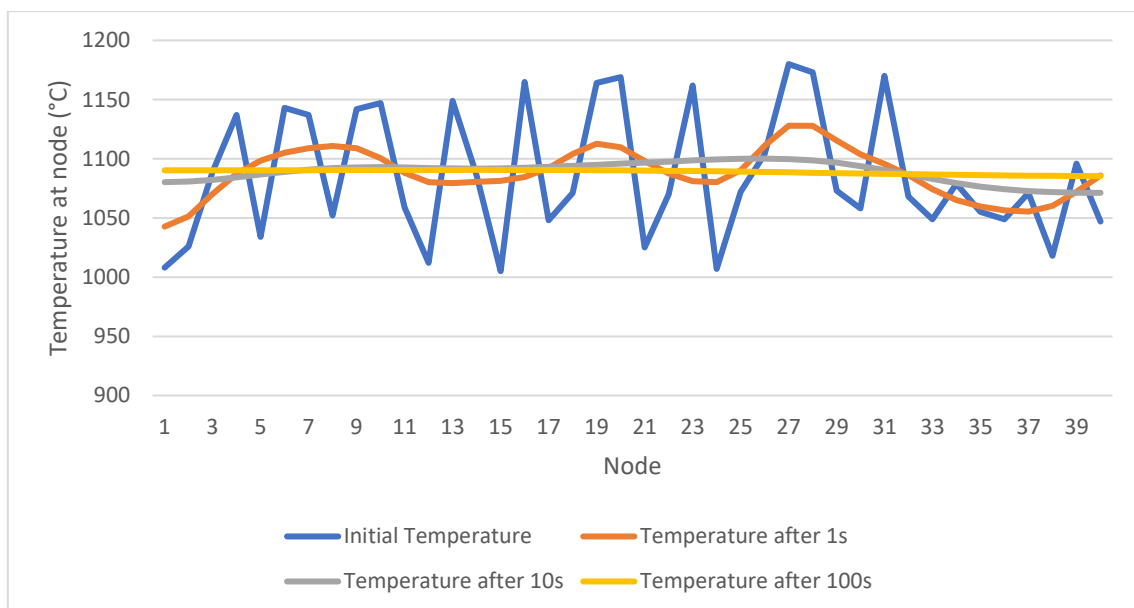

Figure 3.3 – MATLAB 1-dimensional conduction model nodal temperatures

Figure 3.3 shows the initial temperatures of each node as well as each simulation using the same initial values. The data clearly shows the conductive model working as with increasing amounts of time the values of all nodes even out to the average value of the initial temperatures. This is what is expected to be seen from a closed system with no external losses.

The timestep was changed to 0.01 to see if this would result in vastly different temperatures, however, the values were almost the same and the difference could not be seen in the graph. As such those results have not been included.

As the MATLAB model was able to show conduction in 1 dimension, the next steps were to try and adapt the model further into being able to show heat conduction in 2-dimensional space. This will give an idea as to how reasonable it would be to implement a similar model into TiTAN.
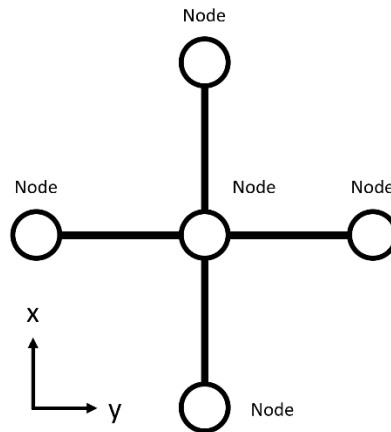
3.2 2-Dimensional Conductive Heat Transfer Model

Figure 3.4 – MATLAB 2-dimensional model mesh adaption

Figure 3.4 shows how the MATLAB model has been adapted. From Figure 3.2 it can be seen how in the 1-dimensional model a single node with 2 connections in the same axis could allow heat to travel in two directions along the same axis. Whereas the 2-dimensional MATLAB model allows each node to have 4 connections in the x and y-axis. This allows heat to be transferred in 4 directions. This would help TiTAN simulate the heat transfer to the calculation point due to the temperature of the layers above and below the calculation point.

To generate a map of node positions in a spiral with several layers, the coordinate plot of the spiral is calculated from the equation.

$$\vartheta = n * 2\pi$$

$$x = (InnerRaduis + PlateThick * \theta/(2\pi)).* cos(\theta)$$

$$y = (InnerRadius + PlateThick * \theta/(2\pi)).* sin(\theta) \quad \text{Eq.8}$$
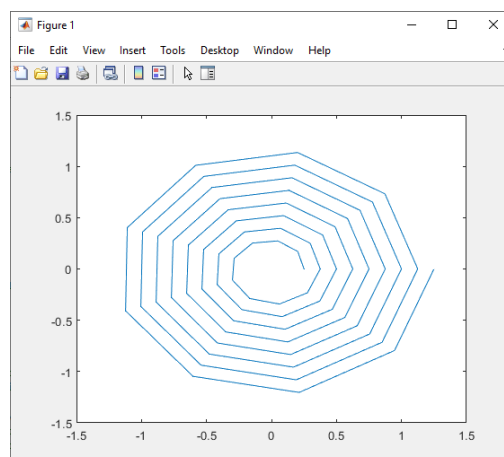

Figure 3.5 – Coordinate plot of coil

The equation allows spirals of any size to be mapped. The coordinate plot in Figure 3.5 was generated using an inner radius of 0.25, plate thickness of 0.125, and 73 nodes with node 1 being the innermost and node 73 the outermost. This was chosen as it produces a spiral with consistent node placing ensuring all nodes are in line with each other, although this is not necessary.

Using these coordinates, the mass and stiffness matrices can be calculated to place nodes above and below each other. As the dimensions of the calculations have increased so too have the matrices from 2x2 to 4x4. The finite element approximation (equation 5) is the same for a 2-dimensional element, however, the matrices increase from 2x2 to 4x4 matrices with typical entries [19-22].

$$[\boldsymbol{K}_e]_{ij} = \frac{1}{h_{xe}\,h_{ye}}\left[\int_{-1}^{1}\int_{-1}^{1} k\left(h^2{}_{ye}\frac{\partial N_j}{\partial \xi}\frac{\partial N_i}{\partial \xi} + h^2{}_{xe}\frac{\partial N_j}{\partial \eta}\frac{\partial N_i}{\partial \eta}\,d\xi d\eta\right)\right]$$

$$\boldsymbol{K}_e = \frac{k_e}{3h_{xe}\,h_{ye}}\begin{bmatrix} h^2{}_{xe}+h^2{}_{ye} & h^2{}_{xe}/2-h^2{}_{ye} & -(h^2{}_{xe}+h^2{}_{ye})/2 & -h^2{}_{xe}+h^2{}_{ye}/2 \\ h^2{}_{xe}/2-h^2{}_{ye} & h^2{}_{xe}+h^2{}_{ye} & -h^2{}_{xe}+h^2{}_{ye}/2 & -(h^2{}_{xe}+h^2{}_{ye})/2 \\ -(h^2{}_{xe}+h^2{}_{ye})/2 & -h^2{}_{xe}+h^2{}_{ye}/2 & h^2{}_{xe}+h^2{}_{ye} & h^2{}_{xe}/2-h^2{}_{ye} \\ -h^2{}_{xe}+h^2{}_{ye}/2 & -(h^2{}_{xe}+h^2{}_{ye})/2 & h^2{}_{xe}/2-h^2{}_{ye} & h^2{}_{xe}+h^2{}_{ye} \end{bmatrix}$$

$$[\boldsymbol{M}_e]_{ij} = \frac{h_{xe}\,h_{ye}}{2}\left[\int_{-1}^{1}\int_{-1}^{1} N_j N_i\,d\xi d\eta\right]$$

$$\boldsymbol{M}_e = \frac{h_{xe}\,h_{ye}}{36}\begin{bmatrix} 4 & 2 & 1 & 2 \\ 2 & 4 & 2 & 1 \\ 1 & 2 & 4 & 2 \\ 2 & 1 & 2 & 4 \end{bmatrix} \qquad \text{Eq.9 [25]}$$

This model was run with and without external boundary conditions. In the case of no boundary conditions $\boldsymbol{Q}_e$ and $\boldsymbol{q}_e$ are zero as with the 1-dimensional example. However, in the case that there are boundary conditions the vectors $\boldsymbol{Q}_e$, $\boldsymbol{q}_e$, and $\boldsymbol{T}_e$ are given by.

$$\boldsymbol{T}_e = \begin{bmatrix} T_1 \\ T_2 \\ T_3 \\ T_4 \end{bmatrix} \quad \boldsymbol{Q}_e = \begin{bmatrix} Q_1 \\ Q_2 \\ Q_3 \\ Q_4 \end{bmatrix} \quad \boldsymbol{q}_e = \begin{bmatrix} q_1 \\ q_2 \\ q_3 \\ q_4 \end{bmatrix} \qquad \text{Eq.10 [25]}$$

Similarly, to the 1-dimensional MATLAB model to test how well the code works three simulations were performed in MATLAB using the same material property values as mentioned in Chapter 3.1. Each simulation has 73 nodes, this number was chosen as the spiral it generates is very uniform with nodes in regular places other values would also work. The temperatures of each node are randomly generated values between 1000°C and 1200°C, table shown in the appendix, this was chosen as the temperature of the strip as it enters the coilbox is around 1100°C and so the simulation will deal

with temperatures that are expected to be present. The simulations were run for 1, 10, and 100 seconds respectively with a timestep of 0.1 seconds.
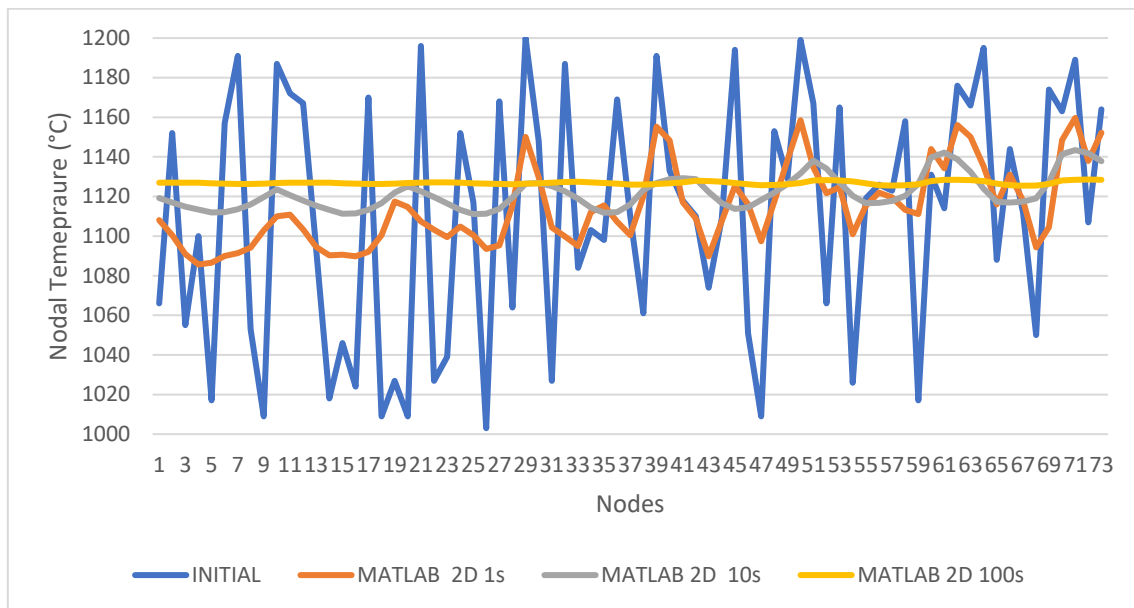

Figure 3.6 - 2-dimensional MATLAB model nodal temperatures over time(s)

Figure 3.6 shows the plot of each node temperature from the 2-dimensional MATLAB model. Again, this data shows that the system reaches equilibrium in the same way as the 1-dimensional model. However, it is not clear to see if the 2-dimensional system is working as the data looks very similar to the 1-dimensional analysis. Therefore, another test was run with all nodes at the same temperature, of 1000°C, apart from one which was set at 1500, the test was run for 2 seconds.
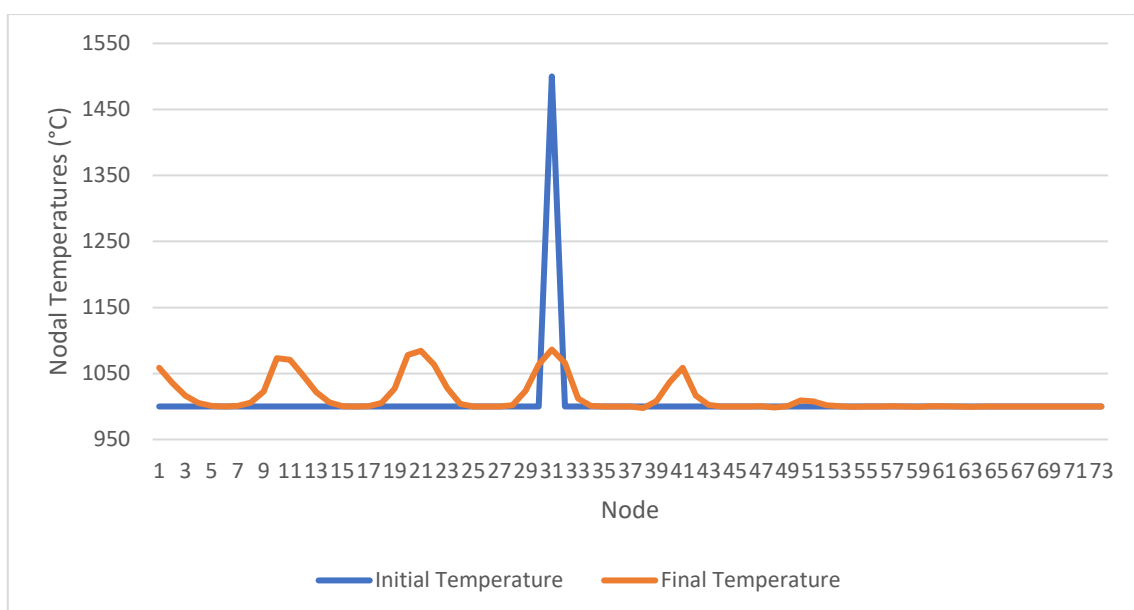
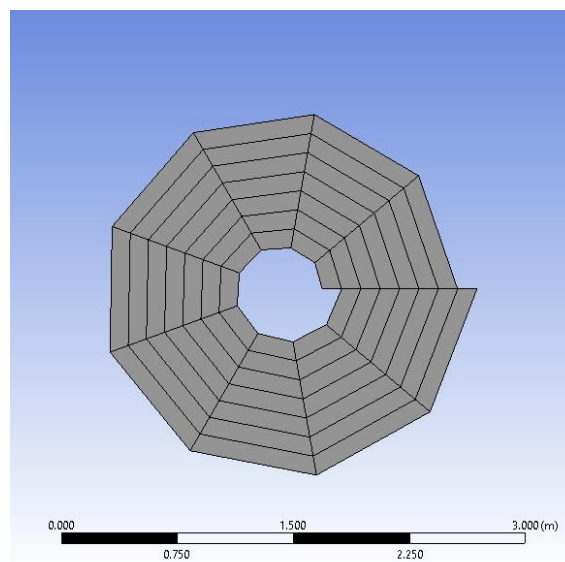*Figure 3.7 - 2-dimensional MATLAB model 2D conductivity test*

Figure 3.7 shows temperature increases at nodes above and below the peak value, as well as those immediately next to them. showing that the system is capable of 2-dimensional conduction as with 1-dimensional conduction it is expected that only nodes consecutive to the temperature peak show conduction.

3.3   Confirming accuracy of simulation

The results from both the 1-dimensional and 2-dimensional MATLAB simulation react in an expected way, with no boundary conditions and in an isolated system, the temperature diffuses until equilibrium is reached. However, to confirm the accuracy of the MATLAB simulations a replica of the 2-dimensional system will be created and tested in ANSYS to compare results.

ANSYS is a general-purpose, finite element modelling package for numerically solving a wide variety of problems. These can include static/dynamic structural analysis, heat transfer, and fluid problems [17].

Using the ANSYS transient thermal module and geometry modeller it is possible to simulate both the MATLAB model and recreate a similar model as used in TiTAN. This is a useful tool to allowing to compare the accuracy of each model. The 2-Dimensional MATLAB FEM Model was recreated in ANSYS using transient thermal models, taking care to model the mesh exactly in the same manner as the MATLAB model.

Figure 3.8 – ANSYS MATLAB mesh model

The ANSYS model uses the same number of nodes, 73, as well as the same number of elements in the same positions relative to each other as the 2-dimensional MATLAB model. The ANSYS model also uses the same initial temperatures, with the same material properties as mentioned in Chapter 3.1. The ANSYS model also had no external losses as radiation and convective heat loss models were turned off only simulating internal diffusion. The simulation was run for the same amount of time and timestep as the 2-dimensional MATLAB model.
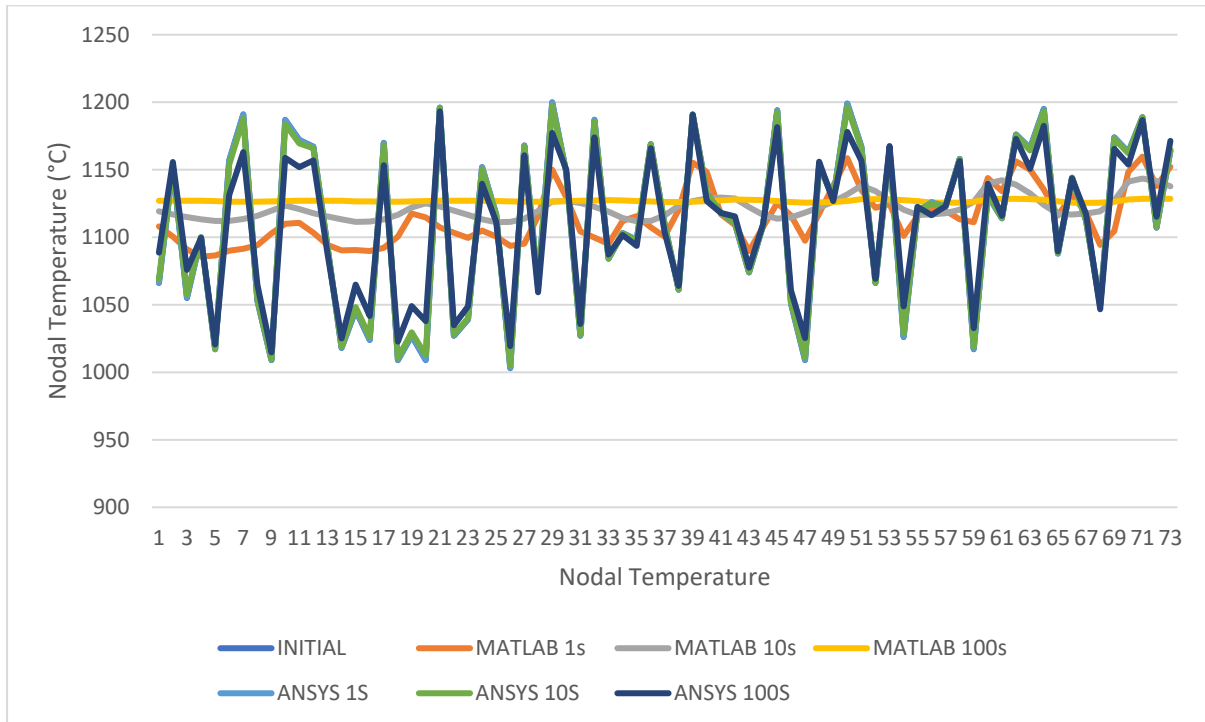
Figure 3.9 – 2-Dimensional MATLAB model temperatures compared with ANSYS model temperatures over time(s)

Figure 3.9 shows a comparison of the temperature of each node in the system at different times. From the data, it is clear to see that for each runtime the MATLAB model is progressing too quickly and showing too much conduction.

3.4 Discussion of FEM models

The finite element models developed in MATLAB intended to provide insight into TiTANs heat transfer methods. The one-dimensional model developed shows how the conduction of temperatures within a steel strip may occur. The one-dimensional model shows conduction and the system expectedly reaching equilibrium, with temperatures evening out over time.

The expansion of the model into two-dimensional FEM intended to assess how difficult it would be to implement into TiTAN and whether such a system would be beneficial in the advantages that it could provide over a 1-dimensional model. Namely, heat transfer between the layers of the coil would be possible.

The 2-dimensional system developed in this study shows how chains of nodes and elements can be connected and show heat conduction in multiple axes of movement. However, implementing the system in such a way to calculate accurate conduction over time is still challenging.

Furthermore, implementing a system that looks at the steel strip as a whole would require more user inputs to dictate the total temperatures of the steel strip. If the steel strip was to go through a previous module within TiTAN that was still a 1-dimensional model information may be lost, thereby reducing the accuracy of the 2-dimensional model.

Although it is possible to implement a 2-dimensional system into TiTAN the benefit of improved accuracy of the model would be offset by the increase in computational time and resources. As Titan is used for low fidelity, quick simulations implementing a resource-intensive model will increase simulation time.

3.5   Conclusions from MATLAB Model

This chapter looked at the possibility of expanding TiTAN into a 2-dimensional FEM model to better capture the heat transfer mechanics that occur in the coilbox. Upgrading TiTAN to be able to calculate heat transfer in 2 dimensions would allow for TiTAN to calculate heat transfer to and from layers above and below the calculation position.

Although a successful 1-dimensional model was produced and expanding the model into 2 dimensions shows heat transfer between layers. The model developed in MATLAB when compared to a comparison model developed in ANSYS showed the MATLAB model to be progressing too quickly.

Furthermore, at this stage the models were closed systems with no boundary conditions and environmental losses and with access to TiTAN finally granted, we were able to compare the MATLAB code with TiTANs programming. Although the time stepping issue could be solved and boundary conditions added to the inner and outer edges of the coil in the MATLAB model implanting such a system into TiTAN would be outside the scope of this project as time restrictions would mean that work on TiTAN would need to be started and the MATLAB code put on hold.

In conclusion, to maintain synergy with TiTAN as a whole, maintain calculation times, and due to time restrictions of the project, it was decided that the best approach would be to try and work around the 1-dimensional system already in place in Titan. As 80% accuracy with real temperature data is expected to be achieved, it should be satisfactory to modify the 1-dimensional system where needed to maintain this level of accuracy.

4   Coilbox Movement

In Chapter Two plant data analysis figure 2.6 showed how the movement of the coil through the coilbox as well as the layer position is important in determining the temperature change in the coil. The figure showed an increase in layer temperature due to the coil moving position to further cradle positions. It is essential that TiTAN can capture this information.

This section looks at the movement of the steel strip as it navigates through the coilbox. TiTAN has limited knowledge of the strip. As previously mentioned, TiTAN only performs calculations at the calculation position chosen by the user. Regarding the rest of the strip, the program keeps track of the head and tail position of the strip as it moves through different process simulation modules as a function of displacement. With the information available through TiTAN, the program must calculate how many revolutions the coil will have, the outer diameter, and within which layer of the coil the calculation point is present. Once these values are found the amount of time that the calculation point is coiled for can also be determined and the environmental boundary conditions can be applied.

Furthermore, due to the coiling process itself, the physical configuration of the strip is changed once the strip leaves the coilbox. Once the strip has left the coilbox the head and tail have swapped positions, as the head enters the coilbox first and leaves last. This extends the amount of time the head is coiled and could show a decrease in temperature loss and so must be included in the program.

4.1   Programming Movement in TiTAN

Before programming the movement of the strip in TiTAN it must first be decided what user inputs are required to allow the coilbox to perform as needed. This mainly includes coilbox specific inputs however, to keep the overall consistency and feel of TiTAN, some basic user inputs that are implemented in most modules were also included. Some key user inputs have been outlined in Table 2 below.

Table 2 - User inputs in coilbox module

User Input	Description	Units
Coilbox Length	Input overall length of the coilbox, as the coilbox in the mill has a set length this option will never be changed however as the other modules have this feature, it is included here. Any additional distance added to the length between cradle 2 and cradle 3.	M
Coilbox Passthrough	Allows the user to decide if the coil will pass through cradle 2 while being uncoiled, if selected the coil will uncoil in cradle 1 and move directly to cradle 3.	TICK BOX
Inner Diameter	This value is needed as without at least one coiling variable it is impossible to determine the number of layers in the coil overall and thus the calculation position within the coil.	M
Coiling/ Uncoiling Speed	Allows user to change how quickly the coil is coiled or uncoils, these can be two separate values or the same.	M/S
Coilbox Delay	Allows the user to simulate if the coil is held within the coilbox and how long it has been held.	S

4.2 Movement during coiling and uncoiling

The number of layers of the coil determines which cradles the coil will pass through. The movement of the calculation position is controlled by which layer it resides in within the coil. Therefore, it is important not only to calculate which layer the calculation position is in but also the total number of layers in the coil. The number of layers in the coil can be calculated from Equation 1 below.

$$n = \frac{D_O - D_I}{h} = \frac{h - D_I + \sqrt{(D_I - h)^2 + \frac{4hL}{\pi}}}{2h} \qquad \text{Eq.11 [32]}$$

Where n denotes the number of layers in the coiled strip, D_I is the inner diameter of the coil (user input), h is the thickness of the strip, and L is the length of the coil.

Replacing L with the calculation position allows the same equation to be used to calculate the layer in which the calculation position resides. The value from these equations is rounded to the nearest whole number, as the relative position of the calculation position within the layer will not impact the TiTAN simulation, rather it is more important to view each layer regarding the depth of the simulation performed. Knowing the layer in which the calculation position resides when coiled is now used to determine the length of time the position spends coiled and when it is uncoiled.

The movement of the calculation position in the coil is circular as it rotates in the same fixed position in the coilbox until the strip has been coiled. This varies from position to position, for example in a 14-layer coil, which is the average layers of a strip that was looked at in the study, the calculation position in layer 1 will rotate around the same point 14 times to allow the entire strip to be coiled, on the other hand, calculation position in layer 14 will only rotate once around the same point as it is the last layer. By knowing the layer in which the calculation position resides, and the total number of layers in the coil, using the thickness of the strip, the diameter of the circular path the point will rotate around can be determined. By combining this with the coiling/uncoiling speed the total time it takes for the position to be coiled can be determined, equation 2.

$$Coiling/Uncoiling\ Time = \frac{\pi(D_I + 2hn)}{Coiling/Uncoiling\ Speed} \qquad \text{Eq.12}$$

The movement of the strip in the coilbox must show a 2-dimensional circular movement in 1 dimension. To achieve this, equation of a spiral shown can be modified, $x(\emptyset) = R\cos(\emptyset)$. Where R is the radius of the spiral and $\emptyset$ is the angle between the x-axis and the point of the spiral. By replacing R with the coiling/uncoiling speed of the speed of the strip as its coiled can be determined, equation 3.

$$StripSpeed = (Coiling/Uncoiling\ Speed)\cos\emptyset \qquad \text{Eq.13}$$
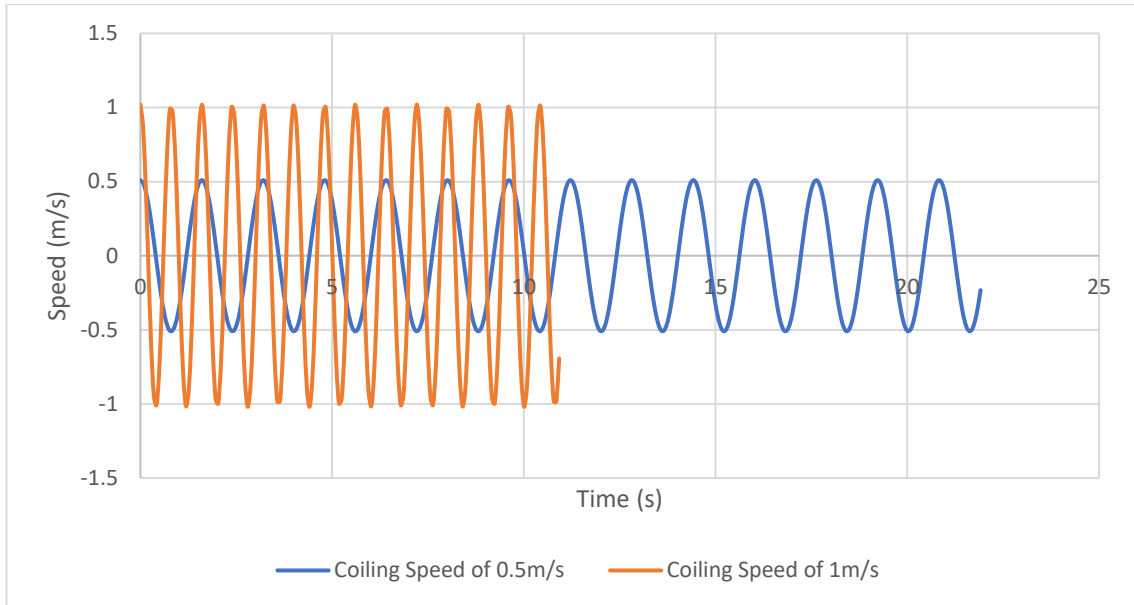
Where $\emptyset = 2\pi \cdot$ Current Timestep.

Figure 4.1 - MATLAB graph showing strip speed at 0.5m/s and 1m/s.

Figure 4.1 shows a graph of steel strip speed over time for two different coiling speeds. Both simulations used the same coil properties of a steel strip of length 25m, inner diameter of 0.5m, and strip thickness of 5mm. Both simulations had the calculation position in layer 1 of the coil and therefore experience all 14 revolutions of the coil. Using the same conditions but changing the calculation position to halfway along the length of the coil, 12.5m, would result in the calculation position only experiencing seven rotations.

The last step in programming the movement of the strip is to determine how the strip moves through the coilbox and to set the positions of each cradle. Using the schematic above the movement of the coil was split into four distinct movements. As the strip enters the coilbox the strip decelerates to reach coiling speed using equation 14

$$a = \frac{v^2 - u^2}{2s} \qquad \text{Eq. 14 [33]}$$

Where v is the coiling speed, u is the initial speed of the strip, and s is the distance from the entry of the coilbox to the cradle roll 1. Cradle 1 uses the coiling equation 2 as show above until coiling time has been reached, at which point the coil can either wait if a delay has been added or start uncoiling. The uncoiling process uses the same coiling equation as before, however when a certain number of revolutions have been completed, determined by multiplying the revolution time by the number of layers removed from the strip by uncoiling, the strip moves between cradles.

The strip moves to a given cradle at a constant speed and moves uniformly until the cradle position has been reached, either cradle 2 or 3 depending on the coilbox passthrough and layer of the coil that CalcPos is in. The current timestep is paused when this process happens so the uncoiling resumes at the point at which it stopped.
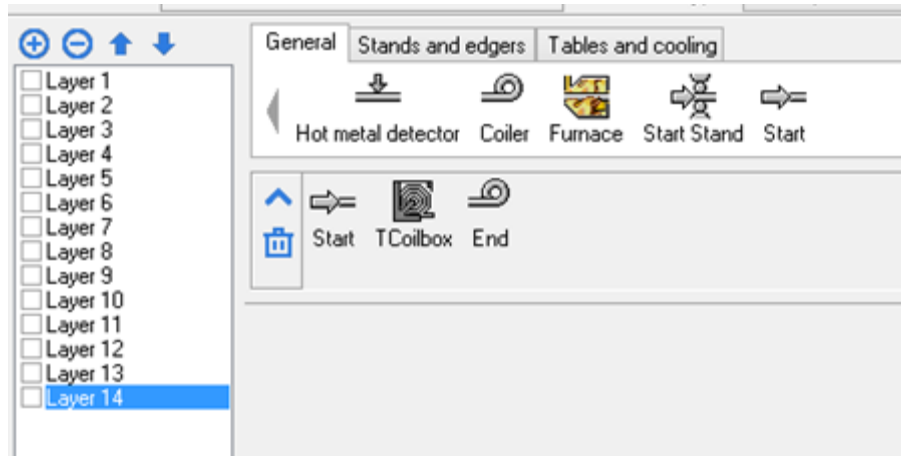
Figure 4.2 - Coilbox movement test TiTAN configuration

Once the movement mechanics had been implemented the system was tested using the setup shown in figure 4.2. The system uses a series of identical strips with different calculation positions to allow the testing of all possible locations the strip may be in. The system was tested with a strip of length 40 meters, with an inner diameter of 0.5m, strip thickness of 40mm which should give a coil with 14 layers, a coiling speed of 2.5m/s, an uncoiling speed of 0.5m/s, and a delay of 6 seconds between coiling and uncoiling. The system was tested with the coilbox passthrough on and off for each layer.

Figure 4.3 below shows the calculation position withing the strip over time for a calculation in layer 1, the innermost layer of the coil. From the graph, it shows the strip slowing down to coiling speed. Once it has reached cradle one it begins coiling. The strip then waits for the allocated time and begins uncoiling. As it uncoils it can be seen moving through each of the cradles before it leaves the coilbox. Figure 4.4 shows the speed of the same system over time. From this graph the movement of the coil can be clearly seen through each of the cradles.
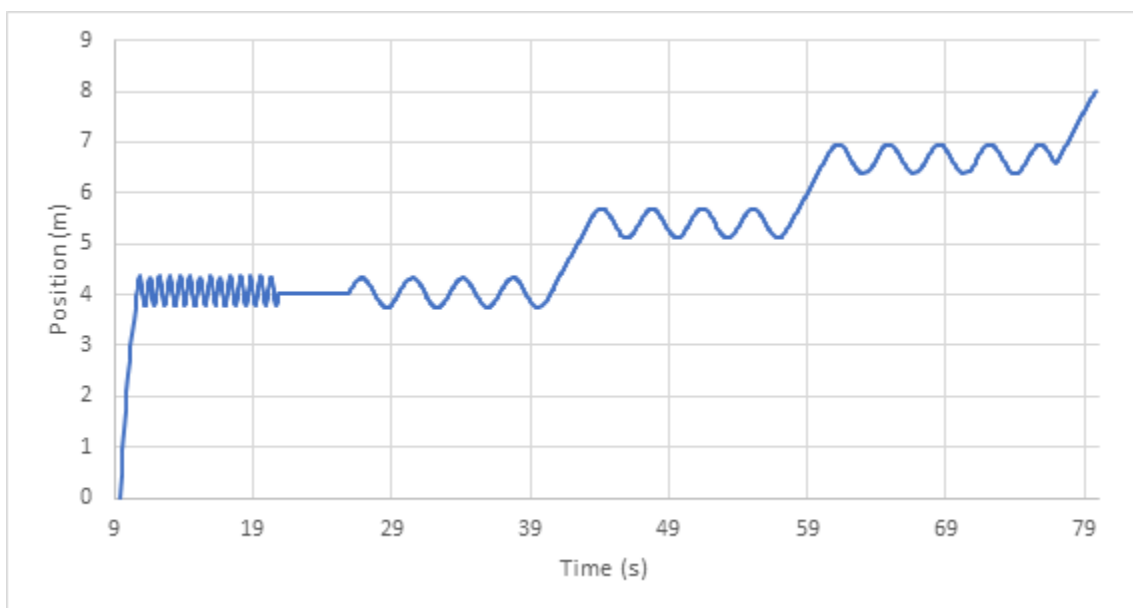
Figure 4.3 - Position of the strip in layer one over time
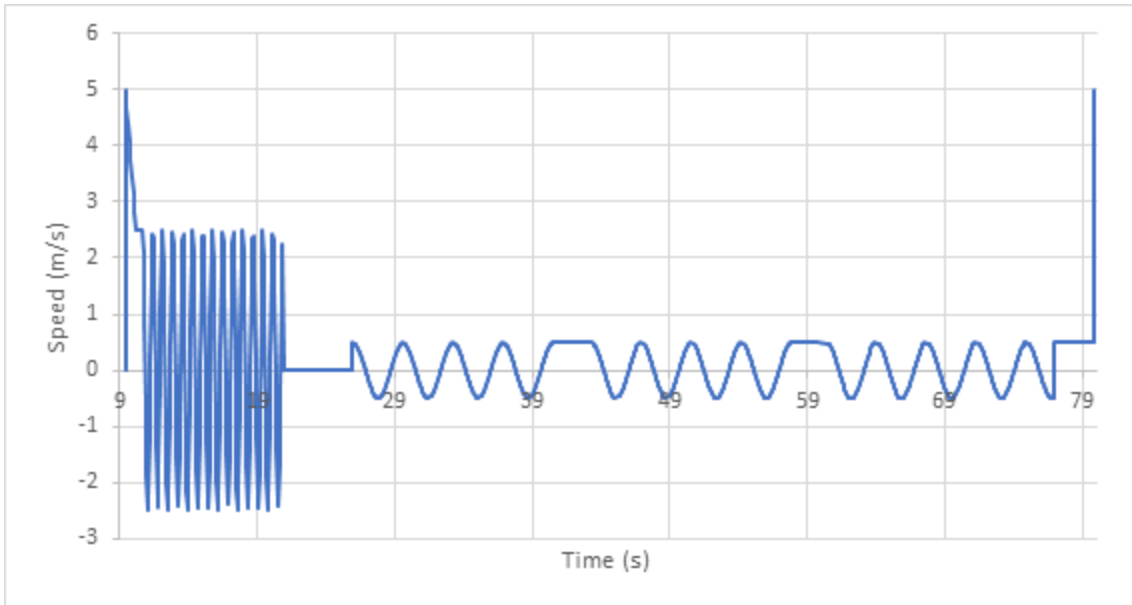
Figure 4.4 - Speed of the strip in layer one over time

The same setup as seen in Figure 4.3 was repeated with the coilbox pass through parameter set to active. In this scenario the coil would skip cradle two and move directly from cradle 1 to cradle 3, Shown below in figure 4.5.
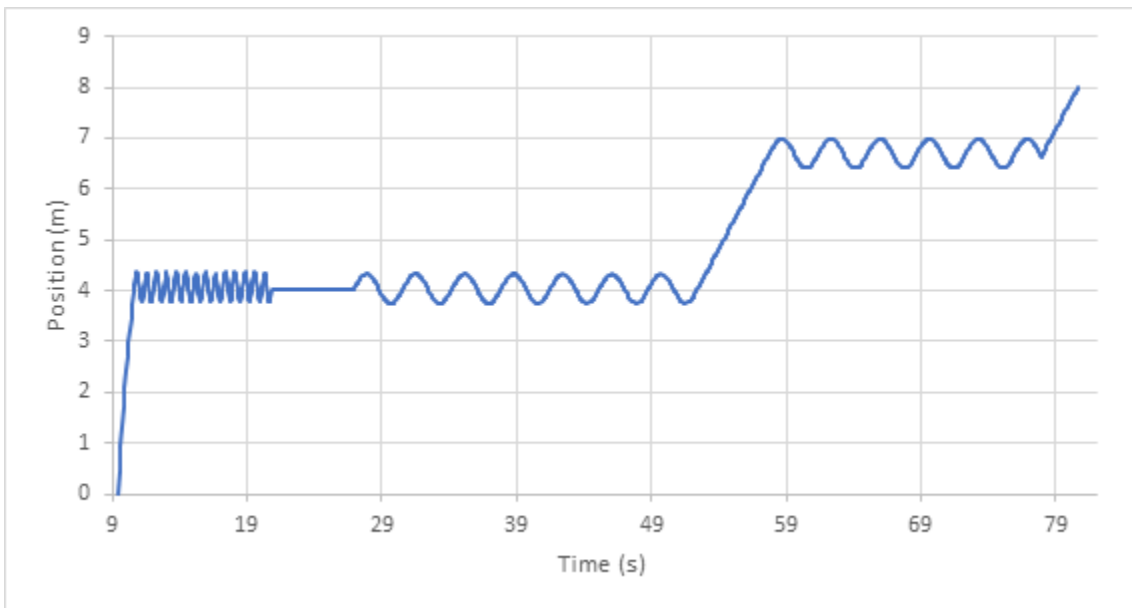
Figure 4.5 - position of the strip in layer one over time, with coilbox passthrough.

4.3   Strip Properties

To change the physical properties to the strip, such as the head and tail switching, as well as the steel strip flipping sides. It was determined that the best approach would just be to override these values in TiTAN as needed. The method used to overwrite these values is shown in the pseudo code below. During the coiling process, once the strip begins coiling the head, tail, and calculation position of the strip are updated to reflect the strip going through the coiling process.

$$\text{Head Store} = \text{Head Position}$$
$$\text{Tail Store} = \text{Tail Position}$$
$$\text{Calc Store} = \text{Calc Position}$$
$$Tail\ Position = Head\ Store$$
$$Head\ Position = Tail\ Store$$
$$Calc\ Position = Tail\ Store - Calc\ Store$$

Another process that occurs in the coilbox is the strip surfaces being flipped, during this process it is important to not only flip the surface cells but the corresponding inner cells also. The cell flip occurs after the coil has finished coiling and before the coil waits or is uncoiled.

$$SurfaceCellStore = SurfaceCell[Top]$$
$$SurfaceCell[Top] = SurfaceCell[Bottom]$$
$$SurfaceCell[Bottom] = SurfaceCellStore$$
$$i = Number of Cells$$
$$n = 0$$
$$while\ i > {number\ of\ cells}/{2}$$
$$\quad i = i - 1$$
$$\quad CellStore = Cell[n]$$
$$\quad Cell[n] = Cell[i]$$
$$\quad Cell[i] = CellStore$$
$$\quad n = n + 1$$

4.4   Conclusion of Coilbox Movement

This Chapter looks at implementing the movement of the calculation position through the coilbox into TiTAN in such a way where it is clear to the user what is occurring how the calculation position is moving through the coilbox.

TiTAN views movement and thermal calculations separately and therefore the movement of the coil can be implemented before the heat transfer equations are modified. TiTAN is able to understand what layer the calculation position is in during coiling and uncoiling, as well as knowing what cradle and how long the calculation position is coiled for. This allows different boundary position to be applied depending on position. TiTAN can apply an environmental boundary condition if the calculation position is on the outer on innermost layer of the coil as well as when it is uncoiled. Furthermore, different boundary conditions can be applied depending on if the calculation position is coiled between two layers.

5   ANSYS Modelling

Chapter 2 analysed some plant data, extracted from TATA Steels plant at port talbot, of the strip temperatures before and after the coilbox. However as mentioned in Chapter 2 plant data discussion. The accuracy and reliability of this data is questionable.

Therefore, to provide another datapoint and to verify the trends in the data. An ANSYS model of the coil was produced. Given the initial temperatures of each coil it is possible to simulate each dataset in ANSYS. This will provide another set of information as to how the layers of the coil interact with each other, as well as if the trends seen in the plant data are also seen in the ANSYS model.

5.1   ANSYS Plant data model

To reduce simulation time and computational power in preparation of programming the model into TiTAN steps were taken such as dimensional analysis, mesh refinement, and confirmation of modelling assumptions in the ANSYS. As the model would be used to help TiTAN development and as the material properties of the strips from the datasets are unknown the model was based on the default material properties TiTAN assigns to materials. As such all ANSYS models will be based on the same material properties of density 7414.3 kg/m³, Thermal Conductivity of 30.054 W/m.°C, and Heat Capacity of 658.23 J/kg.°C

5.1.1   Simulation Dimensional Analysis

The first model made was a representation of TiTAN in 1 dimension with a series of strips one above the other, this is most like how the model would have to be developed in TiTAN (figure 5.1). The model was produced with 14 layers stacked above each other, with each layer having an average thickness of 40mm. This is in line with the plant data collected.
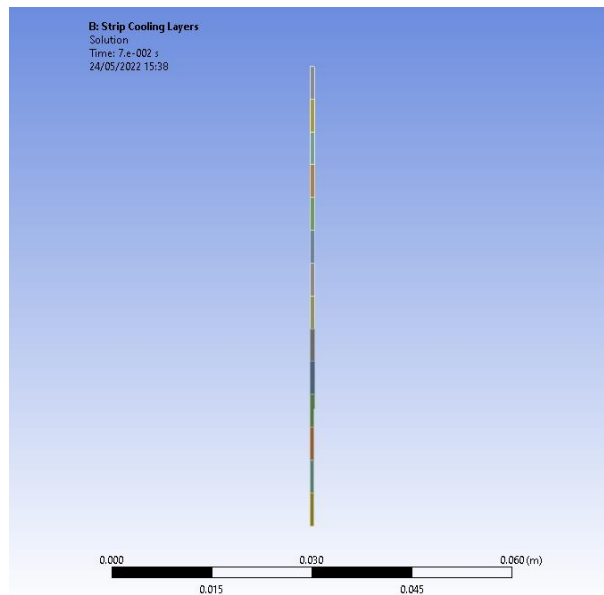
Figure 5.1 - 1 Dimensional representation of coil with 14 layers

The second model developed was a 2-dimensional representation of the coil (figure 5.2). This representation is more realistic than the 1-dimensional representation, as in the 1D model there is no way to accurately capture the varying surface contact areas between layers. In the 1D model it is impossible for it to know whether the plates stacked on top are plates or cylinders. This therefore does not account for the increased surface area the outermost layer would have compared to the inner layers. The 2-dimensional coil has an internal diameter of 0.5m and the same layer height as the 1 dimensional and plant data. The 2D model was developed using concentric cylinders rather than a spiral as the geometry of the simulation would be made easier, and as the purpose of the model is to determine how each layer interacts with each other, it is only important that the layers are in contact with each other.
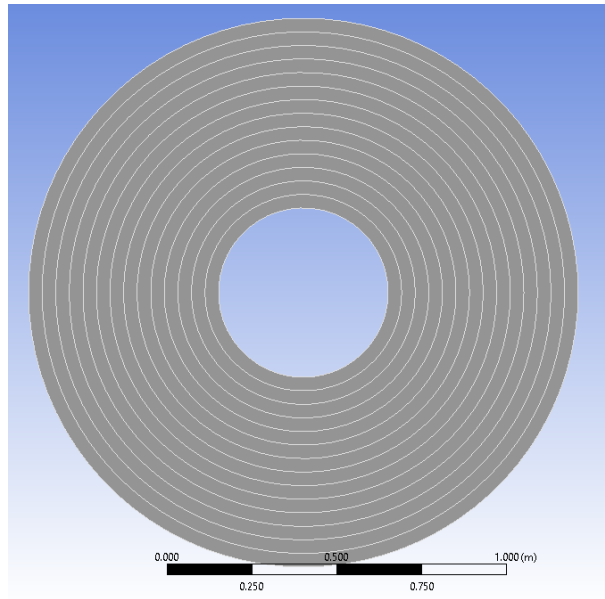
Figure 5.2 - 2-Dimensional representation of coil with 14 layers

Lastly a 3-dimensional model was made by extruding the 2-dimensional model in the z axis, this should represent the plant data most accurately and should give the most accurate comparison to real world data (figure 5.3). The 3-dimensional layer has a depth of 2m which again is accurate to plant data.
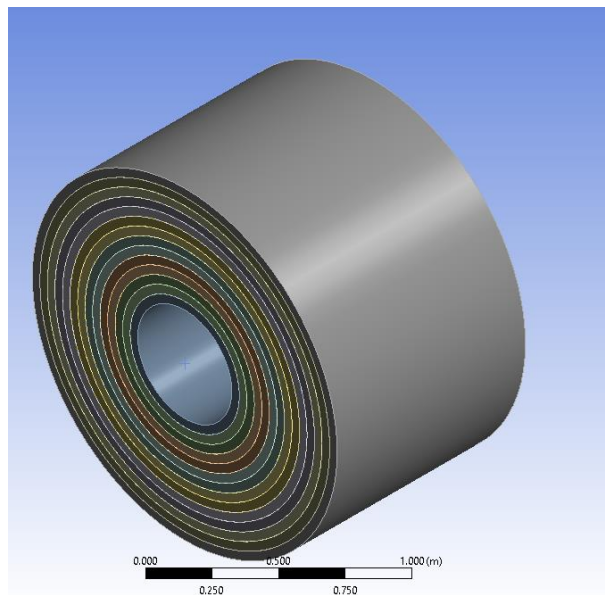
Figure 5.3 - 3-Dimensional representation of a coil with 14 layers

All three simulations had the same boundary conditions applied. With initial temperatures of 1200°C, convection boundary condition applied to the inner and outer most faces/edges with a film coefficient of 10.161e-005 W/mm^2, Radiation to ambient with emissivity of 0.82, and ambient temperature of 20°C. A surface-to-surface radiation model on the inner wall was added to the 2D

and 3D models where it is possible for the innermost layer of the coil to radiate back to itself. All simulation were run for 600 seconds to allow sufficient diffusion and heat losses to occur.
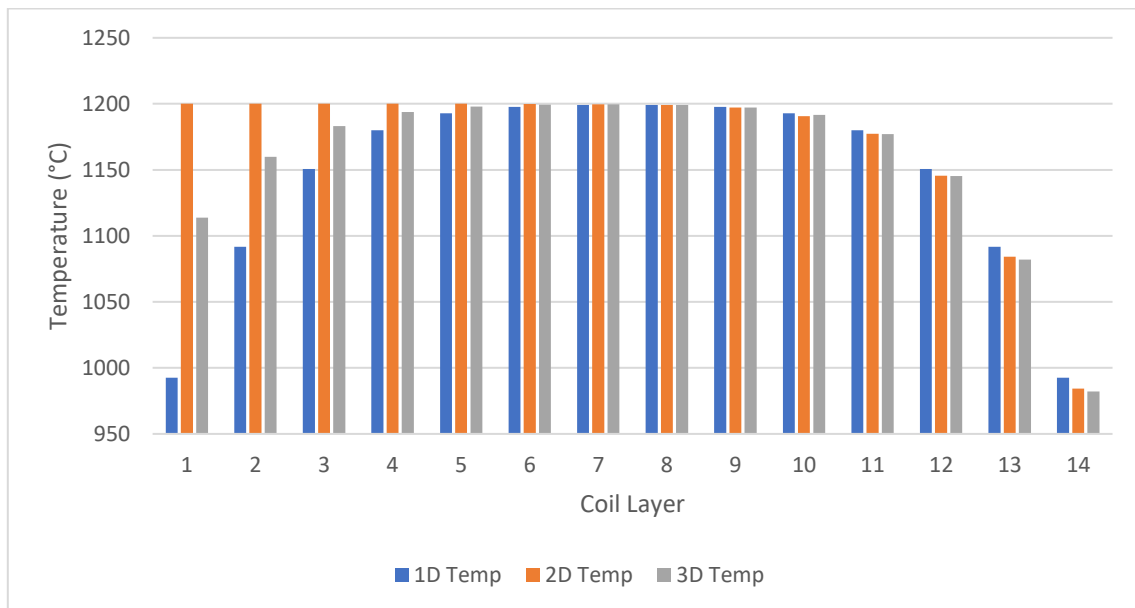
Figure 5.4 - Temperature per layer of each ANSYS model
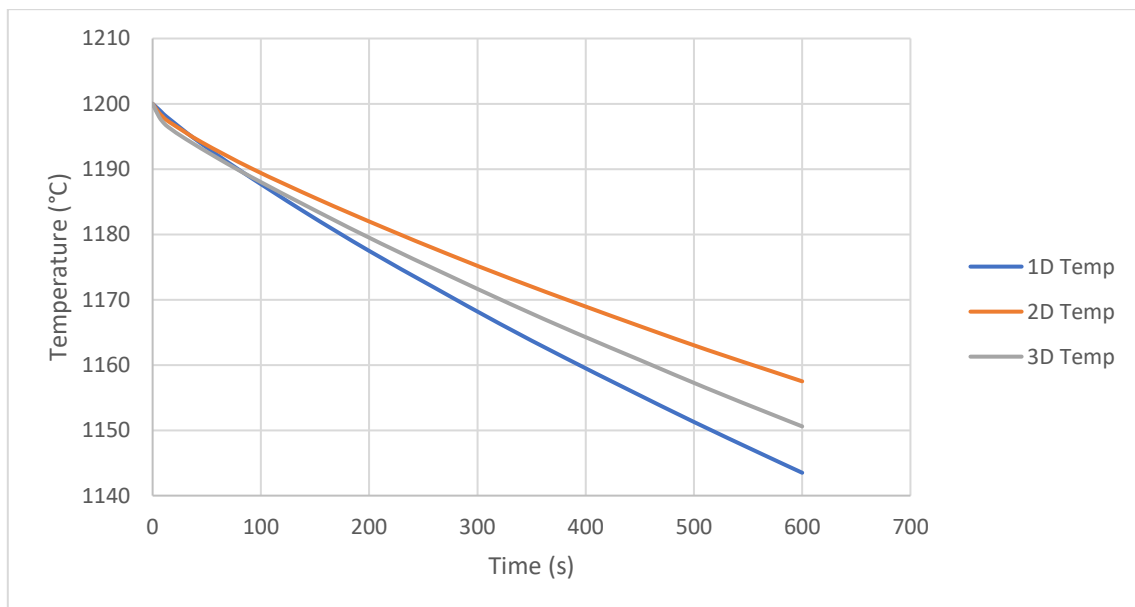
Figure 5.5 - Overall coil temperatures over time

Figure 5.4 shows the end temperatures of each layer of the simulations, from the graph 1-dimensional and 3 dimensional models lose too much heat at the innermost layers, from plant data it is known that this is incorrect. This is due to the 1-dimensional model not having an opposite surface to radiate to and from. The 3D model also shows temperature losses in the inner layer however the cause of this is uncertain. This can be due to the radiation boundary conditions in the

3D model are more affected by the ambient temperature in the simulation as the surface areas emitting radiation increase, however chapter 2 states that the plant data has inaccuracies in the head and tail of the coil as it comes into and out of contact with the pyrometer. Therefore, the 3D model may show more accurate temperature data although there is no real of verifying this information within the scope of this study.

As the 2dimensional model aligns the most with the plant data in terms of trends shown, as well as its simplicity allowing simulation to be run quicker it was chosen to be the main simulation chosen for the analysis.

5.1.2   Modelling Assumptions

Before modelling it is important to understand the scope of the simulation and how accurate it needs to be. For TiTAN's use case it is desirable to be above 80% accuracy of the plant data, as TiTAN is not used to produce accurate models but rather to determine how the strip will behave in the mill, so it is not necessary to produce models that are extremely accurate. Therefore, some assumptions about the heat transfer analysis can be made which will optimise the modelling process and reduce computational costs in the final TiTAN model developed if it can be shown that these assumptions still produce accurate results.

Figure 5.6 - strip after being coiled in coilbox.

Some numerical assumptions are reasonable and do not necessarily need to be validated such as representing the coil as several concentric cylinders with the same thickness. However, although the model does not need to be extremely accurate, it must be a reasonable representation of the heat transfer process in the coilbox, and so assumptions were tested by comparison to models in ANSYS.

The 2-Dimensional model that works well as mentioned in the previous section was chosen to represent the coil. Before undertaking any simulations, a mesh refinement study must be undertaken the results of the simulation are accurate and not dependant on the mesh.
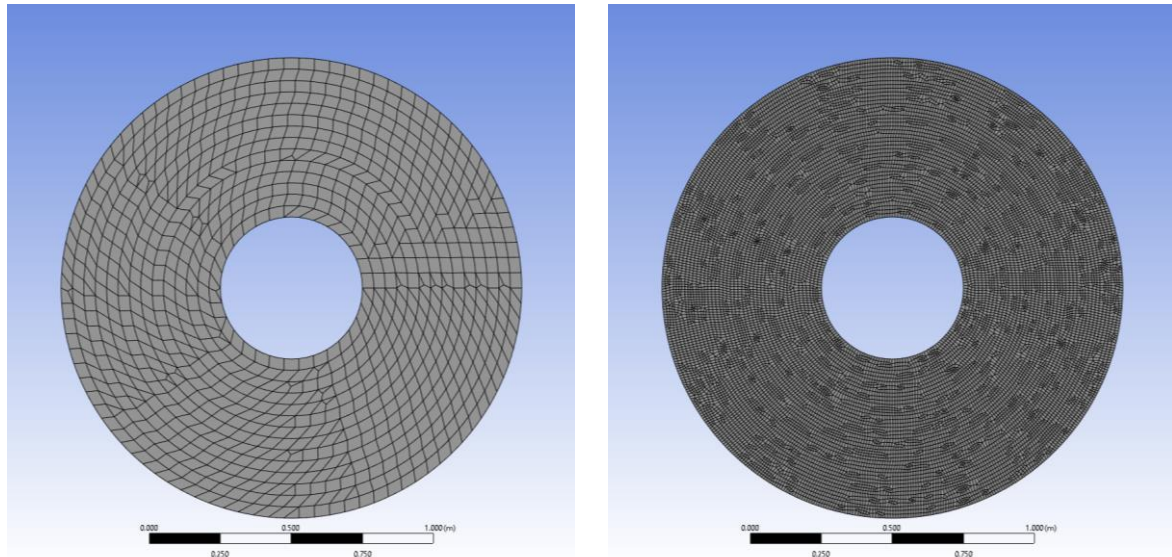
Figure 5.7 - 2D coil with default meshing (left) and higher resolution default meshing (right)

Using the default and increasing the mesh resolution, which allows smaller elements and increases the overall number of nodes in the geometry, gives a messy mesh that has no order, and as such will probably not be accurate as elements may have different number of nodes attached and/or the density of the elements may vary across the face of the geometry (figure 5.7). Each mesh was tested with the same boundary conditions as mentioned in Chapter 5.11.
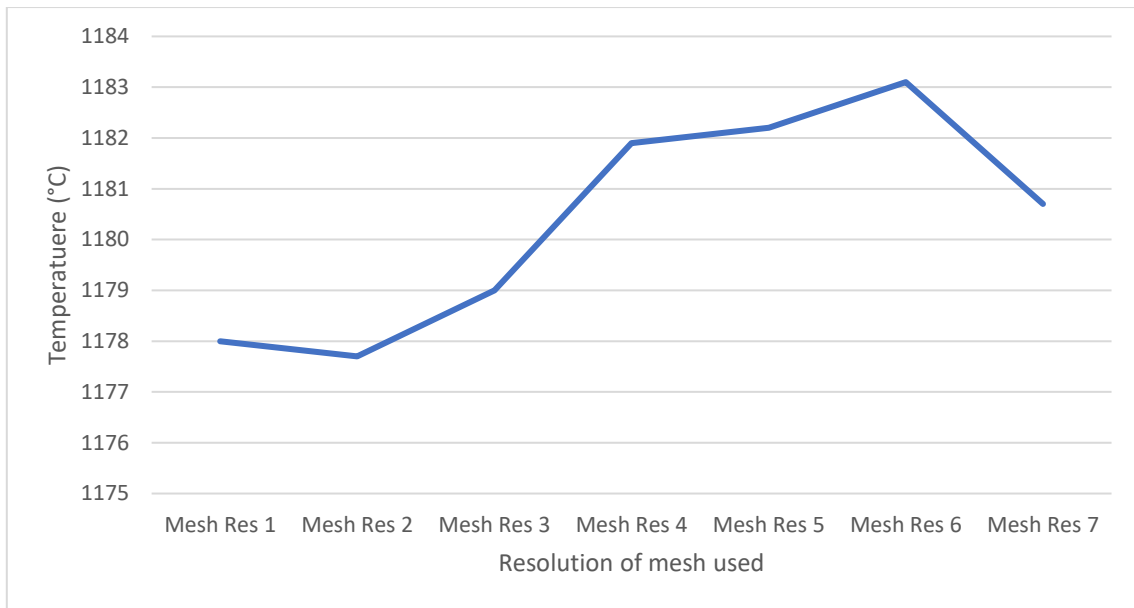
Figure 5.8 - Final temperature of coil with increasing mesh resolution

As the density of the mesh increases, the amount of calculation and computational resources required also increase, which in turn can increase the accuracy of the model. However, due to diminishing returns, at a certain point increasing the density of the mesh increases the calculation cost but does not provide enough increase in accuracy to warrant its use. Therefore, during mesh analysis, the resolution of the mesh is increased incrementally until, in this case, temperatures converge. Figure 5.8 shows a plot of final temperatures for each mesh tested and convergence can be seen around mesh 4 to mesh 6, therefore standard mesh with refinement 5 would be suitable.
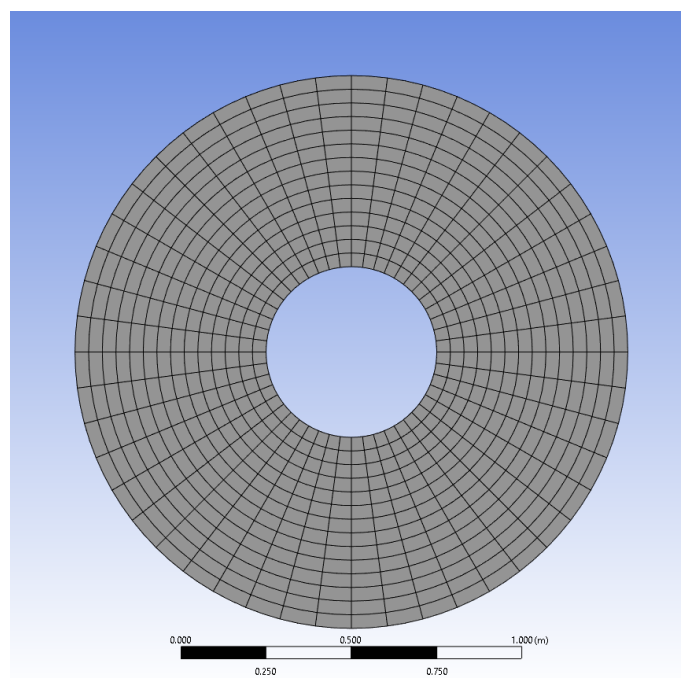
Figure 5.9 - 2D Coil with resolution 5 mesh and face meshing

58

By adding face meshing to the surface of the coil the mesh is much more uniform and increasing the resolution of the mesh keeps a unform element distribution across the coil. However, the cells closer to the centre of the coil are smaller than those on the outer edges (figure 5.9).
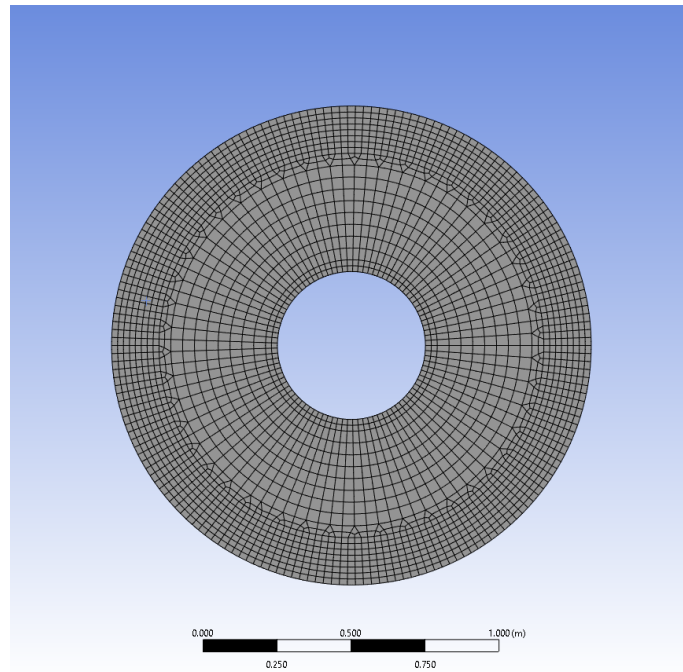
Figure 5.10 - 2D coil with face meshing and refinement on outer layers
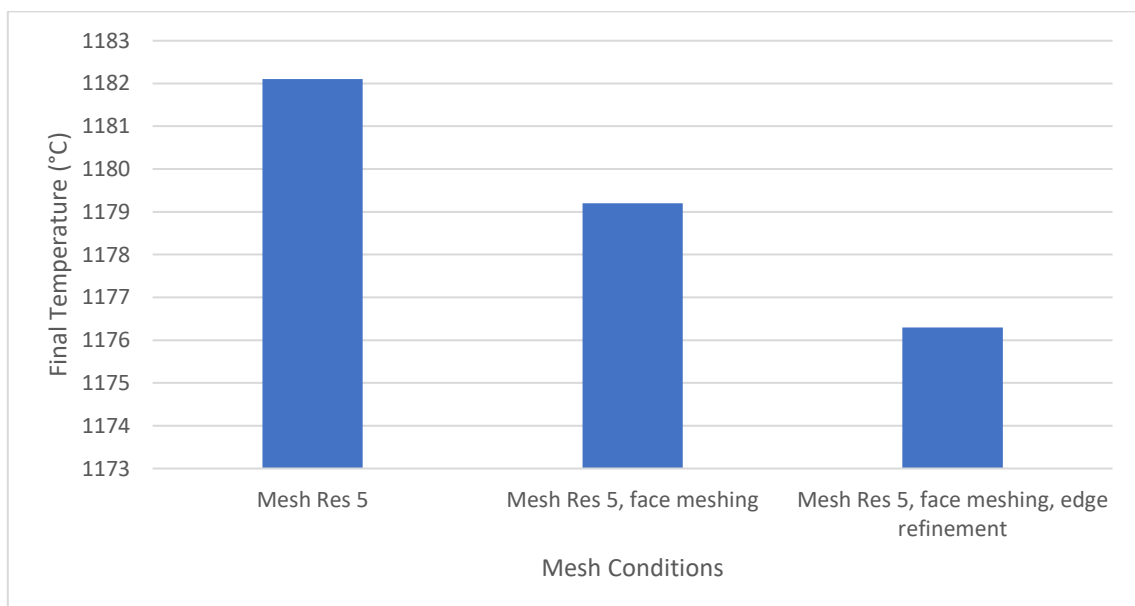
Figure 5.11 – 2D ANSYS model mesh refinement condition temperatures

Adding mesh refinement to the outer edges to match the inner edges of the coil makes the model more accurate overall, as most of the heat losses to the environment happen at the outer edges it is important to have a finer mesh in these regions whereas regions with little movement like the centre of the coil, layer 7 and 8, do not require such a high number of elements. And so, the mesh in figure 5.10 was chosen.

One of the assumptions made in the model is that the main heat transfer mechanism to the environment during the coiling process is radiation and as such convection does not need to be modelled, allowing the model to be simpler. To verify this, the 2D model in ANSYS was used with the mesh in figure 5.10 The model was run twice once with the basic boundary conditions mentioned in Chapter 5.1.1, and again with convection turned off in the model.
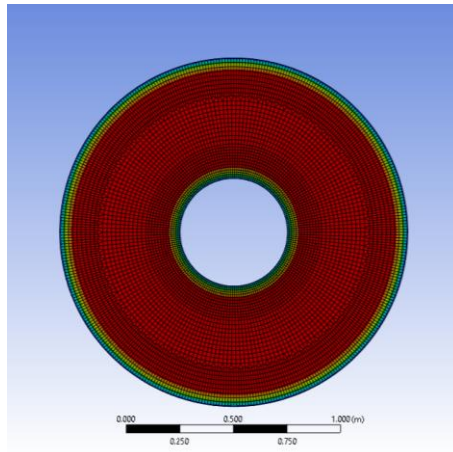
Figure 5.12 - 2D coil final temperature with boundary conditions applied.
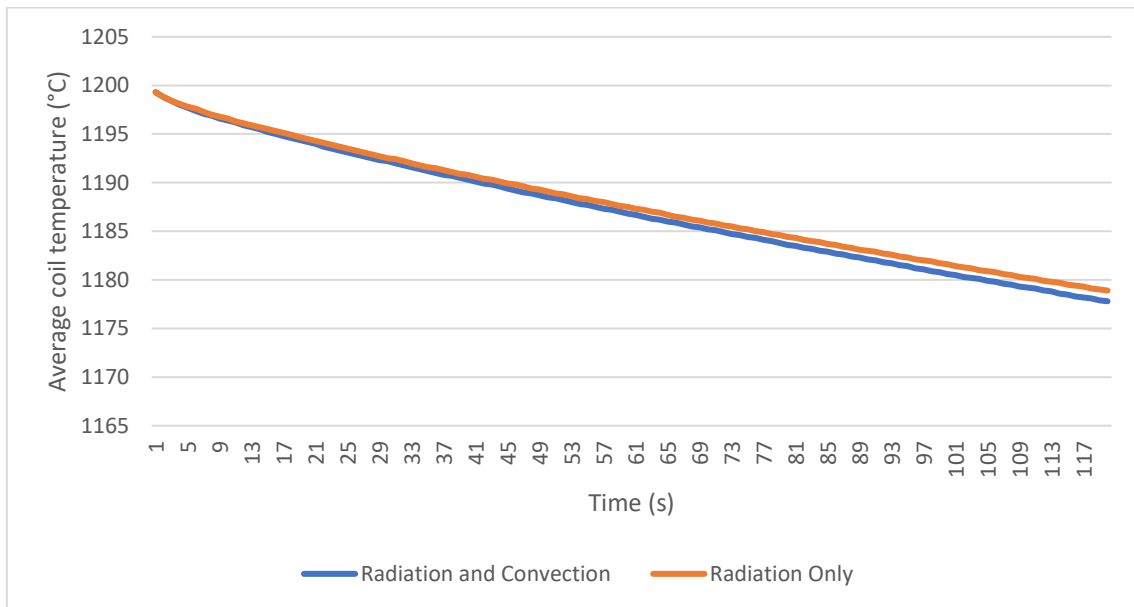
Figure 5.13 - Temperature over time for each boundary conditions

61
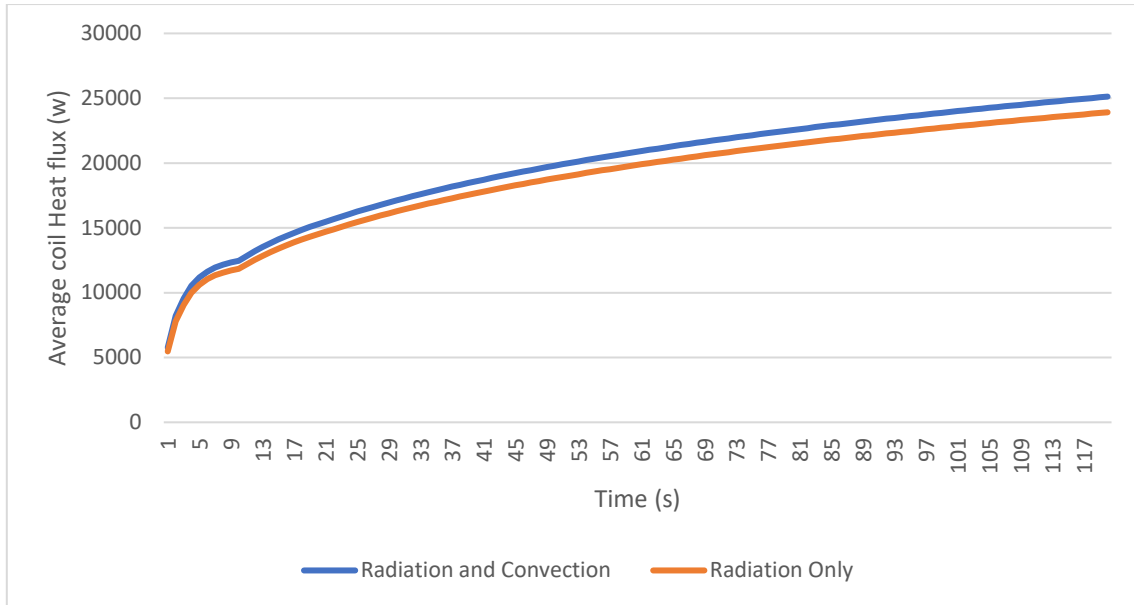
Figure 5.14 - Heat flux over time for each boundary conditions

Figure 5.13 shows that the temperature with radiation, and the radiation and convection models are less than 2°C different from each other. Both models lose heat uniformly over 120 seconds. The models showed a difference in temperature of just 1°C. Figure 5.14 shows the heat flux of both systems over time, and again both models show 1000w heat flux difference, therefore it is reasonable to assume no convection in the TiTAN model.

During the coiling process, the strip is not in perfect contact at each layer, from videos of the coiling process taken from the steel mill, small gaps can be seen across the layers in the coil. Although most of the surfaces are in contact and the gaps in the coil are small, the gaps were simulated in ANSYS to determine if the amount of heat loss from these gaps needs to be programmed into the TiTAN model.
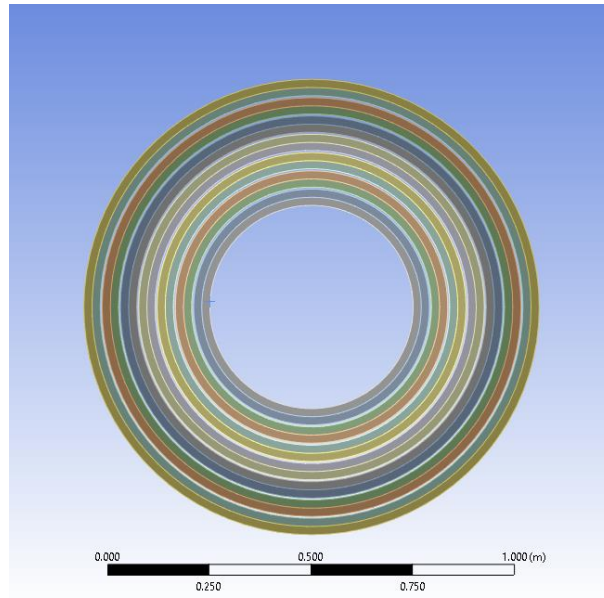
Figure 5.14 - 2D model of coil showing each layer.

It is difficult to estimate how big the gaps in the coil are and where they occur, as access to the coil on the mill was not possible and the plant data only has 1 camera source to try and determine this. Instead, three models were tested in ANSYS (figure 5.14) with varying degrees of separation between each layer. The first model was in 100% perfect contact, the next model had a uniform 5mm gap between each layer, and the last model had a uniform 10mm gap between each layer to determine how much of an impact this could have on the model. Each model had the outer dimensions of the coils increase to account for the new gap between the layers.
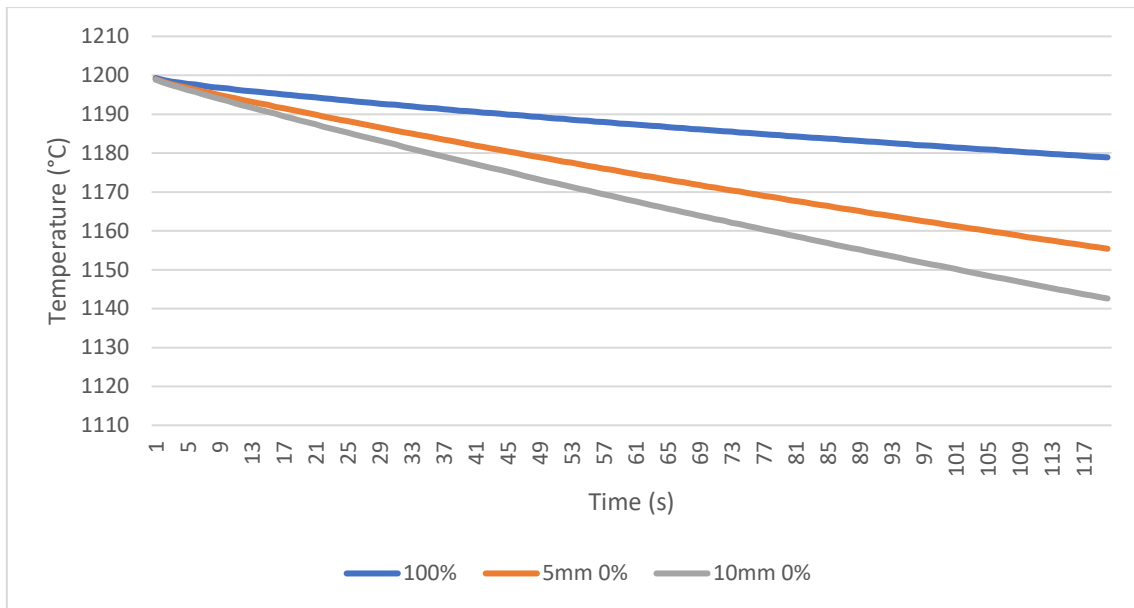
Figure 5.15 - Temperature over time for each contact percentage of coil

Figure 5.15 shows the temperature data over time for each simulation. A spiral with 0% contact and 5mm gaps all around shows a final temperature difference of 20°C where a 10mm gap shows a temperature drop of 40°C, as in reality more than 80% of the strip will be in contact it is reasonable to assume that the heat loss will be significantly less than this, potentially less than 10°C over 120 seconds. Therefore, the inclusion of the gaps would overestimate the effect that they are observed to have making it reasonable to assume perfect contact between the layers of the coiled strip.

5.2   ANSYS Plant Data Comparison

Using the assumptions previously stated all 10 datasets were modelled in the ANSYS 2D system to try and better understand how accurate the results are and how well they portray the heat transfer within the coil. Using material properties discussed in Chapter 5.1, radiation to ambient with emissivity of 0.82, and ambient temperature of 20°C boundary condition applied to the inner and outer edges. As well as a surface-to-surface radiation model on the innermost edge.
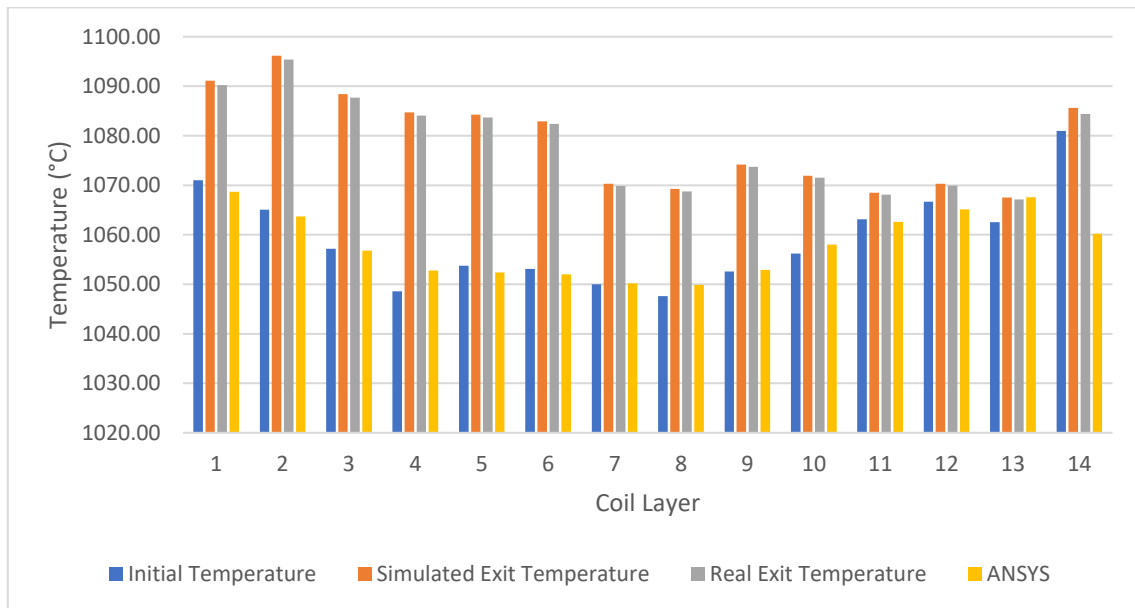
Figure 4.16 – Dataset 6 temperature comparisons of ANSYS and plant data
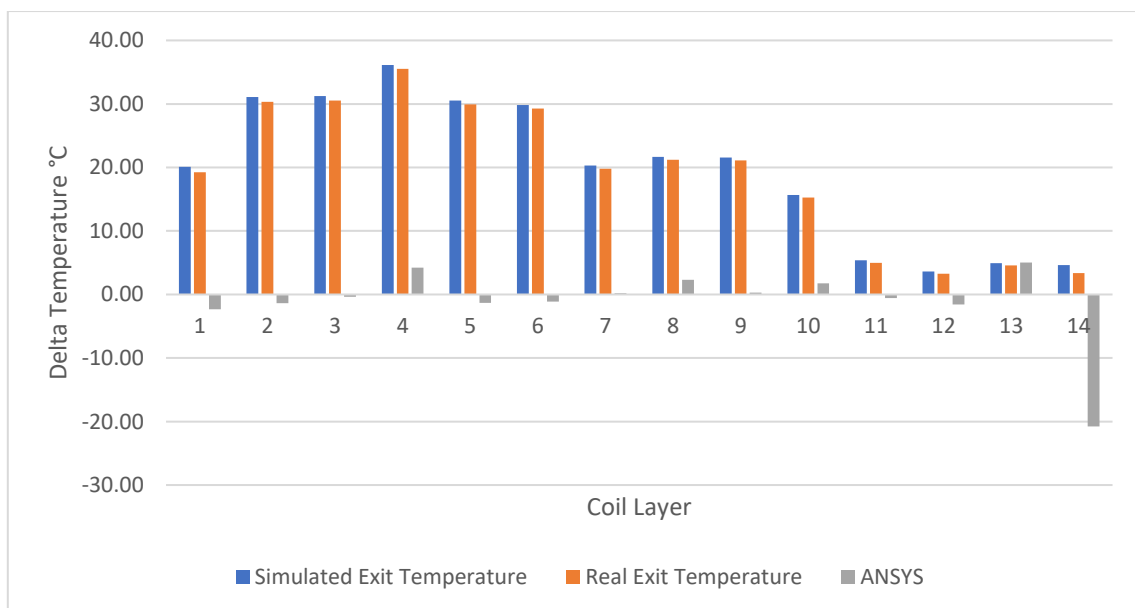
Figure 5.17 - Dataset 6 delta temperature comparisons of ANSYS and plant data
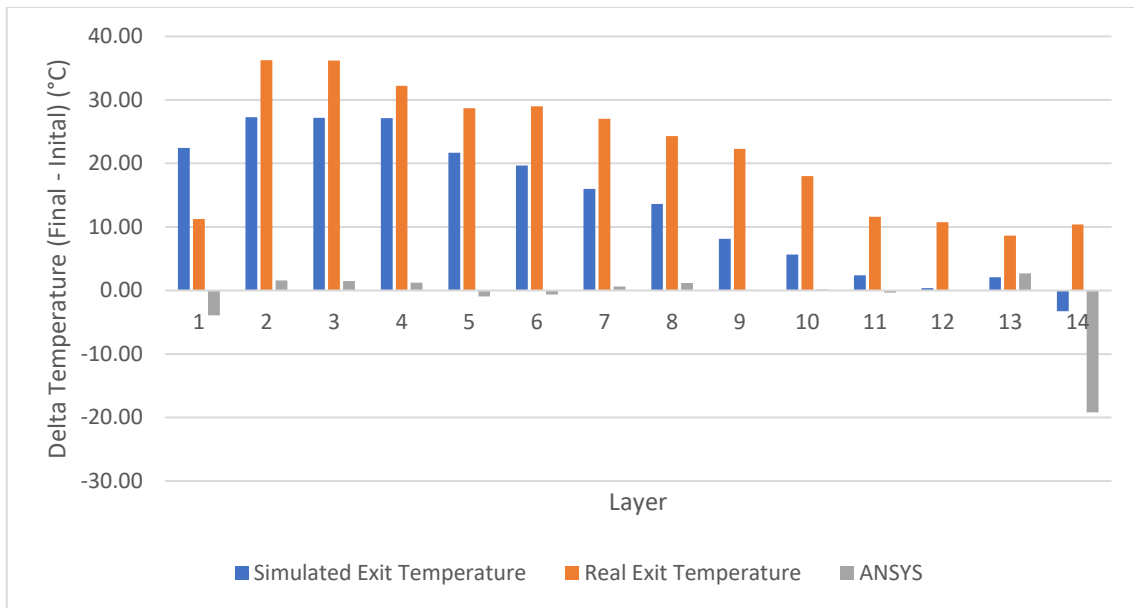
Figure 5.18 - Average delta temperatures of ANSYS and plant data

Figure 5.16 shows the exit temperatures of both plant data variables, real and simulated, as well as the ANSYS simulation compared to the initial temperature. The data shows some similarity with the plant data showing that the innermost layer of the coil does not lose too much temperature to the environment. Possible due to any temperature losses through radiation being reabsorbed by the coil.

Figure 5.17 shows the average temperature data per layer for dataset 6. From ANSYS the coil loses a lot more heat in the outer layers than the plant data, whilst the other layers have minimal heat losses and gains as they diffuse into average temperatures which is as expected. Figure 5.18 is a comparison of all the datasets for both plant data sets and the ANSYS model developed which again shows a similar trend that can be seen in Chapter 2.3

5.3   ANSYS Model Discussion

The ANSYS model was developed to provide another comparison point against the plant data analysed in Chapter 2. The plant data is known to have issues and therefore not a perfect representation of the coiling process. Therefore, the ANSYS model allows for a chance to validate these results as there is no access to TATA Steels calibration records for their equipment or other sites that would be able to compare these results.

The ANSYS results showed more heat losses on the outermost layer, which is an expected result as the final layer has the most surface exposed to the environment. It also showed little to no heat transfer in the innermost and middle layers suggesting that the temperatures there are stable, and no major heat transfer is occurring. All 10 datasets were simulated in ANSYS and are shown in the appendix.

Although the ANSYS model may be more representative of the thermal losses of the coil, it does not consider the movement of the coil during uncoiling. As the coil moves across cradles, a temperature jump can be seen in the remaining coils. This can be accounted for this in the ANSYS model by only comparing temperature when the strip has been coiled.

5.4   ANSYS Plant Data Model Conclusions

In this chapter, a model of the coil was developed in ANSYS which was able to use the initial temperature of each dataset gathered from chapter 2: Plant Data Analysis. Due to the difficulties in confirming the accuracies of the plant data, as discussed in Chapter 2.4, the ANSYS model allowed for another point of comparison to further understand the heat transfer mechanics of the coiling process.

Once a model was developed and optimised to reduce computational time and to form a base for assumptions that can be made when developing the TiTAN model, the ANSYS model was run for the same duration of time that the strip was coiled for in each dataset. The initial temperature of each layer was set to the initial average layer temperature calculated in Chapter 2.

The ANSYS temperatures of each coil are more realistic as compared to the plant data temperatures. The ANSYS temperatures show minimal heat transfer between the inner layers of the coil. Some heat transfer occurs as the temperature in the coil tries to equalise. The innermost layer also shows little heat loss, although slightly more than the inner layers as shown in Figure 5.18. The most significant form of heat loss occurs from the outermost layer. As this is the layer with the most surface area exposed to the environment it shows the greatest temperature losses.

As with the plant data, there are some limitations to the ANSYS data. The ANSYS model does not include the coil moving through cradles, which again shown in Chapter 2, has an impact on the temperature of the steel strip. Furthermore, the ANSYS model used the initial temperatures recorded from the plant data. The inaccuracies discussed with the nature of the plant data also apply to the initial temperatures used in the ANSYS model.

In conclusion, the ANSYS model developed is a useful tool in expanding upon the heat transfer in the coilbox. Mainly by showing how little heat is lost in the layers between the inner and outmost layer of the coil, as well as confirming that heat losses are most pronounced on the outermost coil. Although as with the plant data neither data set is perfect.
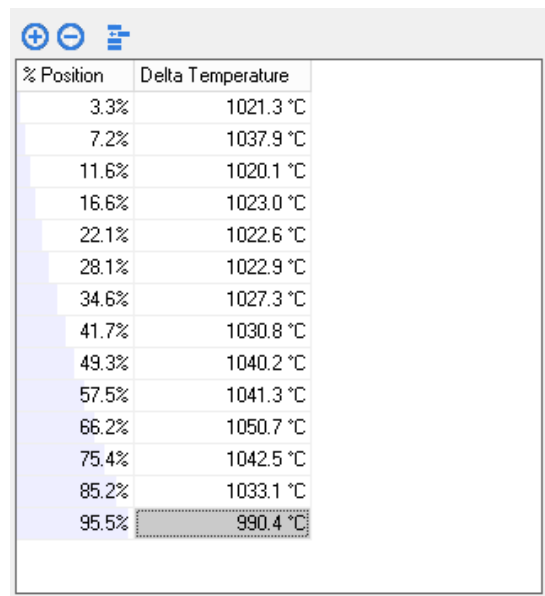
6   TiTAN Heat Transfer Model

This section looks at developing the new heat transfer model for the coilbox. As mentioned before in Chapter 4 the movement of the coil has already been programmed and therefore this section will only look at added heat transfer and boundary conditions to complete the model.

6.1   TiTAN limitations

A limitation of the TiTAN model is it simulates a single point in the strip and has no knowledge of the rest of the strip. This means although TiTAN knows where the calculation point is within the coil the temperature deltas are unknown. To address this directly it was decided to allow the user to input strip temperature data before the simulation is started.

Figure 6.1 shows the current user interface allowing TiTAN to know the relative temperature of the entire strip. In Figure 6.1 temperature data is inserted at relative positions, worked out as a percentage of the overall strip length along the strip shown by % position, to allow for more accurate simulations. However, it is up to the user how much detail is needed. The system is designed to work with no user inputs, assuming constant temperature throughout the strip. If given more time it would even be possible to create a script that would allow the raw pyrometer data from FmObsTemp [10] to be inserted into the temperature data.

% Position	Delta Temperature
3.3%	1021.3 ℃
7.2%	1037.9 ℃
11.6%	1020.1 ℃
16.6%	1023.0 ℃
22.1%	1022.6 ℃
28.1%	1022.9 ℃
34.6%	1027.3 ℃
41.7%	1030.8 ℃
49.3%	1040.2 ℃
57.5%	1041.3 ℃
66.2%	1050.7 ℃
75.4%	1042.5 ℃
85.2%	1033.1 ℃
95.5%	990.4 ℃

Figure 5.1 - TiTAN user strip temperature input for coilbox module

6.2   TiTAN Heat Transfer Model

The heat transfer model developed in TiTAN utilises the outermost surface nodes in the strip. Due to time limitations, it was not feasible to adjust the surface cells and add additional cells above and below each cell to model conduction in the system. The system was modelled by changing the environmental and radiation temperature of the surface nodes to the layer above and below the current calculation point. Refer to figure 1.18 in Chapter 1.4

To calculate the required radiation temperature of the top and bottom surface the heat flow of the strip itself and the potential heat flow to the surface through radiation need to be calculated. The heat flow of the strip is calculated from the heat transfer of conduction equation.

During the coiling and uncoiling process, TiTAN uses the movement data of the strip to determine what surfaces are coiled and at which points. During coiling the bottom surfaces are coiled each revolution before the top surfaces on each layer, whereas when uncoiling the bottom surface of the layer is removed first whilst the top is still in contact. The system can understand which boundary conditions are active at which points and uses the appropriate temperature data. This allows for a more accurate simulation overall, as the amount of time coiled is directly determined through the movement of the coil.
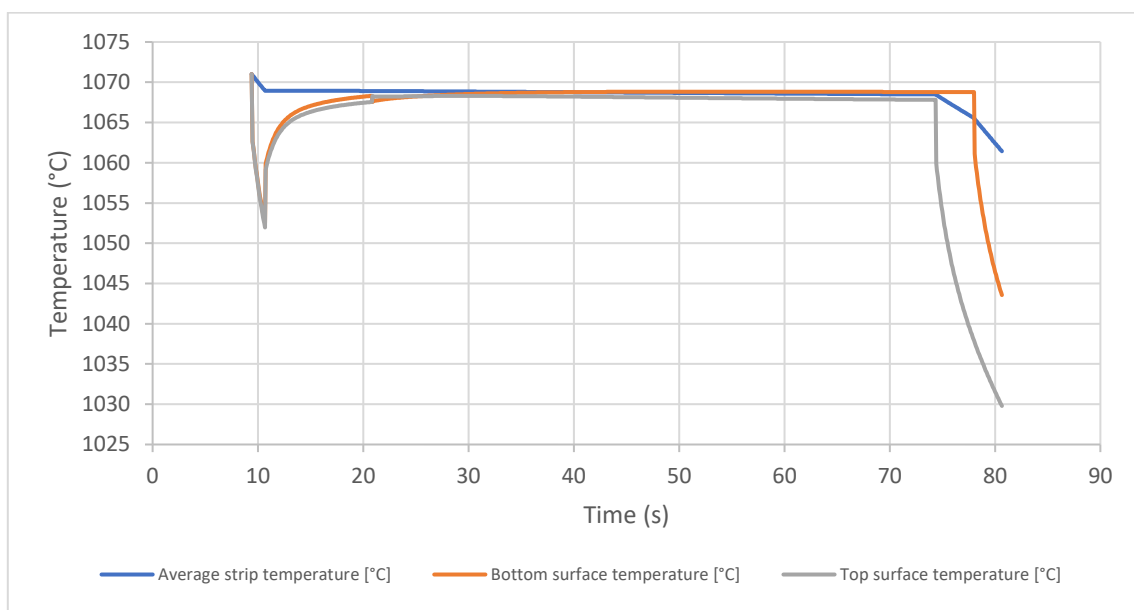
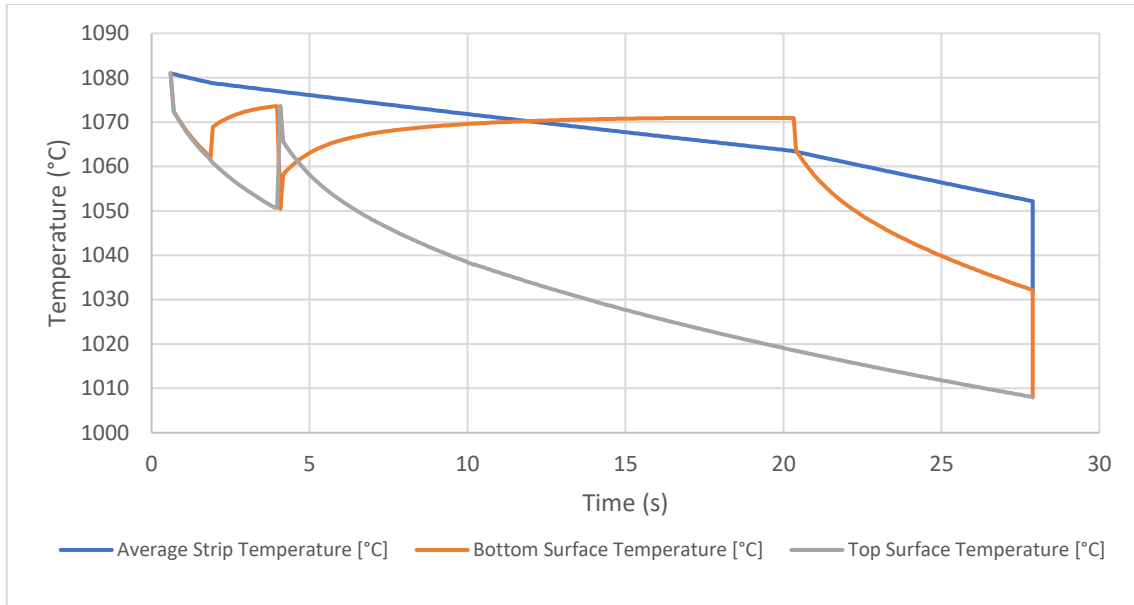*Figure 6.2 - TiTAN layer 1 temperature over time*

Figure 6.3 - TiTAN Layer 14 temperature over time

From Figures 6.2 and 6.3 the strip can be seen losing heat as it enters the coilbox process, once the strip begins coiling the surface temperatures increase back to the average temperature of the strip. From this point, through radiation, the average temperature of the strip decreases or increases depending on the boundary conditions above and below the strip. In Figure 6.2 the strip is in layer 1 and so the innermost surface is radiating to itself, while the top surface is being kept warm by layer 2.

In Figure 6.3 the top surface is exposed to the environment whilst the bottom surface is being heated by layer 13 this causes the average temperature of the strip to fall. Figure 6.3 also clearly shows the strip surfaces being flipped around the 4-second mark. Although this happens for every strip in all positions it is shown most clearly in Figure 6.3 as the calculation position is in the final layer, only the last coiling revolution is shown allowing for a closer resolution of the graph. Lastly, both graphs show each surface of the coil being removed one revolution after the other, allowing the bottom surface to have a slightly hotter surface temperature as the overall coiled time is longer.

6.3   TiTAN Heat Transfer model comparison
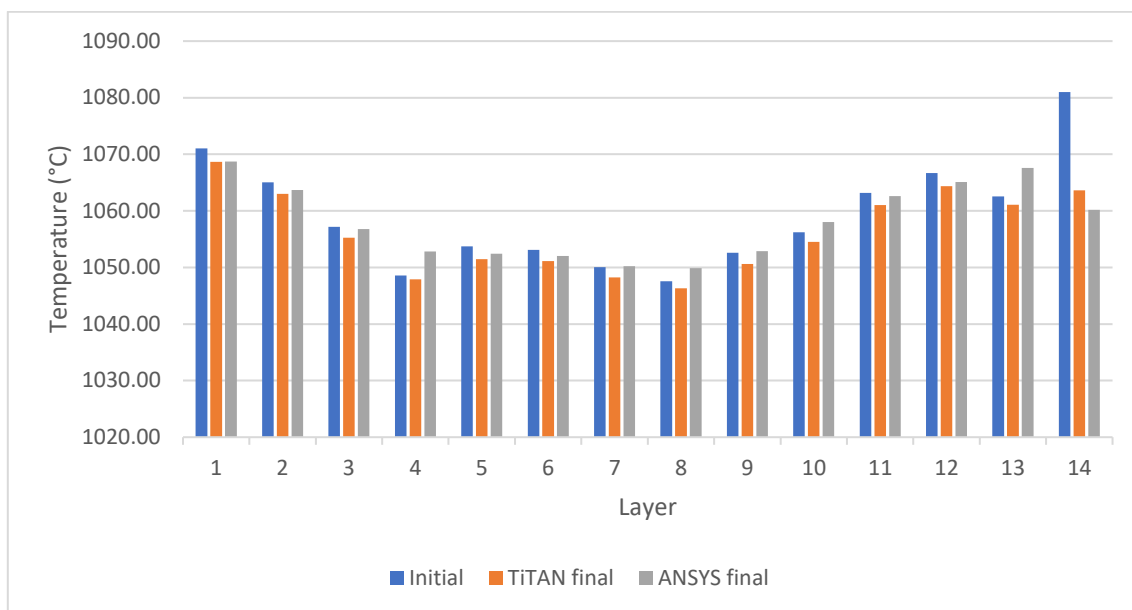
Figure 6.4 - Dataset 6 average layer temps

Figure 6.4 shows the initial temperature data from Initial plant data temperatures compared with the ANSYS and TiTAN model final temperature data. The graph shows a close similarity between both the ANSYS and TiTAN models. This can be seen clearer in figure 6.5 below which shows the average delta temperatures per layer for all the datasets tested.
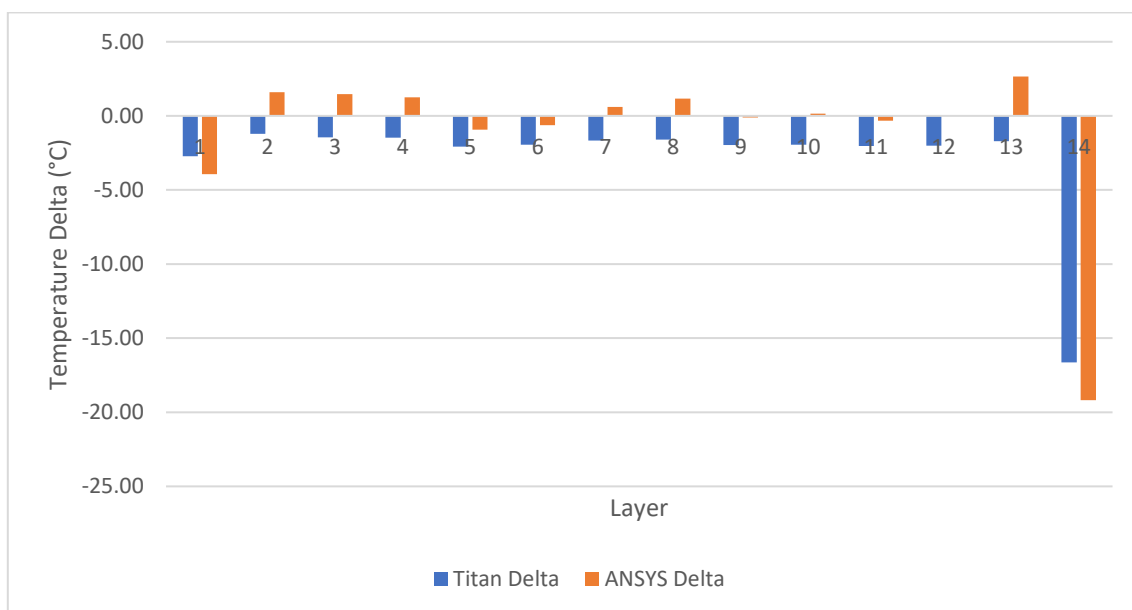

Figure 6.5 – Average layer delta temperature for all datasets

Lastly, a strip with uniform temperature was tested to show how much heat was lost for each layer. The entire strip had a temperature of 1200°C and was simulated comparably to the datasets sharing the same boundary conditions and coiling/uncoiling speeds.
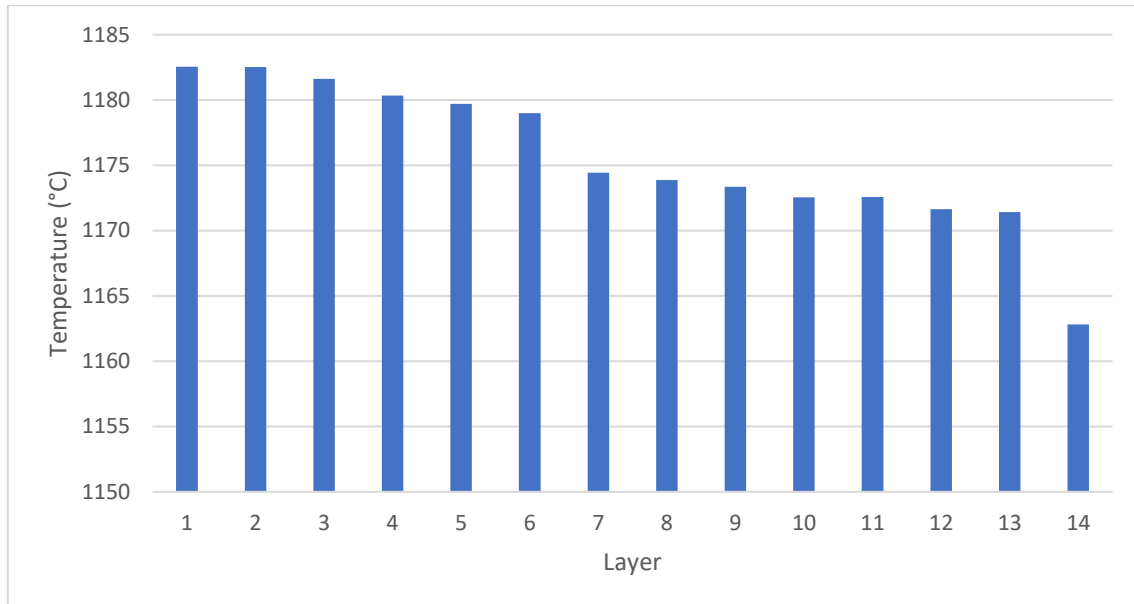
Figure 6.6 - Final temperature of a strip with initial temperature 1200°C for each layer in TiTAN

Figure 6.6 shows all the trends in layer temperature that would be expected. The outermost layer (Layer 14) has the greatest temperature loss, followed by a gradual decrease in layer temperature from Layer 7 to Layer 13. Layers 1 to 6 show a jump in temperature that would be expected with the coil moving to cradle 3 once the outer layers have been removed and so the strip is subjected to environmental conditions for less time. Finally layers 1 to 6 show a gradual decrease in final temperature, indicating layer 1 to be the hottest, which is again what would be expected.
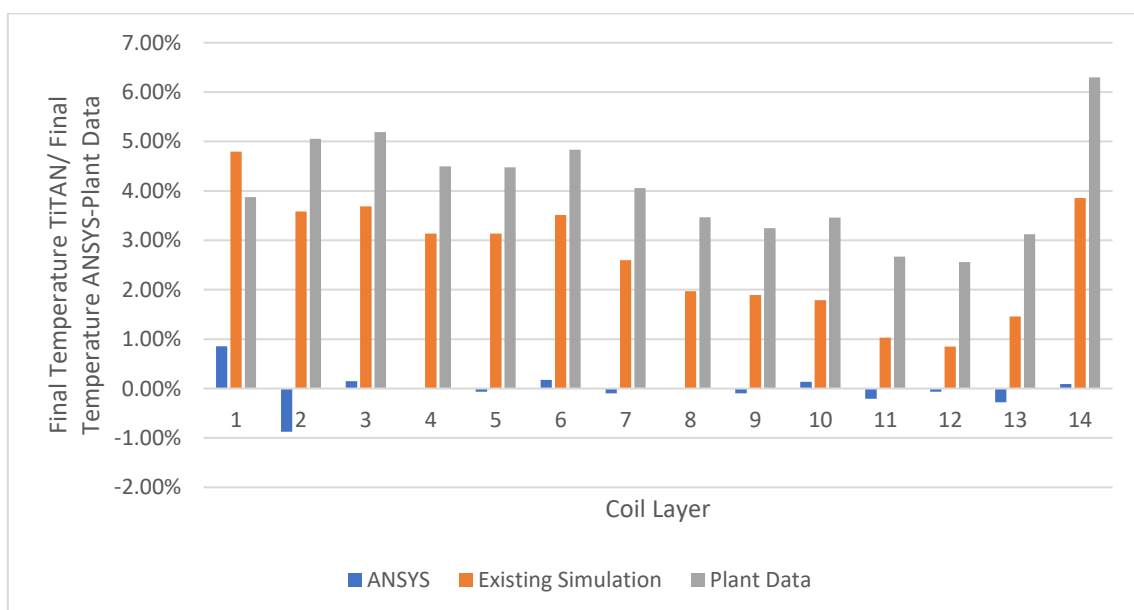
Figure 6.7 – Percentage Error of TiTAN model compared to ANSYS and plant data.

Figure 6.7 shows the percentage error of the Titan model's final temperature compared to the final temperature of the ANSYS simulation and the real exit data from all 10 datasets. From the graph, both models show an average error to be around 5%. The ANSYS comparison shows a consistent accuracy level across all the layers of the spiral, whereas the plant data comparison shows an increase in the accuracy of the model as the layers increase however, due to the nature of the plant data and the inaccuracies of the data gathered it is not possible to fully understand if this is due to the errors in the TiTAN model or the plant data.

As has shown the expected trends from both the plant data, show increases in layer temperature as the coils move through the cradles, as well as the outer layer experiencing the most temperature losses through radiation. The model was fully integrated within TiTAN and the software was handed to the TATA Steel team would validate the simulation with their method.

7   Discussion

TiTAN is a highly specialised tool that is used to predict how a strip will behave on the mill. The main use cases for TiTAN are to outline how the processes of the mill will affect the strip, whether the strip will be able to pass through the mill with the desired temperatures and ensure the steel has the desired mechanical properties. As such the program is highly customizable to allow for a variety of setups and conditions.

Furthermore, it was designed and optimized to be able to run efficiently and intuitively whilst remaining reasonably accurate. Incorporating the coilbox module into TiTAN must keep with TiTAN's design and standards. The system should not feel clumsy, it must integrate seamlessly with the rest of the program, whilst still allowing for quick simulations and remaining accurate. Therefore, compromises had to be made with both the movement and heat transfer aspects of TiTAN.

Portraying the strip movement in 1 dimension as it is coiled is difficult as there is a loss of information on the vertical axis. Despite this, the way the data is represented in TiTAN can relate to the user that the strip is being coiled. The movement of the strip can be traced throughout the coilbox process showing as clear a picture as possible of the behaviour of the strip through the coiling process. The process can model any scenario that may occur in the coilbox, and the coiling speeds and delay times can be adjusted to simulate most real-world occurrences.

Simplifying the heat transfer of the coil was essential to keep the computational cost low, however, accuracy could not be compromised in the process either. As such assumptions were tested to confirm that it would be reasonable to ignore boundary conditions and imperfect contact. To keep the program simple the FEM model was kept 1 dimensional and when modelling the coiled strip instead of adding more nodes to the model throughout the entire coil, the top and bottom surface nodes had boundary conditions adjusted to simulate temperatures above and below the calculation position.
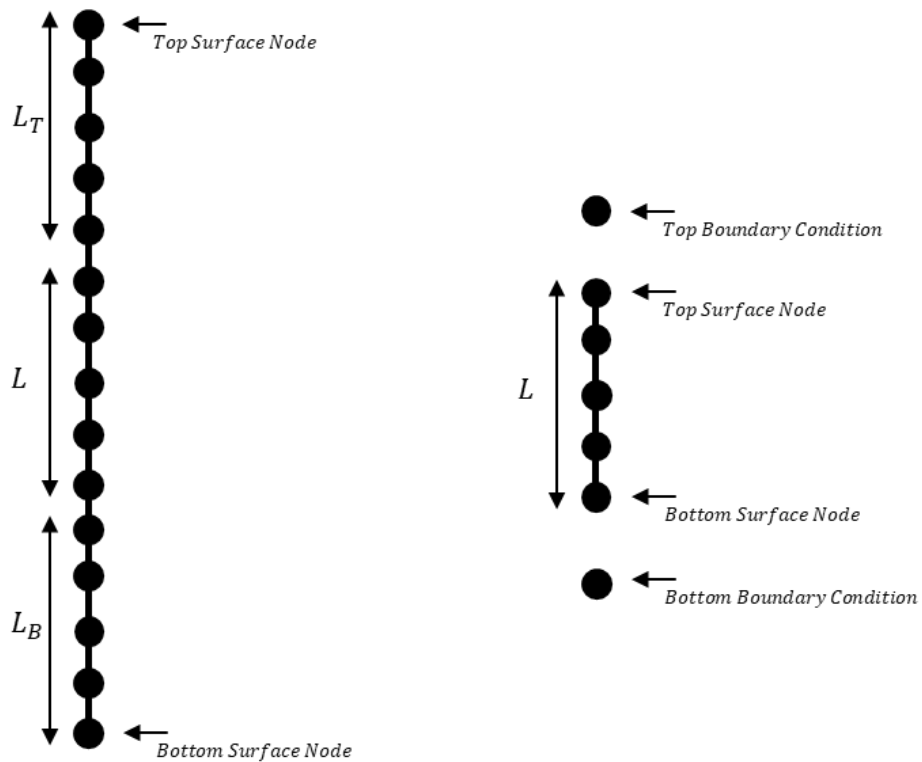
Figure 6.1 - TiTAN through coil model, and developed model

Figure 7.1 shows an example of a system that could be used to model the strip through the entire coil (left) and the model developed (right). Although a system such as this could be implemented in TiTAN, it would require the module to circumvent the programs built-in calculation module and instead do all calculations with the module itself. This would increase the computational time and size of the module and might cause issues with compatibility with other modules. However, if the project had more time an optimised system could be implemented.

8 Overall Conclusion and Future Work

A new installation was added to the TiTAN simulation program, allowing for accurate modelling of the movement and heat transfer of a steel strip as it moves through the coilbox. The model can accurately simulate any point along the strip and setup of the coilbox as defined by the user inputs and is fully integrated into the simulation software working alongside other pre-existing simulations.

The model was developed using the existing FEM process in 1 dimension. Although this system is less accurate than a 2-dimensional model the system is still accurate when compared to the ANSYS data whilst keeping computational time low and integrating well within the program. The model was tested against simulation data developed in ANSYS as plant data was deemed inaccurate. The model shows accuracies of over 90% when compared with datasets in ANSYS.

The model is also able to calculate the movement of the strip through many different user-defined coilbox setups and throughout all the cradle positions. The model is also able to change the direction of the strip and the orientation of the top and bottom surfaces and relay this information forward to the next installation in TiTAN.

Throughout the project some challenges and issues restricted the total amount of time TiTAN was available, as the NDA took some time to be signed, other ideas into using FEM and expanding TiTAN were explored, but ultimately had to be abandoned due to time constraints.

Another limitation of the study was due to the nature of the plant data attained. Without more knowledge and further comparison points it is not possible to determine the accuracy of the plant data. This was a big limitation in the study as the model would be compared to real working temperatures observed in the coilbox. Whilst in the end, the TiTAN model can provide temperatures within 80% of observed temperatures ultimately ANSYS was used to determine how the heat transfer occurs between layers.

With the time the project had allocated the module is up to an acceptable working standard using the tools that TiTAN had available. If further time was allocated a potential 2-dimensional FEM solution could have been implemented within the coilbox module and optimised to provide quick and accurate data about the strip.

9 References

[1] Tata Steel Europe Annual Report 2020-21. (2021).
     https://www.tatasteeleurope.com/sites/default/files/Tata Steel UK Limited Annual Report
     2020-21.pdf

[2] Jang, J. Y., Lee, Y. W., Lin, C. N., & Wang, C. H. (2015). 3-D Transient Heat Transfer Analysis of
     Slab Heating Characteristics in a Reheating Furnace in Hot Strip Mills. 9(11), 1923–1927.

[3] Lenard, J. G. (2014). 2 - History of Hot Strip Mills11Contributed by Donald R. Adair, flat
     rolling manager, Quad Engineering Inc. and Edwin B. Intong, former technical manager for
     Electrical & Automation, US Steel Engineers and Consultants. In J. G. Lenard (Ed.), Primer on
     Flat Rolling (Second Edition) (Second Edi, pp. 17–29). Elsevier.
     https://doi.org/https://doi.org/10.1016/B978-0-08-099418-5.00002-0

[4] Tata Steel Europe. (2020). Tata Steel in the UK Fact Sheet.
     http://web.archive.org/web/20080207010024/http://www.808multimedia.com/winnt/kern
     el.htmx

[5] Sharma, K. L. S. (2017). 19 - Management of Industrial Processes. In K. L. S. Sharma (Ed.),
     Overview of Industrial Process Automation (Second Edition) (Second Edition, pp. 321–357).
     Elsevier. https://doi.org/https://doi.org/10.1016/B978-0-12-805354-6.00019-0

[6] Lenard, J. G. (2014). 1 - Introduction. In J. G. Lenard (Ed.), Primer on Flat Rolling (Second
     Edition) (Second Edition, pp. 1–15). Elsevier. https://doi.org/https://doi.org/10.1016/B978-
     0-08-099418-5.00001-9

[7] Tata Steel Media Kit: Gallery. Tata Steel Media Kit | Gallery. (n.d.).
     https://www.tatasteel.com/media/media-kit/gallery/

[8] López, B., & Rodriguez-Ibabe, J. M. (2012). 4 - Recrystallisation and grain growth in hot
     working of steels. In J. Lin, D. Balint, & M. Pietrzyk (Eds.), Microstructure Evolution in Metal
     Forming Processes (pp. 67–113). Woodhead Publishing.
     https://doi.org/https://doi.org/10.1533/9780857096340.1.67

[9] Suebsomran, A., & Butdee, S. (2013). Case Studies in Thermal Engineering Cooling process
     on a run-out table by the simulation method. Case Studies in Thermal Engineering, 1(1), 51–
     56. https://doi.org/10.1016/j.csite.2013.07.002

[10] Shen, S., Guye, D., Ma, X., Yue, S., & Armanfard, N. (2022). Multistep networks for roll force
     prediction in hot strip rolling mill. Machine Learning with Applications, 7(March 2021),
     100245. https://doi.org/10.1016/j.mlwa.2021.100245

[11] Panjkovic, V. (2007). Model for prediction of strip temperature in hot strip steel mill.
     Applied Thermal Engineering, 27(14–15), 2404–2414.
     https://doi.org/10.1016/j.applthermaleng.2007.03.009

[12] Yildiz, S. K., Forbes, J. F., Huang, B., Zhang, Y., Wang, F., Vaculik, V., & Dudzic, M. (2009). Dynamic modelling and simulation of a hot strip finishing mill. Applied Mathematical Modelling, 33(7), 3208–3225. https://doi.org/10.1016/j.apm.2008.10.035

[13] delphi @ www.embarcadero.com. (n.d.). https://www.embarcadero.com/products/delphi

[14] Col, R. (2015). Modelling heat transfer during hot rolling of steel strip Modelling heat transfer during hot rolling of steel strip. June. https://doi.org/10.1088/0965-0393/3/4/002

[15] Park, S. J., Hong, B. H., Baik, S. C., & Oh, K. H. (1998). Finite element analysis of hot rolled coil cooling. *ISIJ International*, *38*(11), 1262–1269. https://doi.org/10.2355/isijinternational.38.1262

[16] Karlberg, M. (2011). Modelling of the temperature distribution of coiled hot strip products. *ISIJ International*, *51*(3), 416–422. https://doi.org/10.2355/isijinternational.51.416

[17] S. . Park, B. H. Hong, and S. C. Baik, "Finite element analysis of hot rolled coil cooling," ISIJ Int., vol. 38, no. 11, pp. 1262–1269, 1998.

[18] Mori, K. I., & Oketani, N. (1999). Prediction of coiling conditions of plate in coilbox by controlled FEM simulation. International Journal of Machine Tools and Manufacture, 39(3), 403–413. https://doi.org/10.1016/S0890-6955(98)00043-1

[19] Kukhar, V., Kurpe, O., Klimov, E., Balalayeva, E., & Dragobetskii, V. (2018). Improvement of the method for calculating the metal temperature loss on a Coilbox unit at the rolling on hot strip mills. International Journal of Engineering and Technology(UAE), 7(4), 35–39. https://doi.org/10.14419/ijet.v7i4.3.19548

[20] Steel Mill, Rebar Rolling Mill Machinery Hot Steel Rolling Mill Plant. (n.d.).

[21] Peyton, A. J. (2015). 3 - Electromagnetic induction tomography. In M. Wang (Ed.), Industrial Tomography (pp. 61–107). Woodhead Publishing. https://doi.org/https://doi.org/10.1016/B978-1-78242-118-4.00003-4

[22] Pradhan, K. K., & Chakraverty, S. (2019). Finite Element Method. In Computational Structural Mechanics (pp. 25–28). https://doi.org/10.1016/B978-0-12-815492-2.00010-1

[23] Rapp, B. E. (2017). Chapter 32 - Finite Element Method. In B. E. Rapp (Ed.), Microfluidics: Modelling, Mechanics and Mathematics (pp. 655–678). Elsevier. https://doi.org/https://doi.org/10.1016/B978-1-4557-3141-1.50032-0

[24] Pradhan, K. K., & Chakraverty, S. (2019). Chapter Four - Finite Element Method. In K. K. Pradhan & S. Chakraverty (Eds.), Computational Structural Mechanics (pp. 25–28). Academic Press. https://doi.org/https://doi.org/10.1016/B978-0-12-815492-2.00010-1

[25] Lewis, R. W., Morgan, K., Thomas, H. R., & Seetharamu, K. N. (1996). The Finite Element Method in Heat Transfer Analysis. Wiley. https://books.google.co.uk/books?id=2mVqtW7BDpgC

[26] Segerl7ind L.J., Applied Finite Element Analysis (2nd Edition) John Wiley & Sons, New York (1984).

[27] Hughes T.J.R., Unconditionally stable algorithm for nonlinear heat conduction J. Com. Meth. Apple. Mech. Engg. Des., 51, 389-401 (1979).

[28] Mitchell, A. R. (1982). Finite elements: An introduction. Volume 1, E. B. Becker, G. F. Carey and J. T. Oden, Prentice-Hall. International Journal for Numerical Methods in Engineering, 18(6), 954–955. https://doi.org/https://doi.org/10.1002/nme.1620180613

[29] Morton, K., & Mayers, D. (2005). Numerical Solution of Partial Differential Equations: An Introduction (2nd ed.). Cambridge: Cambridge University Press. doi:10.1017/CBO9780511812248

[30] Reddy, J. N. (2019). *Introduction to the Finite Element Method* (4th Edition). McGraw-Hill Education. https://www.accessengineeringlibrary.com/content/book/9781259861901

[31] Hughes T.J.R., Unconditionally stable algorithm for nonlinear heat conduction J. Com. Meth. Apple. Mech. Engg. Des., 51, 389-401 (1979).

[32] Hussain, I. (2022). Inductance Calculation of Single-Layer Planar Spiral Coil.

[33] Poznyak, A. S. (2021). 1 - Kinematics of a point. In A. S. Poznyak (Ed.), Classical and Analytical Mechanics (pp. 1–30). Elsevier. https://doi.org/https://doi.org/10.1016/B978-0-32-389816-4.00012-0

10 Appendix

10.1 MATLAB Initial Temperatures

The table Below shows in the initial temperature for each node in both the 1 and 2-dimensional MATLAB simulations, as well as the ANSYS verification model mentioned in Chapter 3

Table 3 - MATLAB Node Initial Temperatures

Node	Temp (°C)	Node	Temp (°C)	Node	Temp (°C)	Node	Temp (°C)	Node	Temp (°C)
1	1066	16	1024	31	1027	46	1051	61	1114
2	1152	17	1170	32	1187	47	1009	62	1176
3	1055	18	1009	33	1084	48	1153	63	1166
4	1100	19	1027	34	1103	49	1129	64	1195
5	1017	20	1009	35	1098	50	1199	65	1088
6	1157	21	1196	36	1169	51	1167	66	1144
7	1191	22	1027	37	1110	52	1066	67	1112
8	1053	23	1039	38	1061	53	1165	68	1050
9	1009	24	1152	39	1191	54	1026	69	1174
10	1187	25	1117	40	1133	55	1119	70	1163
11	1172	26	1003	41	1118	56	1126	71	1189
12	1167	27	1168	42	1110	57	1123	72	1107
13	1093	28	1064	43	1074	58	1158	73	1164
14	1018	29	1200	44	1109	59	1017		
15	1046	30	1148	45	1194	60	1131		

10.2 Plant Data Datasets

Below all plant data datasets from 1 to 10 are shown.
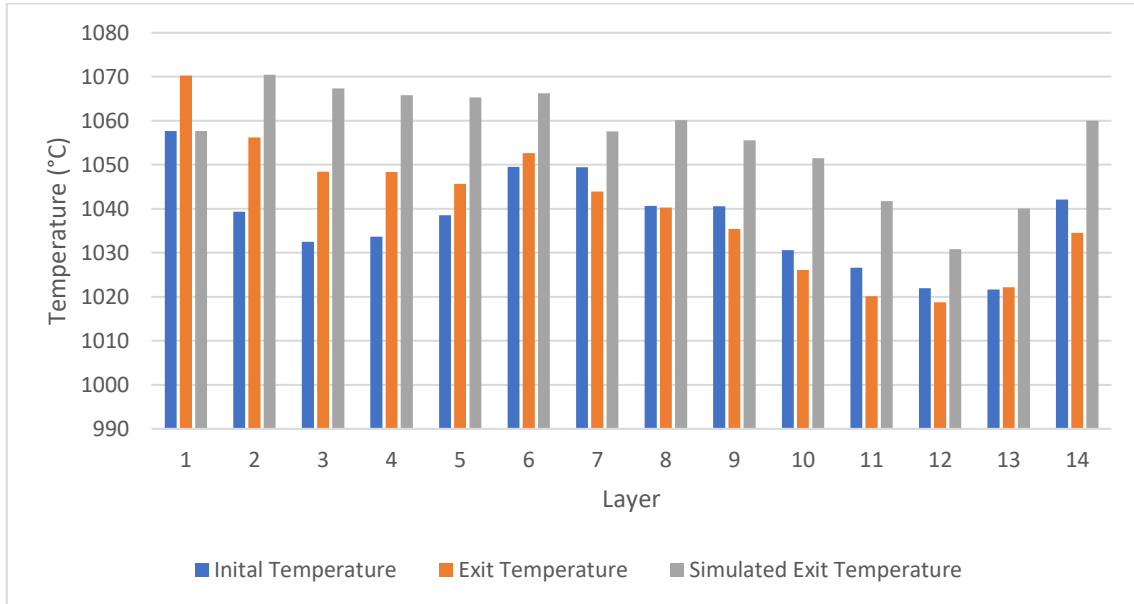
Figure 10.1 – Dataset 1 Pyrometer Data
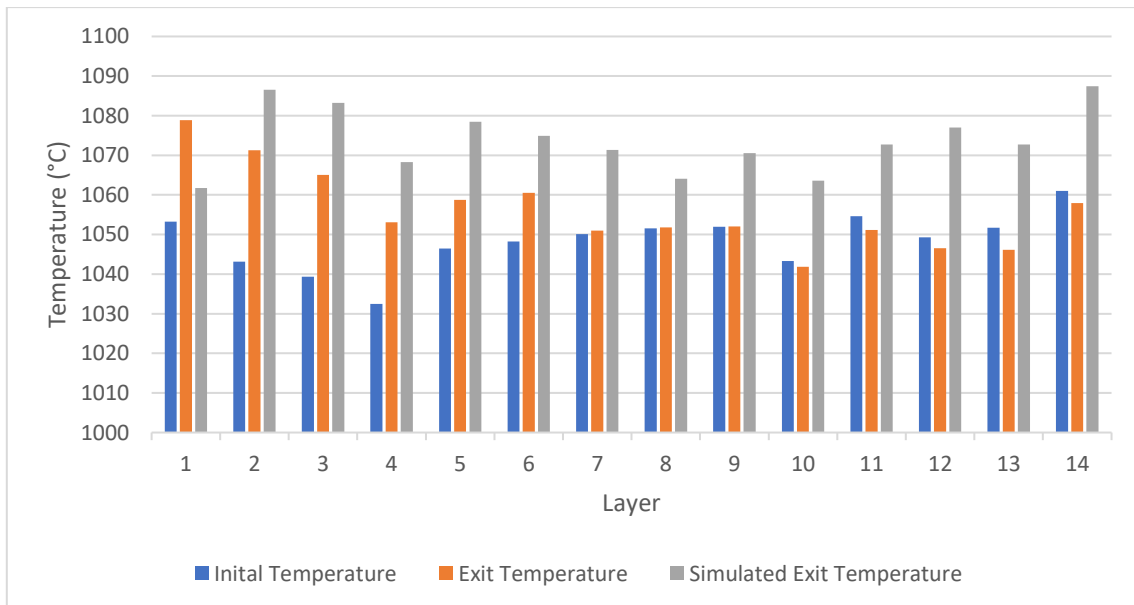
Figure 10.2 – Dataset 2 Pyrometer Data
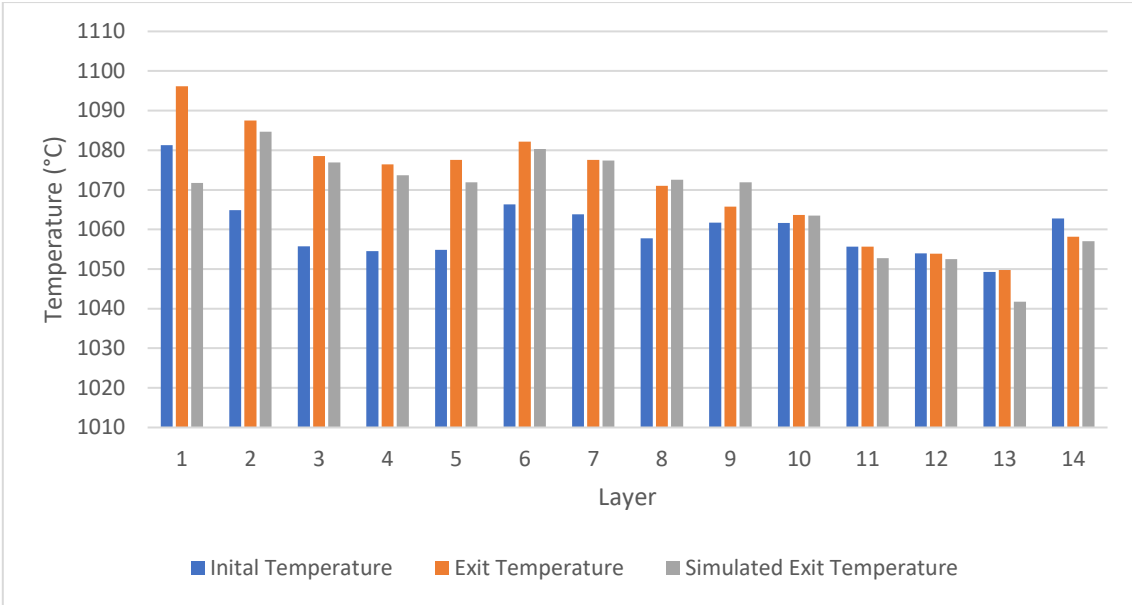
Figure 10.3 – Dataset 3 Pyrometer Data
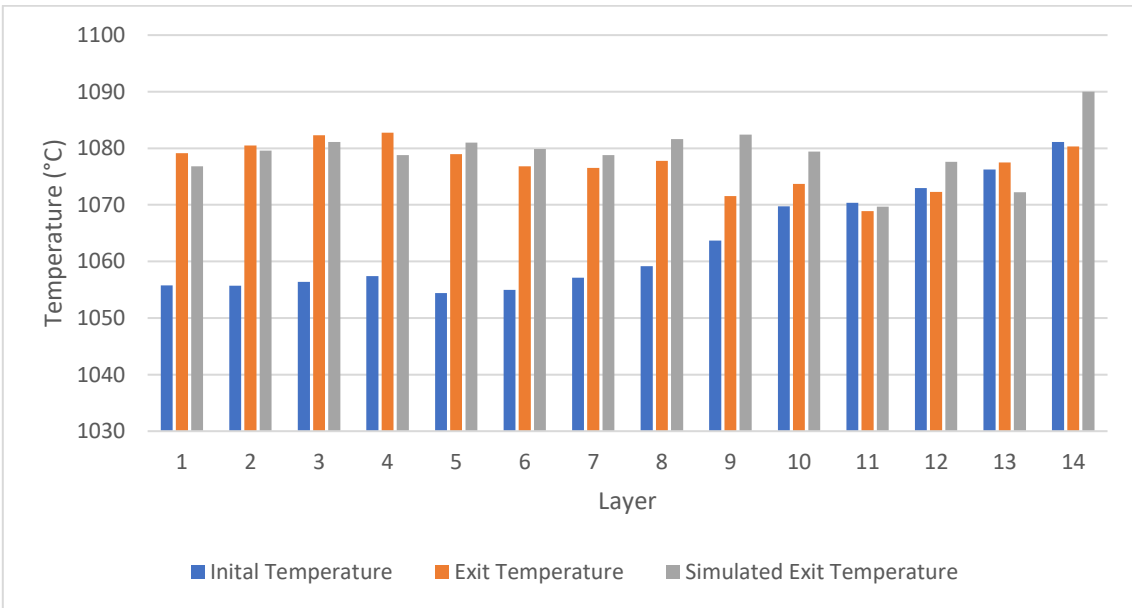
Figure 10.4 – Dataset 4 Pyrometer Data
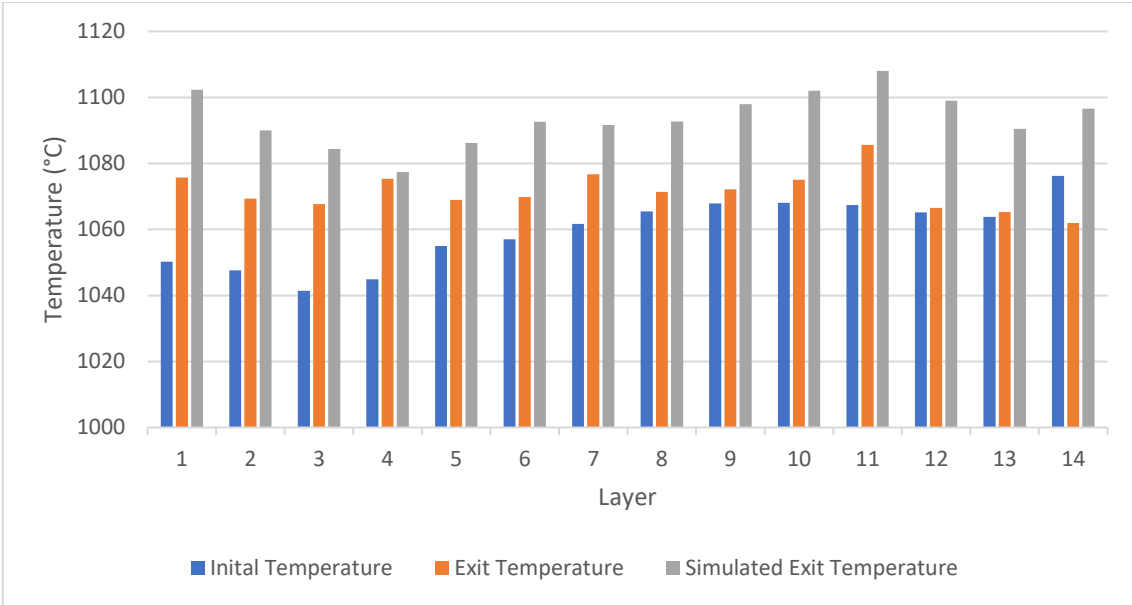
Figure 10.5 – Dataset 5 Pyrometer Data
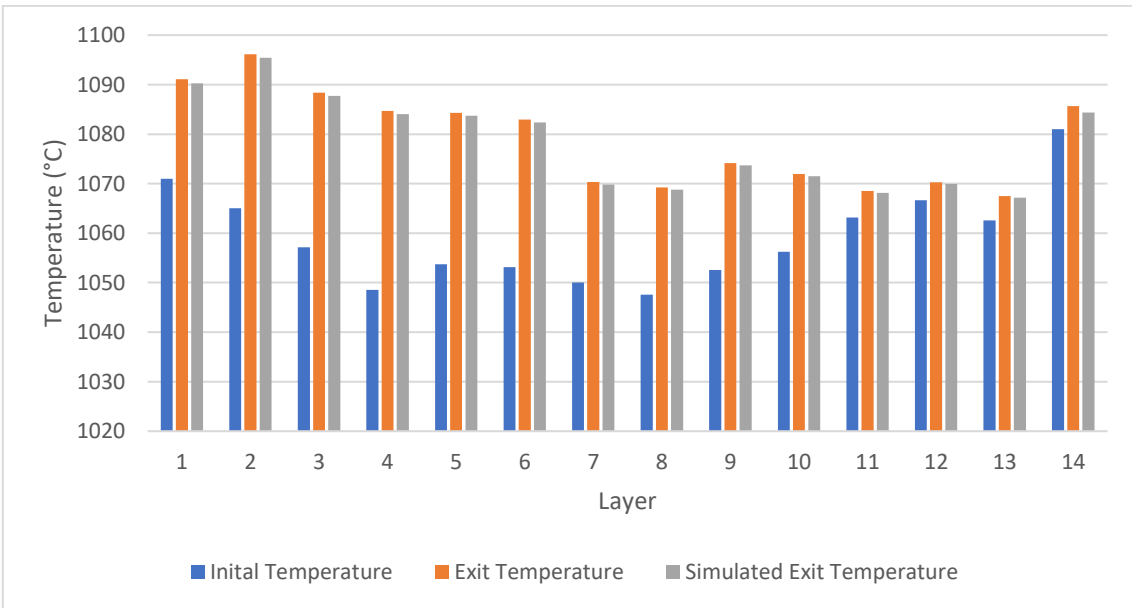
Figure 10.6 – Dataset 6 Pyrometer Data
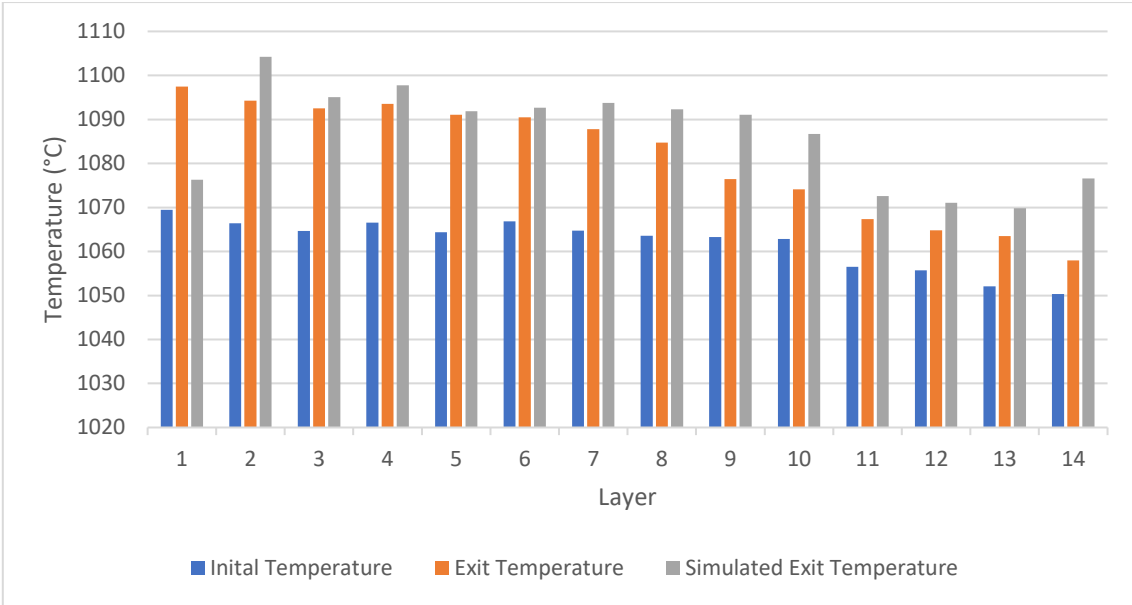
Figure 10.7 – Dataset 7 Pyrometer Data
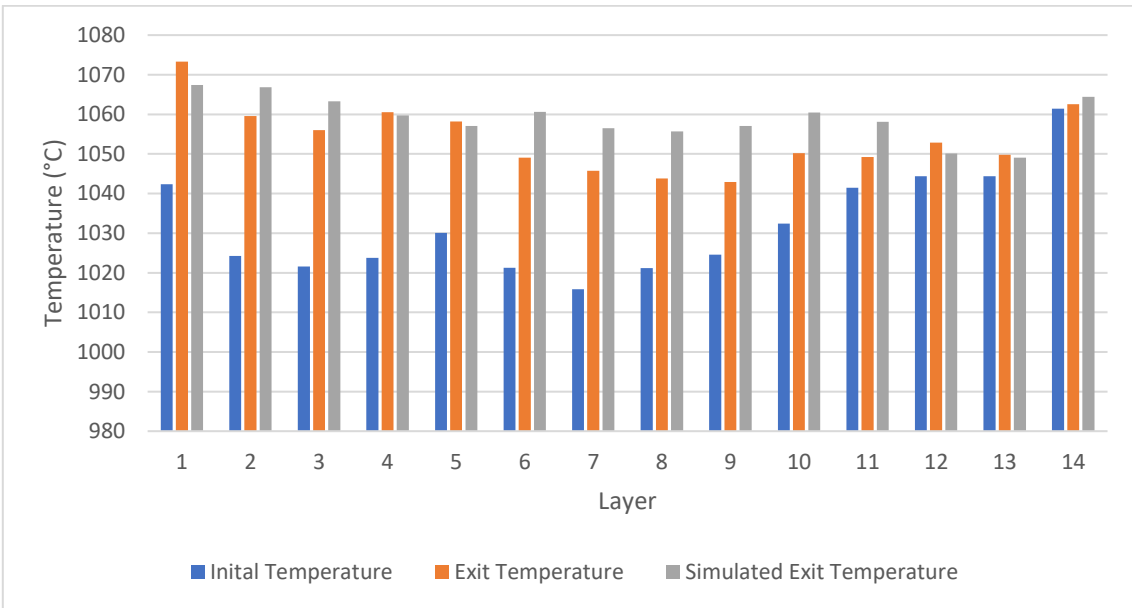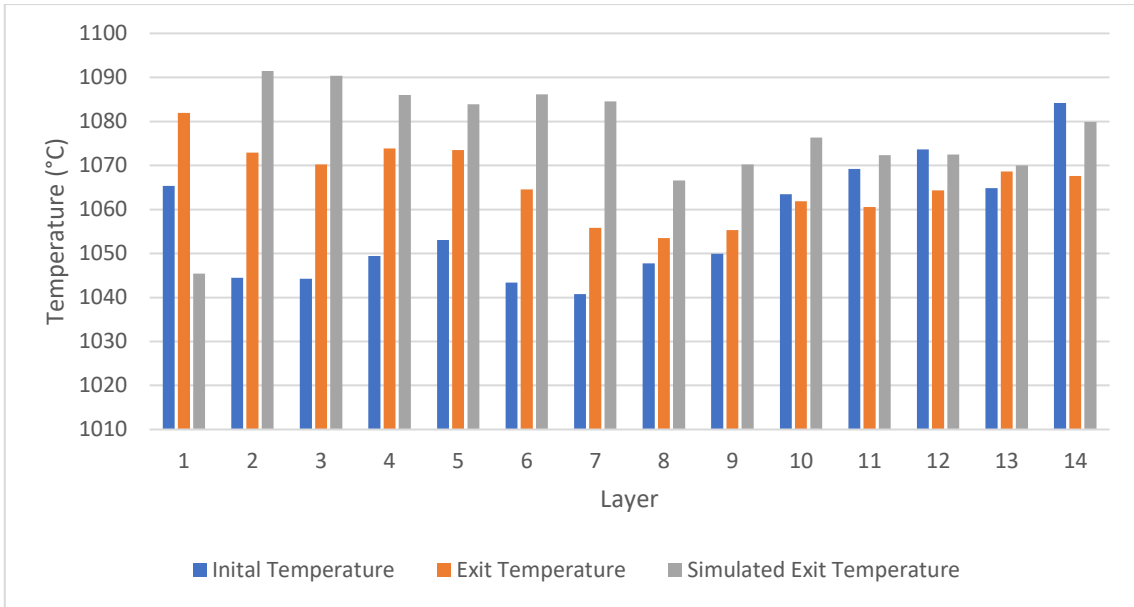

Figure 10.8 – Dataset 8 Pyrometer Data

84

Figure 10.9 – Dataset 9 Pyrometer Data
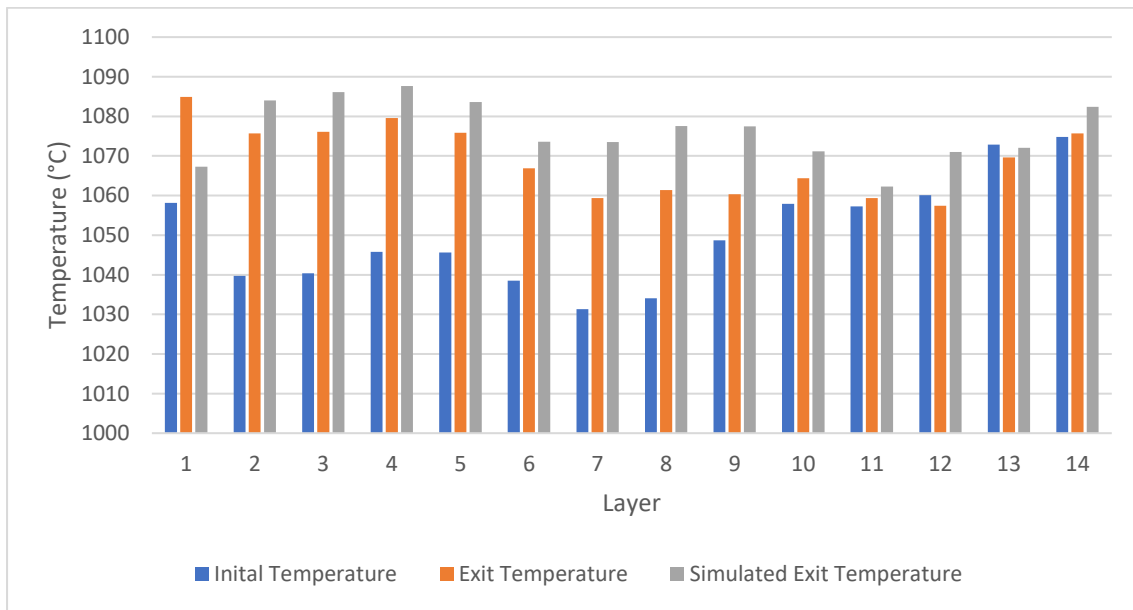
Figure 10.10 – Dataset 10 Pyrometer Data

10.3 ANSYS Plant Data Comparison

Below all datasets from 1 to 10 are shown. The data is represented as delta temperature, which is the final temperature, from both plant data (FmObsTemp[11] and CropShearEntryTemp) and simulation data (ANSYS), subtracted from the initial temperature of FmObsTemp[10], before the strip enters the coilbox.
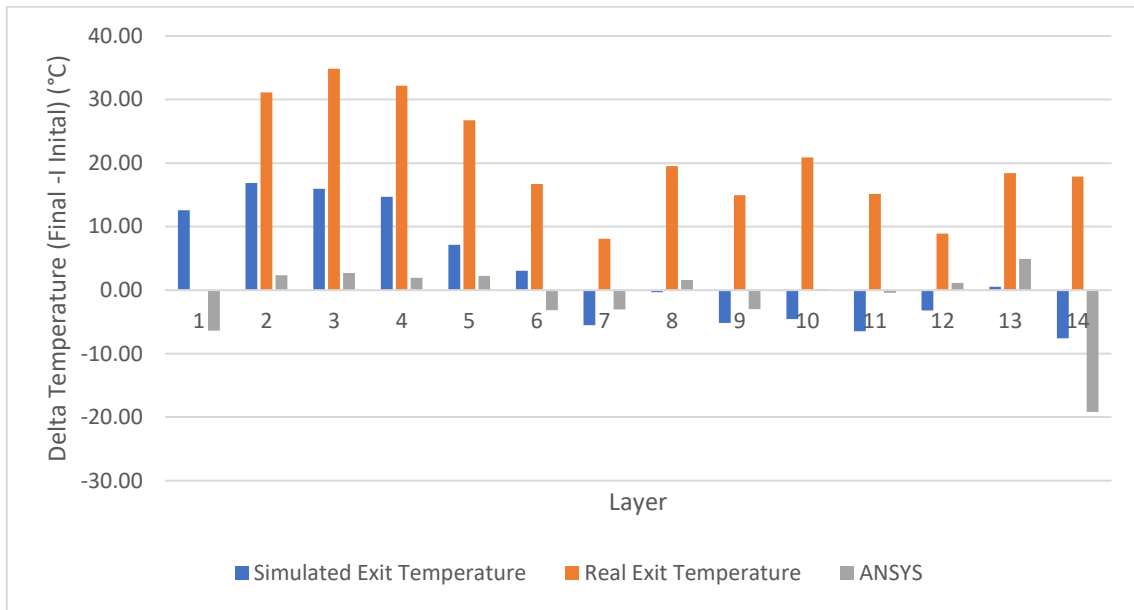
Figure 10.11 - Dataset 1 delta temperature
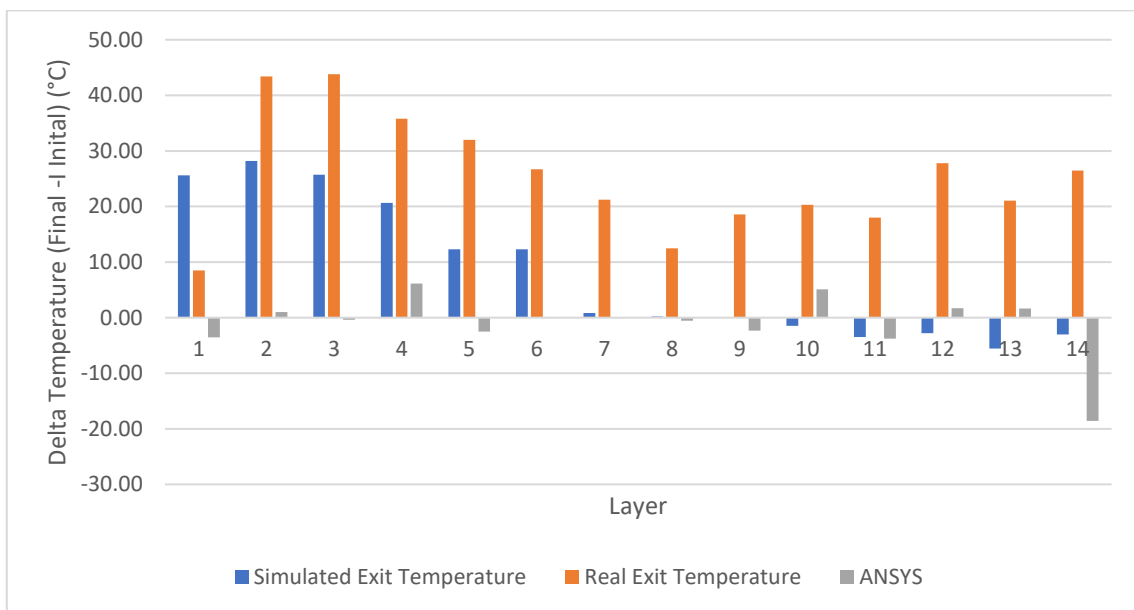
Figure 10.12 - Dataset 2 delta temperature
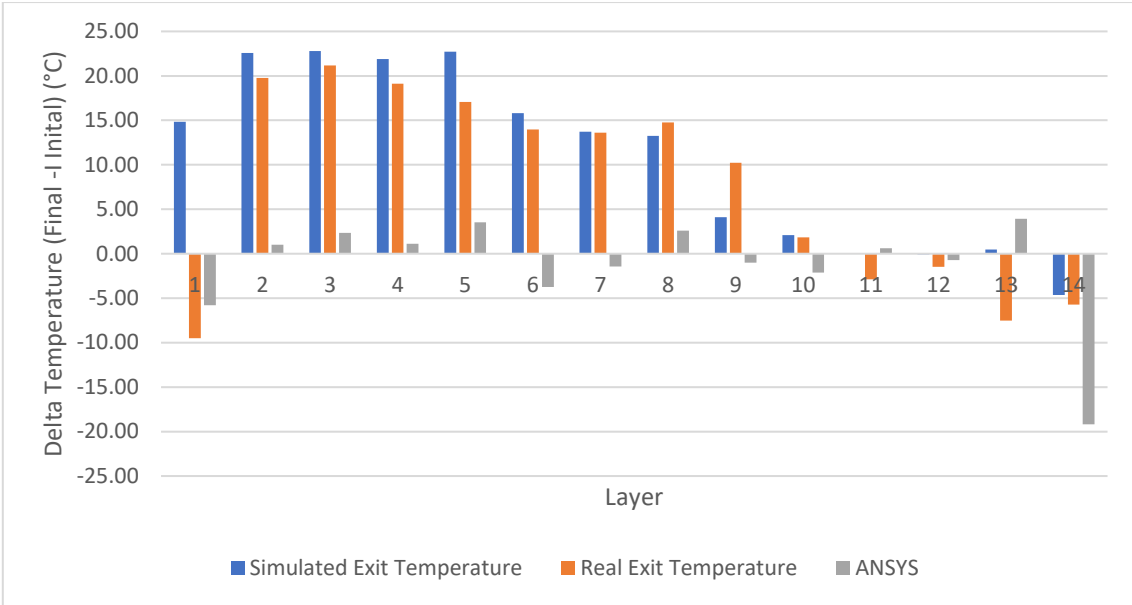
Figure10.13 - Dataset 3 delta temperature
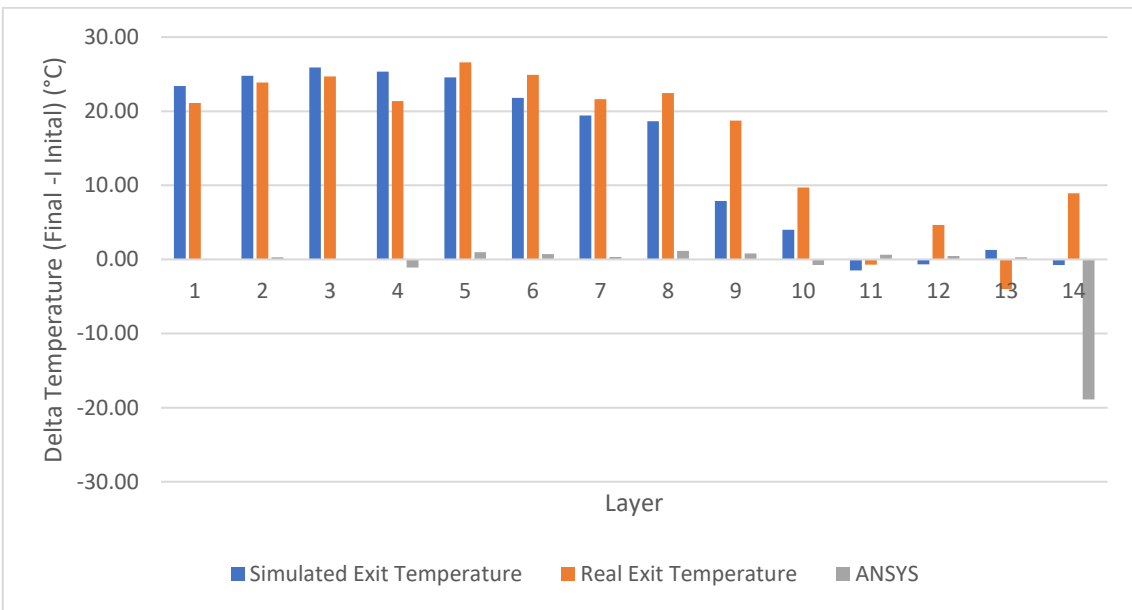
Figure 10.14 - Dataset 4 delta temperature
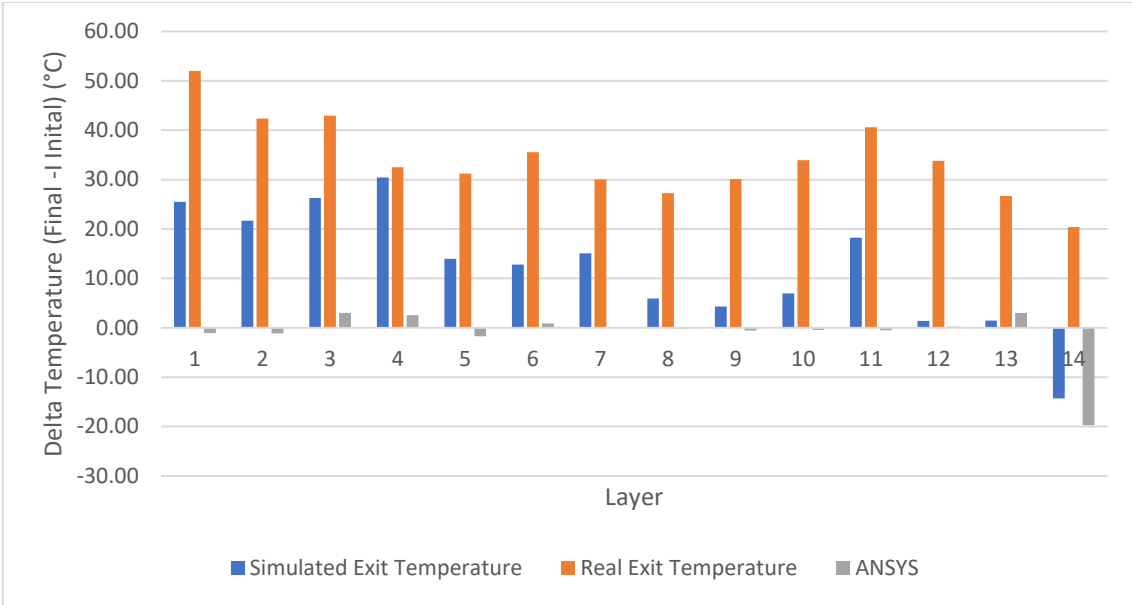
Figure 10.15 - Dataset 5 delta temperature
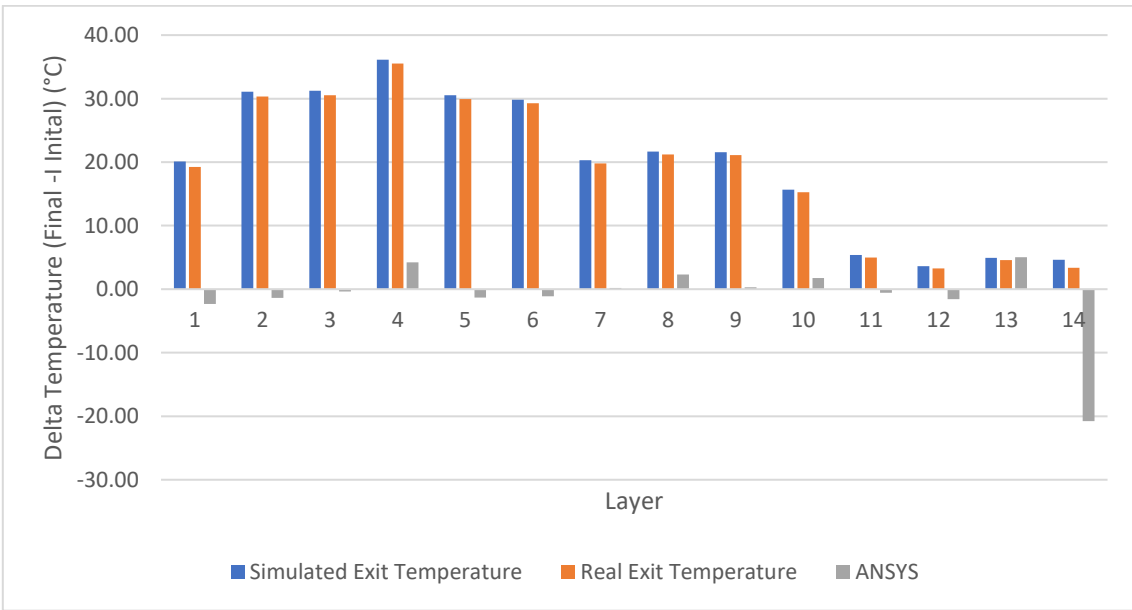
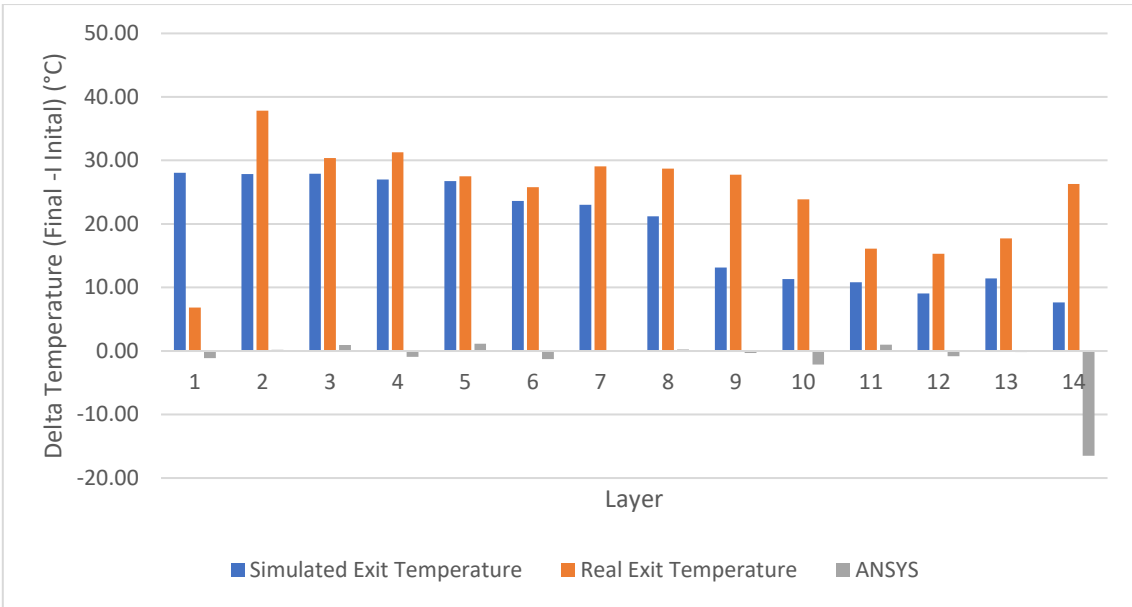*Graph 10.16 - Dataset 6 delta temperature*

Figure 10.17 - Dataset 7 delta temperature

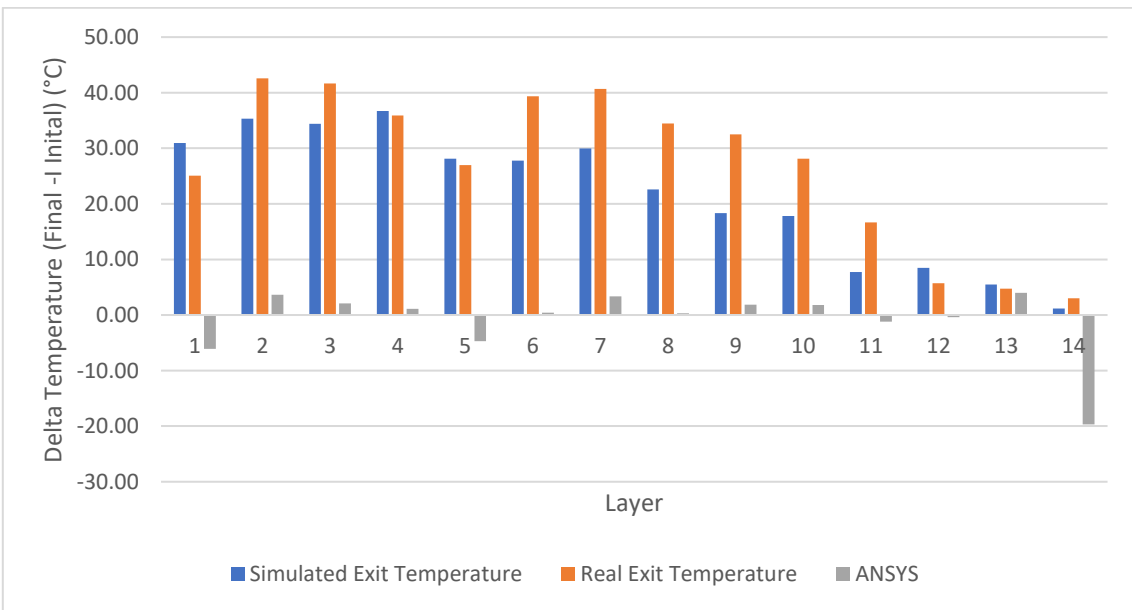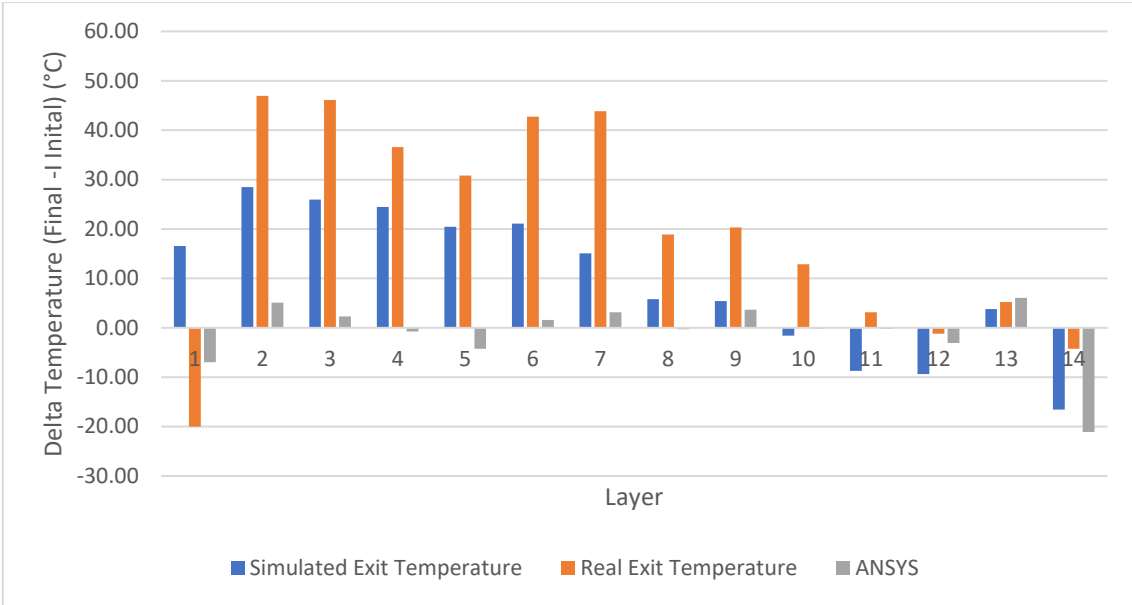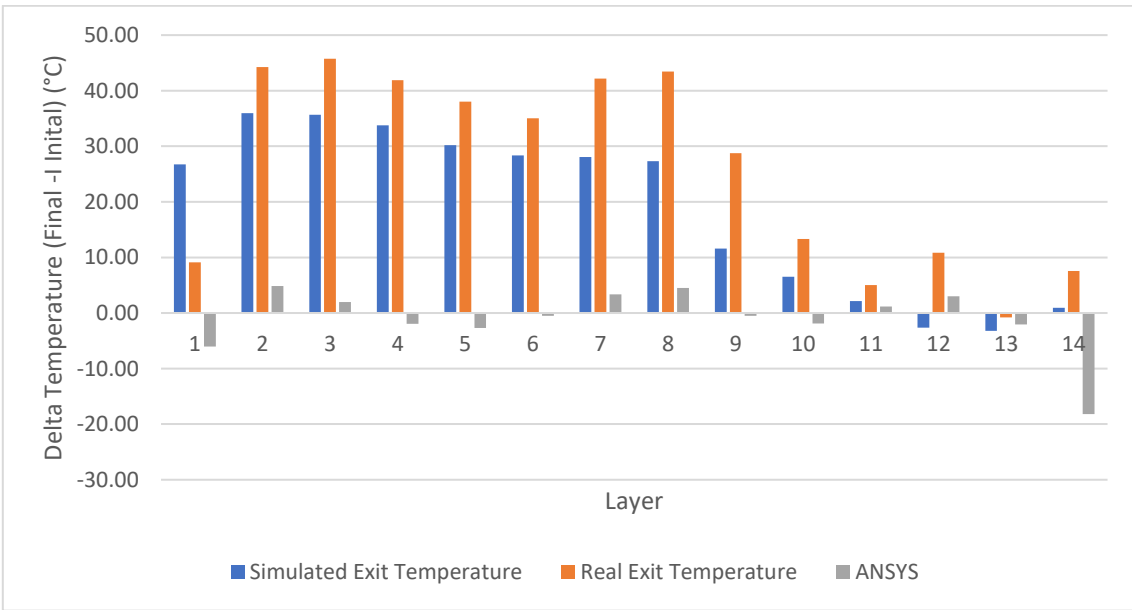*Figure 10.18 - Dataset 8 delta temperature*

Figure 10.19 - Dataset 9 delta temperature

Figure 10.10 - Dataset 10 delta temperature